

**Interactions between latent fingerprints, deposition surfaces and  
development agents.**

A thesis submitted for the degree of Master of Philosophy

Simon Richard Bacon  
Experimental Techniques Centre  
Brunel University  
2012

## **ACKNOWLEDGMENTS**

I would like to thank my supervisors, Dr Ben Jones and Dr Jesús Ojeda, for their guidance and assistance throughout this project. I would also like to thank Dr Alan Reynolds and Lorna Anguilano of ETCbrunel, as well as Vaughn Sears and Rory Downham of the Centre for Applied Science and Technology (CAST, part of the UK Home Office) for their technical assistance. This work is funded by the UK Home Office project 7121939. Finally, to my parents, Richard and Sue; your continued faith and support means a great deal.

## ABSTRACT

Fingerprints have provided a crucial source of forensic evidence for well over a century. Their power lies in an inherent ability for human identification and individualisation, which is based on two fundamental properties: uniqueness and lifelong permanence. Latent fingermarks represent by far the most evidentially common and challenging form of deposition, whereby an invisible copy of the unique friction ridge fingertip pattern is left as an amalgamated secretory residue on any surface that is touched. Dry powder dusting, the first and most iconic method for visualising or developing these deposits, was developed in the latter part of the 19<sup>th</sup> Century. In the period since, a great number of additional techniques, utilising physical, chemical and optical interactions in isolation or combined, have been devised for the same purpose. By selecting the correct technique in the correct order, it is now possible to extract significant print details from an unprecedented variety of surfaces. In the UK, such operational choices are recommended via Home Office issued protocol tables, which offer an optimum guide based on substrate type, substrate properties and fingermark conditions. Development technique specificity has improved in the last half-century alongside increased biochemical understanding of residue composition, however, the sheer variety of potential deposition substrates that exist within a heavily industrialised world inevitably causes disparities in efficiency, even within single protocol classifications. These effects are compounded by the enormous potential for pre- and post-deposition residue composition variation, relating to donor factors (age, sex, diet, lifestyle, etc.) and time dependant changes (environmental, biological, etc.) respectively. As a result, routine technique application can cause sub-optimal development.

This research utilises high resolution imaging and analysis techniques to demonstrate how subtle surface chemistry and topography features can selectively influence routine technique efficiency within a single protocol classification (smooth, non-porous plastics). Titanium dioxide, a widely used white pigment, has been shown as prevalent in a range of polymers following SEM and EDX analysis, either in a patchy or ubiquitous distribution. SEM analysis demonstrates a strong interaction between the pigment and carbon powder suspension, which causes detrimental overdevelopment effects in off-ridge areas. ToF-SIMS mapping of a Formica substrate places a significant amount of patchy distributed titanium dioxide in the top 30nm of the surface. Mapping also indicated the presence of an aluminosilicate pigment coating; however, it's involvement in the possible surface potential or surface energy interaction mechanism is unknown. The effects of linear surface features, which have previously been implicated in off-ridge cyanoacrylate overdevelopment on two operationally relevant polymers, were also analysed by creating a silicon wafer model for micro-FTIR analysis. Fingermark residues, including hydroxyl groups, have been shown to migrate significant distances along induced scratches in the model substrate over a 48hr period. It is likely that observed overdevelopment along large valley-like features (uPVC) and scratches (polyethylene) in the operationally relevant polymers is caused by a similar migration of residues.

## CONTENTS

|  |           |
|--|-----------|
| Title  | i         |
| Acknowledgments  | ii        |
| Abstract   | iii       |
| Contents   | iv        |
| List of figures  | vii       |
| List of tables   | xi        |
| Declaration  | xii       |
| Common abbreviations   | xiii      |
| <br>   |           |
| <b>1 INTRODUCTION</b>  | <b>1</b>  |
| <b>1.1 Fingerprints in history</b>                                 | <b>6</b>  |
| <i>1.1.1 Ancient history</i>                                       | 6         |
| <i>1.1.2 Early dactyloscopy</i>                                    | 7         |
| <i>1.1.3 Individuality, permanence &amp; classification</i>        | 7         |
| <b>1.2 Friction ridge skin and fingermark residue biochemistry</b> | <b>9</b>  |
| <i>1.2.1 Structure &amp; function</i>                              | 9         |
| <i>1.2.2 Morphogenesis</i>   | 12        |
| <i>1.2.3 Residue composition</i>                                   | 14        |
| <b>1.3 Latent fingermark development</b>                           | <b>17</b> |
| <i>1.3.1 Surface porosity</i>                                      | 18        |
| <i>1.3.2 Optical techniques</i>                                    | 20        |
| <i>1.3.3 Dry &amp; wet powders</i>                                 | 21        |
| <i>1.3.4 Physical developer &amp; multi-metal deposition</i>       | 22        |
| <i>1.3.5 Vacuum metal deposition</i>                               | 23        |
| <i>1.3.6 Ninhydrin</i>   | 24        |
| <i>1.3.7 Cyanoacrylate fuming</i>                                  | 24        |
| <i>1.3.8 Development sequencing</i>                                | 25        |
| <b>1.4 Summary &amp; research objectives</b>                       | <b>27</b> |
| <br>   |           |
| <b>2 IMAGING &amp; ANALYSIS</b>                                    | <b>29</b> |
| <b>2.1 Scanning electron microscopy (SEM)</b>                      | <b>29</b> |
| <i>2.1.1 Instrumentation</i>                                       | 30        |
| <i>2.1.2 Image generation</i>                                      | 32        |
| <i>2.1.3 Contrast &amp; resolution</i>                             | 33        |
|  | iv        |

|            |   |    |
|------------|---|----|
| 2.1.4      | <i>Energy dispersive X-ray (EDX) analysis</i>   | 34 |
| 2.1.5      | <i>Applications in dactyloscopy</i>   | 35 |
| <b>2.2</b> | <b>Time-of-flight secondary ion mass spectrometry (ToF-SIMS)</b>                            | 35 |
| 2.2.1      | <i>Instrumentation</i>  | 36 |
| 2.2.2      | <i>Spectral interpretation</i>  | 38 |
| 2.2.3      | <i>Imaging maps</i>   | 39 |
| 2.2.4      | <i>Applications in dactyloscopy</i>   | 39 |
| <b>2.3</b> | <b>Fourier transform infrared (FTIR) spectroscopy</b>                                       | 40 |
| 2.3.1      | <i>Instrumentation</i>  | 41 |
| 2.3.2      | <i>Spectral interpretation &amp; experimental modes</i>                                     | 42 |
| 2.3.3      | <i>Applications in dactyloscopy</i>   | 44 |
| <b>2.4</b> | <b>Atomic force microscopy (AFM)</b>  | 45 |
| 2.4.1      | <i>Instrumentation</i>  | 46 |
| 2.4.2      | <i>Modes of operation</i>   | 47 |
| 2.4.3      | <i>Applications in dactyloscopy</i>   | 50 |
| <br>       |   |    |
| <b>3</b>   | <b>THE EFFECTS OF POLYMER PIGMENTATION ON FINGERMARK DEVELOPMENT TECHNIQUES</b>             | 51 |
| <b>3.1</b> | <b>Introduction</b>   | 51 |
| <b>3.2</b> | <b>Experimental</b>   | 51 |
| 3.2.1      | <i>CAST polymers</i>  | 51 |
| 3.2.2      | <i>Sample development</i>   | 52 |
| 3.2.3      | <i>Brunel polymers</i>  | 53 |
| 3.2.4      | <i>FTIR polymer characterisation</i>  | 53 |
| 3.2.5      | <i>SEM analysis</i>   | 53 |
| 3.2.6      | <i>ToF-SIMS analysis</i>  | 54 |
| 3.2.7      | <i>SKPM analysis</i>  | 54 |
| <b>3.3</b> | <b>Results &amp; Discussion</b>   | 55 |
| 3.3.1      | <i>Titanium dioxide pigment</i>   | 55 |
| 3.3.2      | <i>Interaction mechanisms</i>   | 62 |
| <b>3.4</b> | <b>Conclusions</b>  | 68 |
| <br>       |   |    |
| <b>4</b>   | <b>THE EFFECTS LINEAR SURFACE FEATURES IN POLYMERS ON FINGERMARK DEVELOPMENT TECHNIQUES</b> | 69 |
| <b>4.1</b> | <b>Introduction</b>   | 69 |
| <b>4.2</b> | <b>Experimental</b>   | 70 |

|                                      |    |
|--------------------------------------|----|
| 4.2.1 <i>Model preparation</i>       | 70 |
| 4.2.2 <i>AFM scratch analysis</i>    | 70 |
| 4.2.3 <i>FTIR microspectroscopy</i>  | 71 |
| <b>4.3 Results &amp; Discussion</b>  | 71 |
| 4.3.1 <i>Silicon model relevance</i> | 71 |
| 4.3.2 <i>Residue migration</i>       | 72 |
| <b>4.4 Conclusions</b>               | 79 |
| <br>                                 |    |
| <b>5 SUMMARY</b>                     | 80 |
| <br>                                 |    |
| <b>APPENDIX A</b>                    | 83 |
| <br>                                 |    |
| <b>APPENDIX B</b>                    | 86 |
| <br>                                 |    |
| <b>REFERENCES</b>                    | 87 |

## LIST OF FIGURES

|   |    |
|---|----|
| Figure 1.1 - Ridge pattern details used for the classification and individualisation of fingerprints.   | 2  |
| Figure 1.2 – A flowchart for latent fingermark examination.   | 4  |
| Figure 1.3 – Neolithic carvings of fingerprint ridge patterns found on Gavrinis Island off the coast of France in 1971.                                 | 6  |
| Figure 1.4 – A cross-sectional representation of the anatomy of human skin.   | 10 |
| Figure 1.5 – Diagrammatic representation of primary and secondary dermal structures in relation to external friction ridge skin structure.              | 11 |
| Figure 1.6 – Volar pad locations on the hand of a developing foetus during the first ~8 weeks of pregnancy.   | 13 |
| Figure 1.7 – A cross-sectional representation of the aging of a fingermark following deposition on a porous substrate.                                  | 19 |
| Figure 1.8 – A cross-sectional representation of the aging of a fingermark following deposition on a non-porous substrate.                              | 19 |
| Figure 1.9 – A cross-sectional representation of the physical processes involved with normal VMD development.   | 23 |
| Figure 2.1 – A schematic representation of a typical SEM setup, including features within the two main areas: the electron column and specimen chamber. | 30 |
| Figure 2.2 – Emission signals and their distribution following electron beam-sample interaction.  | 32 |
| Figure 2.3 – The effects of surface topography and tilt angle on the surface area available for electron emission.                                      | 33 |
| Figure 2.4 – The effects of aperture size and working distance on SEM depth of field.   | 34 |
| Figure 2.5 – A schematic representation of a typical SIMS setup, including the two main systems: primary ion and mass analysis.                         | 37 |
| Figure 2.6 – A schematic representation of FTIR interferometer equipment and functionality.   | 41 |
| Figure 2.7 – An absorbance FTIR spectrum of polyoxymethylene, an engineering thermoplastic.   | 43 |
| Figure 2.8 – A diagrammatic representation of a typical AFM setup, including the two principal components: probe and scanner.                           | 46 |
| Figure 2.9 – A diagrammatic representation of the detection of variations in sample surface potential by SKPM analysis.                                 | 49 |

Figure 3.1 – (a) Low magnification SEM image of four fingerprint ridges developed with CPS suspension on the Formica surface. White patches of overdevelopment are visible on and off ridge. (b) Increased magnification SEM image from the centre of (a). (c,d) Two more increases in magnification, revealing a feature within the Formica surface and its association with overdevelopment. 55

Figure 3.2 – (a) SEM image of an MoS<sub>2</sub> powder suspension developed fingermark on Formica showing a level of association between overdevelopment and the presence of a surface feature. (b,c) SEM images of MoS<sub>2</sub> SPR (b) and CA (c) developed fingermark on Formica showing no association between overdevelopment and the same surface feature. 56

Figure 3.3 – An SEM image of an area of Formica containing two distinct surface features., associated with EDX spectra from a location away from both surface features (1), a location containing only the small ‘particulate’ feature (2) and a location containing only the large ‘flake’ shaped feature (3). 57

Figure 3.4 – A low kV SEM image (a) of a blank Formica sample developed with CPS alongside an increased kV, backscattered electron detection SEM image of the same area (b). While overdevelopment is clearly associated with titania, not all areas of the compound exhibit this effect. 58

Figure 3.5 – (a) An EDX map of a blank Formica sample (green-aluminium, red-titanium) alongside an SEM image of the corresponding area (b), illustrating two frequent subsurface structures (1-aluminosilicate, 2-titanium dioxide) and a localised spread of titanium. (c) An SEM image of a CPS developed uPVC surface highlighting the problems with ‘blanket’ development and ridge-boundary contrast (boundary running from bottom left to top right). Alongside is a representative EDX map of a blank uPVC sample (d), showing a ubiquitous spread of titanium (red). 59

Figure 3.6 – A comparison between CPS development on a blank transparent uPVC surface containing no titanium (a) and a blank white uPVC surface (PP3) containing surface wide titanium (b). The level of carbon powder adhesion is significantly higher on the titanium containing substrate. 60

Figure 3.7 – A low kV SEM image (a) of a blank NP2 sample developed with CPS alongside an increased kV, backscattered electron detection SEM image of the same area (b). Overdevelopment in the central region is associated with underlying titania, however, a large patch of overdevelopment is also associated with a topographic feature in the top left corner of the images. 62

Figure 3.8 – A high kV SEM image (a) of a titania doped epoxy resin alongside a low kV image of the same area (b). Localised patches of titania are significantly rougher in texture



than the surrounding areas, which may explain increased levels of powder adhesion over these patches when this surface is developed with CPS (c,d). 63

Figure 3.9 – An area of Formica with patchy titania as imaged using secondary electron SEM (a), tapping mode AFM (b) and SKPM (c). Significant variation in surface potential in this small area is visible as contrast in image C; however, this does not correlate entirely with titanium dioxide localisation as seen in image A. 64

Figure 3.10 – Maps of the 2<sup>nd</sup> (a), 3<sup>rd</sup> (b) and 4<sup>th</sup> (c) successive ToF-SIMS acquisitions from area C, showing localised titanium signal by the 3<sup>rd</sup> acquisition. Alongside is a retrospective SEM image of the same area (d) - larger patches of titanium are visible here, owing to the greater penetration depth of the technique. 65

Figure 3.11 – Distribution of titanium (a), aluminium (b) and silicon (c) in the surface of Formica, as demonstrated by maps from area B and compared to a retrospective SEM image of the same area. Co-localisation of the three elements suggests a coating around the titania pigment. 67

Figure 4.1 – CA overdevelopment into off-ridge areas following development of fingermarks on PE (a) and uPVC (b). Overdevelopment is associated with large wave-like surface features and sharp scratches respectively. 69

Figure 4.2 – A representative cross-sectional view of one area from one scratch on the donor A sample substrate. Slopes either side of the scratch opening, caused by physical stresses during scratching, are clearly evident 72

Figure 4.3 – FTIR absorbance spectra taken from the same area of tape on the donor A (donor B is not shown, however, can be represented by these spectra) sample substrate from day 1 (a) and day 3 (b). The high levels of similarity are sufficient to allow comparisons between over the 48hr period for all scans. 73

Figure 4.4 – An FTIR spectrum from a Donor A fingerprint residue location (indicated by the cross on a representative micro-FTIR hydroxyl group map image) showing the peak bands to be mapped. 74

Figure 4.5 – A light microscope image of the donor A sample, including each area chosen for micro-FTIR mapping 75

Figure 4.6 – Control region hydroxyl group maps taken with a 25µm aperture on day 1 (a) and day 3 (b) showing no significant contrast along the scratch line (situated approximately a quarter from the top of the images). Fingerprint region maps taken with a 25µm aperture on day 1 (c) and day 3 (d) showing residue movement and droplet size reduction associated with scratch lines (situated) approximately a quarter and three quarters from the top of the images). 76

Figure 4.7 – Control region hydroxyl maps of the scratch line from figures 4.5a,b taken with a 6.25µm aperture on day 1 (a) and day 3 (a) showing no significant contrast. Fingerprint region maps of the bottom scratch line from figures 4.5c,d taken with a 6.25µm aperture on day 1 (c) and day 3 (d). The increased resolution provided by a smaller aperture highlights scratch associated residue migration and droplet size reduction. 77

Figure 4.8 – Residue migration and droplet size reduction demonstrated with 6.25µm maps for the remaining residues, including fatty acids/triglycerides (a,b), sugars/phospholipids (c,d), hydrocarbons (e,f) and proteins (g,h), on days 1 and 3 respectively. (Note: Arbitrary colour scales are comparable between the two analysis days, but not between individual residue types) 78

## **LIST OF TABLES**

|  |    |
|--|----|
| Table 1.1 – A summary of fingerprint residue composition as contributed by secretions from the three primary sweat glands. | 15 |
| Table 3.1 – An overview of all primary and secondary polymers used during this study.                                      | 61 |
| Table 4.1 – Wave bands selected for micro-FTIR mapping of fingerprint residue components                                   | 73 |

## **DECLARATION**

The work described in this thesis has not been previously submitted for a degree in this or any other university, and unless otherwise referenced it is the author's own work.

### **Statement of copyright**

The copyright of this thesis rests with the author. No quotation from it should be published without prior written consent and any information derived from it should be acknowledged.

## COMMON ABBRIVIATIONS

ACE-V – Analysis, comparison, evaluation and verification

AFM – Atomic force microscopy

ATR – Attenuated total reflectance

BSE – Backscattered electrons

CA – Cyanoacrylate

CAST – Centre for Applied Science and Technology

CP – Cast polymer

CPS – Carbon powder suspension

EDX – Energy dispersive X-ray

FTIR – Fourier transform infrared

NP – New polymer

PE – Polyethylene

PS – Powder suspension

SE – Secondary electrons

SEM – Scanning electron microscopy

SKPM – Scanning Kelvin probe microscopy

SPR – Small particle reagent

ToF-SIMS – Time-of-flight secondary ion mass spectrometry

UHV – Ultra high vacuum

UP – Used polymer

uPVC – Unplasticised polyvinyl chloride

VP – Variable pressure

**INTRODUCTION****1**

Human fingerprints can broadly be classified as one of a number of biometric markers that are used for identification based on one or more intrinsic anatomical or behavioural characteristic (DNA, retina, face, voice etc.) [1]. Their use forensically is individualisation, whereby a sample can be demonstrated as unique or of known origin [2]. Fingerprints are, in terms of individualisation, the archetypical piece of forensic evidence. Each surface (substrate) that a human fingertip comes into contact with gets left with unique information about that person based on skin ridge patterns and secretions. These patterns are established midway through pregnancy, they remain constant throughout life and, as a result of being encoded at the interface between dermis and epidermis, are resistant to superficial skin injuries [3]. A fingerprint's forensic power, therefore, lies with the extremely robust variation in ridge details created during foetal development, together with the secretive properties of skin. It is no surprise then that the word 'fingerprint' turns up in numerous disciplines, almost as a scientific synonym for 'uniqueness'. One might think immediately towards DNA fingerprinting or, reading on, to descriptions of the spectral data created by the techniques featured in this study to analyse print residues along with their substrates and development agents. Such references reinforce the general belief in fingerprint evidence and are built up from decades of ridge detail understanding.

Skin ridges and furrows are visible to the naked eye in complicated patterns on the palms of the hand and the soles of the feet, and together they provide the basic structures for identification. The evolution of this friction ridge (or volar) skin predates the emergence of our species from its closest ancestor and occurred to fulfil three primary functions; perspiration, touch and grip [2]. Documented observations and detailed drawings of fingerprint anatomy can be dated as far back as the end of the 17<sup>th</sup> Century, but it was not until the mid-1800s, when the individual uniqueness and lifelong consistency of fingerprints was discovered, that their use for identification began [2]. This paved the way for the world's first classification system, allowing for far less laborious one-to-many fingerprint identification searches. The Henry System, named after its creator, utilises four basic fingerprint patterns in order

to classify print records into primary groups, thereby simplifying any subsequent ridge detail (minutiae) comparisons (Fig 1.1) [4].












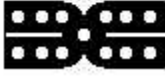
| Ridge minutiae    |   | Basic ridge patterns |   |
|-------------------|---|----------------------|---|
| Ridge ending      |    | Arch                 |    |
| Bifurcation       |    |                      |   |
| Lake              |    | Tent                 |    |
| Independent ridge |    |                      |   |
| Dot/Island        |    | Loop (left or right) |   |
| Spur              |   |                      |   |
| Bridge            |  | Whorl                |  |
| Crossing          |  |                      |   |

Figure 1.1 – Ridge pattern details used for the classification and individualisation of fingerprints. (Source: Berry & Stoney (2001) [2])

Along with more modern systems based on ridge flow characteristics, the fundamentals of Sir Edward Henry's invention still operate within today's international automated fingerprint identification systems (AFIS) [4]. Such systems are employed to conduct two main types of forensic search: tenprint search and latent search. A tenprint consists of rolled or plain impression prints from each of the 10 fingers of a subject, searched against a database of known individuals. Since rolled and plain impression prints (obtained as an inked impressions on paper or using a digital scanning by rolling the finger from nail-to-nail or pressing the finger down flat respectively) are collected in a controlled manner, they are invariably of sufficient quality to provide all the information required for a match [5]. Latent searches,

however, represent a far greater challenge. A latent (invisible) fingermark is one of three types typically found at a crime scene, along with the patent (visible) and impression (plastic) kind. All three suffer from being deposited in an uncontrolled manner (i.e. unwittingly on surfaces and objects that are touched) and will therefore show a greater range in quality than rolled or plain impression prints. Latent fingermarks are by far the most evidentially common and their searches against the same database of known individuals represent the highest importance in forensic fingerprinting [5]. Unlike patent and impression prints, which can simply be photographed *in situ*, latent marks first require some form of development in order to visualise them for subsequent identification. In the period since the forensic importance of fingerprints became apparent, a great number of development techniques have been devised, ranging from methods for enhanced illumination to those for physical adhesion and chemical reaction [2].

Dactyloscopy is the modern term used to describe the science of fingerprint identification, when translated literally it means ‘to examine the finger’, and in practice it is achieved based on three levels of features [2,30]:

- 1) Overall pattern type;
- 2) Minutiae details;
- 3) Ridge and pore morphology.

Whilst automated computer based systems are now almost universally employed by law enforcement agencies across the globe to take the burden of comparing these features within entire populations, a manual process for verifying a latent match is still necessary [5]. In the UK and many other countries this is a four step procedure known as ACE-V or analysis, comparison, evaluation and verification [5]. Analysis is the initial stage of determining whether the latent contains enough ridge detail and is of sufficient quality for identification, if so the necessary features are marked. The next step involves comparing the three levels of features with the paired print in order to quantify their level of similarity. Evaluation refers to the classification of the latent fingermark and paired fingerprint as individualisation (identification/match), exclusion (non-match) or inconclusive, based on the prior comparisons. The final verification step is essentially a replication of the first three steps and involves



independent re-examination of the latent by one or two additional fingerprint experts [5,6].

Crucially, from a forensic standpoint, fingerprint ridges are lined with pores that cover their surface with perspiration from sweat glands. This fact, together with friction ridge skin's ability to retain other bodily secretions and external contaminants on its surface following contact, effectively turns each fingertip into a biochemical "rubber stamp" [2]. In theory then, everything we touch is deposited with this combined residue and has the potential to subsequently reveal that occurrence. In practice, however, there is significant room for error. Considering the same stamp analogy: by pressing too hard or too lightly detail might be hidden, movement during impression will smudge ink, and consecutive impressions without replenishing ink will progressively diminish detail. These effects are accentuated by the delicate intricacy of fingerprint patterns and compounded when taking into account the enormous possible variations in substrate properties, intra and inter donor residue biochemistry and post deposition ageing and environmental effects. The first step in the ACE-V procedure is designed to reveal any such possible obstructions to comparison and as a result, a latent fingermark's capacity for individualisation is reduced or partial in the overwhelming majority of evidential circumstances.

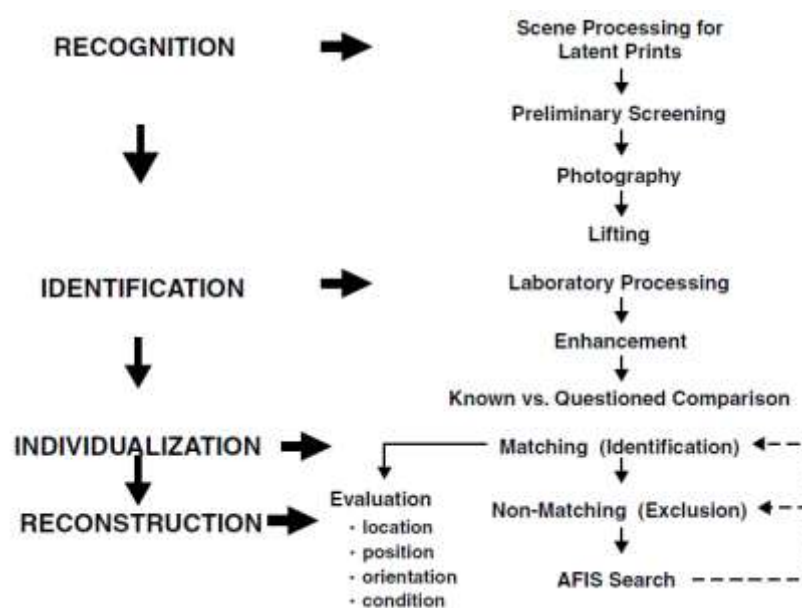


Figure 1.2 – A flowchart for latent fingermark examination. (Source: Olsen & Lee (2001) [7])

Enhancing this capacity is therefore a combination of an examiner's ability to recognise potential latent mark areas and their subsequent utilisation of the optimum development technique(s) for that specific situation. Efficient recognition of areas within a crime scene that are likely to contain marks is the first step in latent examination and since all other steps are dependant on the success of this process, it is also the most important (Fig. 1.2) [7]. Success requires a careful consideration of the surfaces an examiner is presented with and its relative properties [8-12]; as such the recognition process is intrinsically linked to the choice of development technique. The official system for development technique choice in the UK is governed by Home Office issued protocol tables, which offer the examiner a guideline as to the most effective technique for a given situation based on certain print conditions (fresh/aged) and a number of substrate properties (wet/dry, smooth/rough, porous/non-porous/semi-porous) [8,9]. Specificity with regard to technique choice and surface variability is an issue with such encompassing classifications. In certain cases this may render the routine technique sub-optimal or inefficient and manifest in either weak development, superfluous background development or no development [10-12].

Modern techniques for micro- and nanoscale analysis of fingermarks, substrates and development techniques are increasingly being utilised to investigate the interactions taking place between these three entities, while relating observations to development discrepancies and highlighting ways improve protocol specificity. A recent study using a combination of high resolution imaging and powerful analytical instruments, for example, demonstrates very subtle topological variations between a subset of polymers within a single protocol classification (smooth, non-porous plastics), which heavily affected the performance of powder suspension development [12]. The potential for protocol refinements that result from such work not only increases development efficiency, which simultaneously saves individual police forces time and money, but also adds scientific credibility to fingerprint evidence amidst an ever growing trend towards public and judicial scrutiny of criminal forensics [13,14]. Indeed, the notion that a fingerprint match is evidentially infallible has been questioned more in the last decade than the entire preceding century [15,16]. It has been suggested that the main challenges stem from a lack of empirical data regarding the robustness of the identification process and flaws in the standardised ACE-V

identification protocol leading to false positive identifications [16,17]. Despite this, most would agree that the rationale behind a fingerprint's evidential value, i.e. its individual uniqueness and permanence, is valid [16]. A crucial step to increasing the efficiency of the entire fingerprint identification process begins with maximising the quality and quantity of prints developed from an exhibit or crime scene surface [17]. Research into optimising development techniques for specific substrate and latent fingermark conditions is helping to achieve this and ensure the future of fingerprinting is as robust as its history.

## 1.1 Fingerprints in history

### 1.1.1 Ancient history

There is significant archaeological evidence to suggest that members of early civilisations were anatomically aware of their friction ridge skin in terms of its deviation all other areas of skin. For example, carvings discovered at sites off the coast of Ireland and France that are said to depict fingerprint patterns can be dated as far back as 3000 B.C. (Fig. 1.3) [1]. It is generally considered that this awareness did not extend to any knowledge of the individual nature of fingerprints or their potential



Figure 1.3 – Neolithic carvings of fingerprint ridge patterns found on Gavrinis Island off the coast of France in 1971. (Source: Maltoni *et al.* (2009) [1])

for identification, however, the impression of prints into the bricks of newly constructed royal buildings in Mesopotamia and ancient Egypt (*c.* 3000 B.C.) is thought to have represented a form of quality certification [2]. Furthermore, fingerprint impressions in clay are known to have been used on Babylonian contracts (*c.* 1800 B.C.) to prevent forgery and commonly in ancient China to seal official letters and other important documents (*c.* 300 B.C.) [2,6]. An example of the latter, in which a thumb printed clay seal bears the name of the person who made it on the reverse, has even been portrayed as the earliest evidence of fingerprint use for identification purposes [2,18]. It is, however, impossible to

conclude from this source alone than any sort of systematic cognitive approach to document identification was in operation in China during this period.

### *1.1.2 Early dactyloscopy*

The earliest documented descriptions of the intricate anatomical details contained within human fingerprints were made during the late 1600s by two European plant morphologists [2]. In addition to his work on plants, Professor Marcello Malpighi of the University of Bologna was a pioneer in skin physiology research and his contribution was recognised in the naming of the innermost layer of the epidermis (Malpighian layer). In 1686 he published *De Externo Tactus Organo (The External Organ of Touch)*, which contained brief descriptions of friction ridge skin [19]. Two years previously, however, more extensive descriptions were being published for the first time by the English doctor Nehemiah Grew. The first of two papers sent by Grew to *Philosophical Transactions* of the Royal Society of London (1684) included eloquent written observations and detailed drawings of ridges, furrows and pores on the skin of hands and feet [20]. Bizarrely, a world renowned 18<sup>th</sup> Century wood engraver called Thomas Bewick is often credited with bringing fingerprints to the mainstream following the use of his own as a signature on publications [2]. Despite this, it was not until almost 140 years after Grew's paper for *Philosophical Transactions* that fingerprint research made a meaningful return to academic literature. Johannes Evangelista Purkinje, like Grew, was a physiologist and dealt with ridge, furrow and pore functionality in his 1823 thesis [21]. The fifty eight page document, which examines all aspects of the integumentary system in its final section, is a far more scientifically orientated piece of work than Grew's literary observations and significantly it contains the first descriptions of the four basic ridge patterns (1 arch, 1 tent, 2 loops and 5 whorl types) used to classify fingerprints [21].

### *1.1.3 Individuality, permanence & classification*

In order for a fingerprinting system to successfully identify individuals within it and isolate them from everyone else without having to compare every entry, it must feature some form of classification. Additionally, there must be no possibility that two entries are the same or that changes could occur readily with age or superficial injury. The uniqueness of fingerprints was first described in 1788 by a German anatomist

named Johann Mayer, however, it was not until the latter part of the 19<sup>th</sup> century that the permanence of fingerprints was discovered and the idea of uniqueness was given a sound empirical basis [1,22]. Several prominent figures in the history of fingerprinting come to the fore around this period and an element of conjecture still exists with regard to where credit should lie for certain advances. Two British scientists, Sir William James Herschel and Dr Henry Faulds, are known to have separately contributed many years of research in the field of fingerprints and are thought to have each developed novel ideas regarding their uniqueness and potential for identification [23, 24]. In 1917, however, it was conceded by Herschel, who was the first to discover the lifelong consistency of fingerprints, that Faulds had initially conceived the idea of utilising fingerprints to implicate individuals in a crime and conversely to exonerate innocent parties [2].

The legacy of the research by these early fingerprint pioneers for criminal forensics is undoubtedly its culmination in an international classification system. The Henry Classification System, developed by its namesake Sir Edward Henry (a British Inspector General of the Bengal Police in India) and two of his Indian assistants, is the foundation upon which today's modern systems are built [4]. The system numbers digits 1-10 from the right thumb to the left little finger and then assigns each a value based on whorl patterns alone (all other patterns are assigned a value of 0), before ratioing one plus the sum of even digit whorls and one plus the sum of odd digit whorls [25]. It was originally used to classify prisoners in British India towards the end of the 19<sup>th</sup> century [25]. The value of such a system is that it places any individual ten print entry into one of 1024 primary categories, thereby greatly simplifying any subsequent searches based on second or third level detail. The idea of classification was not unique to Henry, indeed Herschel and Faulds had both also worked out means of classification [2] and another British contemporary, Sir Francis Galton, had developed a similar system to Henry and was the first to define specific minutiae details ('Galton's Points'), recognising their role for individualisation [26]. Moreover, a number of years prior to the 1901 operational introduction of the Henry System at Scotland Yard, the world's first fingerprint bureau had already been established by Dr Ivan Vucetich for La Plata Central Police Department in Argentina [2]. Although the Vucetich System remained popular in South America and Vucetich's bureau are

credited with solving the first murder case (F. Rojas, 1893) using fingerprint identification, it was the Henry's system that took on a worldwide appeal [2].

One major limitation of the Henry System is that all ten prints are required. This was sufficient to identify repeat offenders, however, in order to search unknown latent marks from crime scenes against known collections, single-print classifications were required. A number of systems, based on subdivisions of level 1 details and introduction of level 2 and 3 details, were devised for this purpose; however, databases quickly became too large for manual searches [22]. Advances since this period have concentrated on the nationalisation and globalisation of fingerprint based criminal identification through standardisation of the methods employed to achieve individualisation (including latent development) and the incorporation of modern technologies. The latter refers mainly to automated fingerprint identification systems (AFIS), which use complex algorithms based on manual systems to achieve digital fingerprint storage, classification and searching on an international scale [1]. As described, criminal identification must involve the manual human ACE-V process, which relies on the concept of individualisation following a match. Provided sufficient confidence exists within the scientific community regarding the individual uniqueness of fingerprints, which will be discussed in the following subchapter, the main challenges for forensic fingerprinting going into the future relate to eliminating the possibility of subjectivity and errors in the identification process [16]. Several high profile cases of false positive matches since the turn of the century have brought this issue to the fore because such matches can only result from two possible scenarios; two individuals sharing exactly the same fingerprint or an error during identification [16].

## **1.2 Friction ridge skin & fingermark residue biochemistry**

### *1.2.1 Structure & function*

Skin and its appendages (hair, nails and glands) make up the human body's integumentary system, which serves a number of vital functions (protective barrier, temperature regulation, touch sensation, water retention, waste excretion, immunity, blood reservoir and vitamin D synthesis) [27]. This is the body's largest organ system

and the skin itself is the largest single organ, covering, on average, an area between 1.5 and 2 square metres. For such a large, strong and flexible organ the thickness is remarkably small. This is relatively constant at an average of 2mm for most of the body, except for friction ridge skin on palmar surfaces of the hand and fingers and plantar surfaces of the feet and toes, where thickness increases by almost a third [27]. Skin can broadly be divided into two distinct layers: a thin outer layer of epithelial tissue (epidermis), which provides the protective barrier; and dense layer of connective tissue (dermis), which provides support and nutrition [28]. The epidermis is separated from and tightly anchored to the dermis by a basement membrane consisting of elements from both layers. The dermis is connected to underlying muscle and bone by a subcutaneous layer of loose connective tissue and adipose (fat) cells, known as the hypodermis [28]. Although the hypodermis is not technically part of the skin, it contains the blood vessels that supply the organ and the fat tissue functions as an efficient body insulator [28]. Figure 1.4 provides a three dimensional cross section of the skin and all of its appendages.

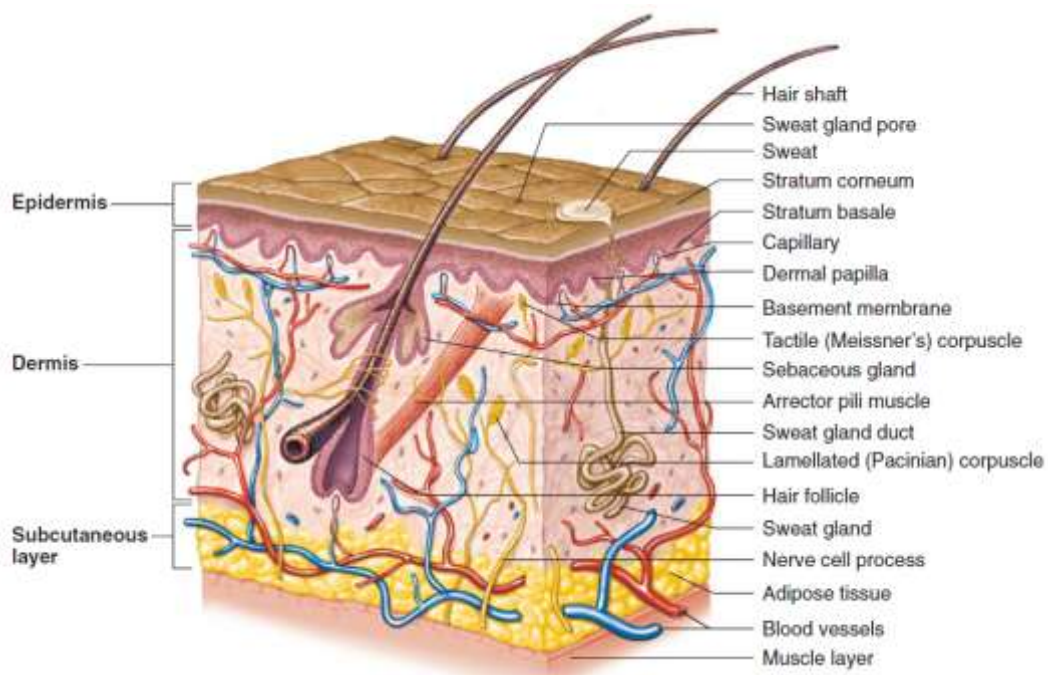


Figure 1.4 – A cross-sectional representation of the anatomy of human skin. (Source: Shier *et al.* (2009) [103])

The dermis accounts for up to 95% of the mass of skin and is formed by two basic layers: papillary and reticular [27]. Together they are significantly thicker than the

overlying epidermis and house the bulk of the skins appendages and secondary tissues (cardiovascular, muscle and nerve). The inner reticular dermis is characterised by dense irregular connective tissue (collagen and elastin fibres) and this provides the skin with strength and flexibility [28]. No basement membrane-like boundary exists between the reticular dermis and the hypodermis, instead a network of fibres interconnect the two regions. Eccrine sweat glands, the only skin appendages that form in friction ridge skin, are rooted at this blurred interface [29]. The outer papillary dermis is characterised by wave-like projections, known as dermal papillae, which indent the inner layers of the overlying epidermis (Fig. 1.5). Their purpose is to increase stability at the basement membrane junction and create extra surface area for the increased networks of capillaries and nerve receptors that are woven into the loose connective tissue of the papillary layer [28]. The dermal papillae of friction ridge skin are mounted on an arrangement of larger dermal waves. The structure and location of these primary and secondary dermal ridges correspond to the patterns of ridges and furrows that appear across the surface of volar skin and at the tips of the fingers as fingerprints (Fig. 1.5) [29].

The epidermis consists exclusively of squamous epithelium in a number of sub-layers and, as the outermost layer of skin, it is directly exposed to the physical stresses of everyday life. To cope with the effects of constant wear and sporadic injury, skin perpetually replenishes its cells from the deepest epidermal layer (*stratum germinativum*, or basal layer) through a combination of cell proliferation, migration and differentiation [29]. The

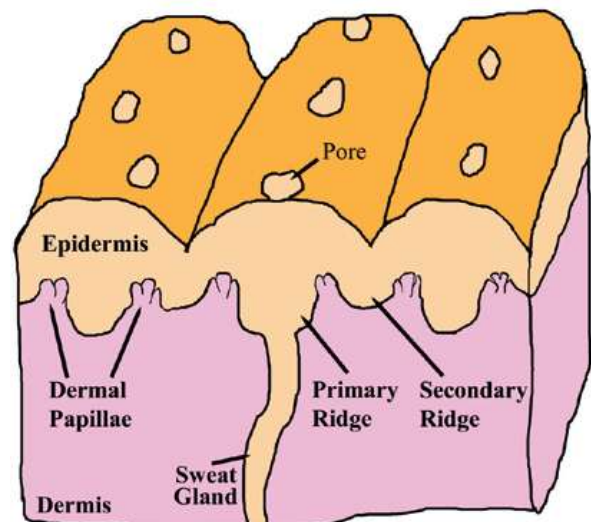


Figure 1.5 – Diagrammatic representation of primary and secondary dermal structures in relation to external friction ridge skin structure. (Source: Maceo (2011) [29])

basal layer is a single row of columnar cells, which are nourished by blood vessels in the dermal papillae allowing for mitosis. This first layer also contains the skins only melanocytes, which are the melanin producing cells that define skin colour [28]. The outermost layer (*stratum corneum*, or cornified layer) is made up of approximately 15



to 20 rows of fully keratinised flat dead epithelial cells, all of which originated from the basal stem cells and comprised each layer in between (*stratum spinosum*, or spinous layer; *stratum granulosum*, or granular layer; *stratum lucidum*, or clear layer) as part of a continuous cycle taking between 25 and 45 days [28]. Basal cells are therefore the only non-mobile cell in the epidermis, each new set of proliferated cells is pushed up the strata while undergoing various morphological changes and stages of terminal differentiation. For this reason, only damage to the basal layer results in permanent alterations to the epidermis and hence an altered ridge pattern appearance [30]. Ridge pattern permanence resulting from the anatomy and physiology of skin is one of the fundamental properties of fingerprints that allow for their use forensically, the other, uniqueness, is determined several months prior to birth.

### 1.2.2 Morphogenesis

The concept of uniqueness in dactyloscopy and the wider field of forensic identification is still a controversial one [15]. In the case of fingerprints it would be next to impossible to prove with one hundred percent clarity that no two prints are alike, since an incomprehensible amount of fingers would need to be compared. However, the general idea of biological uniqueness (i.e. no two organisms are identical) has its foundations in many years of empirical research and it is known that the environmentally interdependent processes governing friction ridge during pregnancy are so complex that even monozygotic twins can develop radically different patterns [31].

These processes begin during the very early stages of gestation with the onset of hand (5-6 weeks) and finger (6-7 weeks) development. Around this period a series of volar pads form sequentially on each volar surface of the foetus. Interdigital pads (~6 weeks) are the first to appear on a developing hand, followed by the thenar and hypothenar pads (~6 weeks), and then one on each fingertip (~7-8 weeks), beginning with the thumb and ending with the little finger (Fig. 1.6) [30,31]. These transient swellings of mesenchyme tissue remain pronounced during their rapid growth until this is overtaken by the growth of the hand itself (~10-11 weeks) and they are no longer visible by week 16. This process is referred to as 'regression' (though technically the pads are covered by surrounding tissue as their growth slows) and it

produces pads with individual shapes and positions from the well rounded precursors [31]. It is during the growth and regression of volar pads that primary dermal ridge proliferation begins and the critical stages in fingerprint pattern development occur [3].

Primary ridge formation coincides with the development of sweat glands and occurs in three distinct locations on a developing finger: the apex of the volar pad, the distal periphery (fingertip) and the distal interphalangeal flexion crease [30]. The initial orientation of proliferation is governed by variations in physical stress on the surfaces of volar pads during regression and

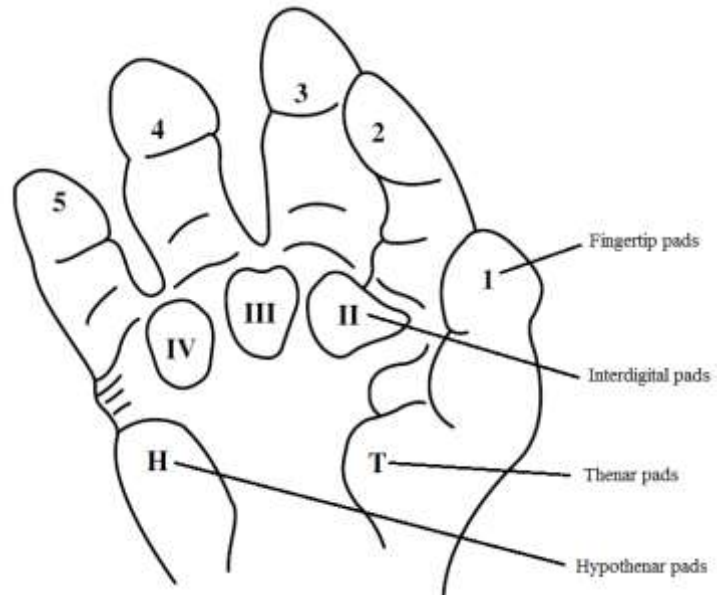


Figure 1.6 – Volar pad locations on the hand of a developing foetus during the first ~8 weeks of pregnancy. (Source: Champod *et al.* (2004) [30])

overall pattern type is thought to be determined by pad height, which in turn is linked to growth and regression timing events [31]. Between the onset and completion of the primary dermal pattern, a number of additional ridge growth properties (count, field convergence and termination) are shaped by a complex combination of volar pad morphology (symmetry, size, height etc.), timing events, underlying bone morphology and external factors (e.g. diet of the mother). By this stage (~16 weeks), both the first (overall pattern type) and second (minutiae) level fingerprint features that will remain consistent throughout life have been established [30,31]. The formation of secondary dermal ridges in between primary ones occurs during the late stages of primary ridge maturation (~15-17 weeks) and causes infolding directly above at the epidermal surface [32]. Secondary ridges continue to mature until week 24, during which time third level (ridge and pore morphology) fingerprint features are sculpted based on general foetus growth and the dermal papillae formation at bridges between primary

and secondary dermal ridges [30]. The resulting dermal pattern of primary fold next to secondary fold is externally mirrored at the epidermis surface as ridges and furrows respectively (Fig. 1.5). It is this pattern that is then left as a fingerprint following contact with any surface.

### *1.2.3 Residue composition*

Human skin accommodates three primary secretory glands: eccrine and apocrine are of the sudoriferous (or ‘sweat producing’) kind, whereas sebaceous produce predominantly lipid content [28]. As previously explained, the pores on friction ridge skin are only fed by eccrine sweat glands. Fluid secreted by these coiled tubular structures is approximately 98% water; however, natural latent fingerprint residue is a complex and highly variable mixture of organic and inorganic substances (Table 1.1) [27]. Aside from the additional eccrine 2%, complexity results from the ability of friction ridge skin for tactile material retention and the transient nature of skins outer layer, which dictate four additional component sources: sebaceous gland secretion, apocrine gland secretion, epidermic substances and external contaminants [33]. Comprehending the contents of any one fingerprint is complicated further by a host of pre- and post-deposition variables. The age, sex, diet and lifestyle of an individual will all have a bearing on secretory composition and when this is considered in conjunction with time dependant factors that can subsequently alter composition (environmental conditions, substrate properties, biological degradation, etc.); it becomes extremely challenging to predict content at the point of development [34]. It is clear then that there is enormous potential for inter- and intra-donor variation in residue content (i.e. within and between donors), however, quantifying this remains a major challenge. Indeed, literature on the composition of individual gland secretions far outweighs that on the amalgamated fingerprint residues and attempts to address this balance are important for development technique selection, new technique advances and determining crime scene chronology [27,33-36].

Eccrine sweat glands in volar skin are larger, more densely situated and more active than any other area of the body [28]. Their secretions will always feature to some degree in fingerprint residues and in addition to water this has been shown to include

Table 1.1 – A summary of fingerprint residue composition as contributed by secretions from the three primary sweat glands. (Source: Ramotowski (2001) [27])

| Source                     | Organic components   | Inorganic components  |
|----------------------------|--|---|
| Eccrine secretions         | Amino acids<br>Proteins<br>Glucose<br>Lactate<br>Urea<br>Pyruvate<br>Creatine<br>Creatinine<br>Glycogen<br>Uric acid<br>Vitamins<br>Fatty acids<br>Sterols<br>Enzymes<br>Immunoglobulins | Sodium<br>Potassium<br>Calcium<br>Iron<br>Chloride<br>Fluoride<br>Bromide<br>Iodide<br>Bicarbonate<br>Phosphate<br>Sulfate<br>Ammonia<br>Trace metals |
| Sebaceous secretions       | Triglycerides<br>Fatty acids<br>Wax esters<br>Squalene<br>Cholesterol<br>Cholesterol esters<br>Trace organics  |   |
| Apocrine secretions        | Proteins<br>Carbohydrates<br>Cholesterol<br>Steroids   | Iron  |
| Miscellaneous contaminants | Drugs<br>Cosmetics<br>Epidermal skin<br>Nicotine<br>Blood  | Drugs<br>Cosmetics  |

a range of organic (e.g. amino acids, proteins, glucose urea and lactate) and inorganic (e.g. sodium, potassium, calcium, ammonia, chlorine, iron and other trace metals) compounds. Lipid content has also been reported in eccrine secretions; however, separating their origin from sebaceous or epidermal contamination is difficult [27]. The relative concentrations of amino acids and proteins are of great importance to

fingermark development techniques and a significant quantity of literature exists on the subject [33,36-39]. The most abundant amino acid in sweat is serine, followed by glycine, orthinine, alanine and a selection of others [27]. A number of studies have effectively shown how inter-donor variations and post-deposition conditions can influence the content of amino acids and other eccrine constituents [36,37]. For example, Croxton *et al.* (2010) [36] found significant amino acid differences with gender, age and diet (vegetarian vs. omnivorous), and an earlier study by Cuthbertson (1969) [37] showed how the concentration of chlorides can vary with age, sex and the porosity of the deposition substrate. Several miscellaneous compounds, including drugs, ethanol, immunoglobulins and enzymes have also been demonstrated in eccrine secretions [27]. Apocrine sweat producing glands are larger and far less abundant than their eccrine counterparts and they are primarily found in association with the follicles of coarse hair in armpit and pubic regions [28]. The presence of apocrine secretions in latent fingermark residue relies on prior digital contact with these areas of skin and the exact characterisation of which is heavily complicated by eccrine and sebaceous contamination. As such, very little literature is available on the contribution of apocrine secretions in latent fingermarks, although certain compounds have been isolated (proteins, carbohydrates, cholesterol and iron) [40].

Sebaceous glands are also generally associated with hair follicles and empty via hair shaft canals, however, unlike apocrine glands they are found all over the body (except volar regions), with a particular abundance in the face and scalp [28]. This results from a primary function of sebaceous secretions, which is to prevent hairs and skin becoming dry and brittle, and because of certain habitual human behaviours (touching of the face and passing of hands through hair) the contents are usually abundant in natural latent fingermarks [27,28]. Sebaceous are an example of holocrine glands, which produce their secretions in cell cytoplasm and deposit them through plasma membrane rupture [28]. In sebaceous glands this is a mixture of lipid based materials (glycerides, fatty acids, wax esters, cholesterol esters, cholesterol and squalene) collectively known as sebum. The composition of sebum is highly susceptible to post-deposition and even post-secretion changes, whereby a number of the initial main constituents are some form of secondary derivative and considerable

breakdown/transformation follows [34]. For example, free fatty acids, which can account for up to 30% of sebum, are produced from the hydrolysis of triglycerides and wax esters. The concentration of squalene has also been shown to be very unstable, with large percentages lost within hours of deposition [41]. Clearly then, time is a critical factor when sebum content is considered in relation to development technique effectiveness, and variations with gender and diet have also been demonstrated [27,36]. However, even more significant are variations in sebum composition that occur with donor age. At the various stages of human development, from newborn and infant to adolescent and post-adolescent, a number of sebum components (e.g. fatty acids, triglycerides, wax esters and cholesterol) alter significantly with regard to their percentage contribution [34]. It has even been suggested, based extrapolation from such data, that chemical analysis of latent fingerprint residues could be a useful biometric gauge for the age of the donor [42].

### **1.3 Latent fingerprint development**

The use of the term ‘latent’ to describe a fingerprint refers to its present state as invisible and the potential for visualisation. Development with some form of physical, chemical or illuminating reaction is required to realise this potential and achieve visualisation. Typically the techniques devised for development have been targeted towards a specific component of the latent fingerprint and it is through detailed understanding of variable biochemical composition that new techniques have evolved and operational choices are made. The content and quality of a latent fingerprint is determined at three stages of deposition: pre, mid and post [34]. Pre-deposition factors are solely influenced by donor conditions (age, sex, diet, lifestyle, etc.) and are very difficult to account for when development is for identification purposes. Mid-deposition factors refer to contact dynamics and the surface properties such as texture, shape and topography. The effect on print quality of contact conditions such as pressure applied and lateral movement during deposition will only be revealed following development, however, evaluation of surface roughness is often important for development choice [8,9,34]. Similarly, the effects of certain post-deposition factors, such as ambient temperature, exposure to water, environmental

contamination, surface chemistry and surface porosity can potentially be anticipated for the optimisation of development effectiveness [30,34].

### *1.3.1 Surface porosity*

Understanding surface porosity is particularly important for development technique choice because it can strongly determine, in a predictable way, what components of the fingerprint are available for interaction as a function of time and environmental conditions [30]. As described in chapter 1.2, fingerprint residue is a water- and lipid-soluble emulsion, which will behave in a characteristic fashion based on how absorbent the substrate is. Also, certain techniques, based on their mode of action, are only suitable for substrates with certain characteristics. For example, a water based technique may physically compromise a surface such as paper. With regard to fingerprint development, surfaces are commonly placed in one of three groups: porous, non-porous and semi-porous [30].

Porous surfaces, such as paper, cardboard and wood, are defined by the rapid absorption of fingerprint residues following deposition. Water-soluble components such as amino acids, urea and chlorides are consumed within seconds and as water evaporates these are left within the surface (Fig. 1.7) [30]. The depth of penetration depends on the level of porosity and the relative size of each constituent, for example most amino acids are larger than urea molecules and will therefore generally penetrate less. Environmental conditions such as relative humidity and temperature will also affect the extent of this initial penetration and as the fingerprint ages these will continue to have a bearing on any further migration [30]. Water-soluble components can remain in the surface for long periods of time as they are protected from mechanical stress, and techniques which target amino acids are particularly effective since their migration is limited, however, any exposure to water will remove this potential for development [34]. Lipid-soluble components remain on the surface of porous substrates for a significantly longer period; most for up to a day and a small amount for extended periods (i.e. many years) [30]. Sensitive techniques like ninhydrin have been shown to develop the small quantities of remaining surface residue on marks as old as 15 years [43]. Any lipid-soluble components that are not

absorbed into the surface can easily be removed by mechanical stress and increases in ambient temperature speeds up their migration and hence diffusion..

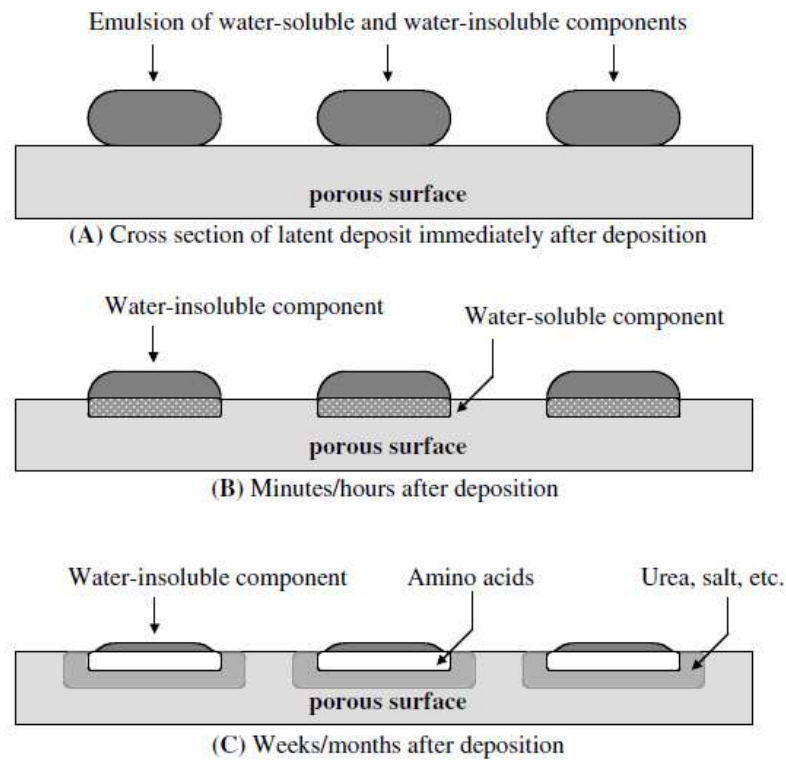


Figure 1.7 – A cross-sectional representation of the aging of a fingerprint following deposition on a porous substrate. (Source: Champod *et al.* (2004) [30])

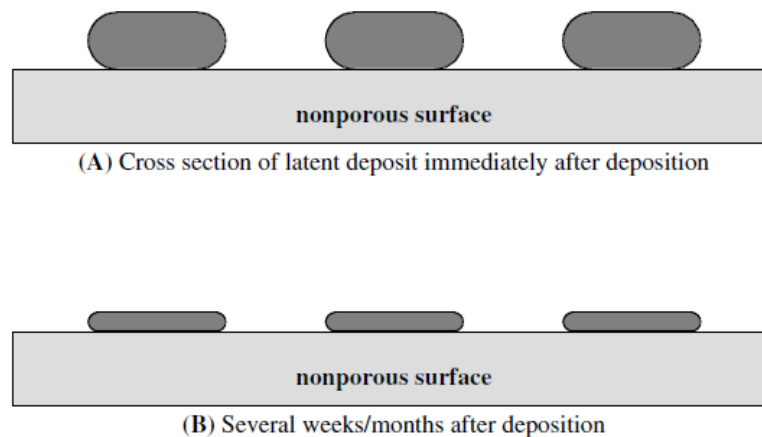


Figure 1.8 – A cross-sectional representation of the aging of a fingerprint following deposition on a non-porous substrate. (Source: Champod *et al.* (2004) [30])



In contrast, a non-porous surface is defined as such if it does not absorb any component of the fingerprint residue. Typical examples include plastics, glass and metallic surfaces. Since the fingerprint remains as a complete emulsion on the substrate surface, both water- and lipid-soluble components can be available indefinitely until they evaporate or degrade (Fig 1.8) [30]. However, being entirely on the surface means greater exposure to degradation in the form mechanical stress and environmental weathering; the effects of which are both compounded as water evaporates and the fingerprint dries out. Exposure to water and organic solvents will also remove water-soluble and lipid-soluble components respectively [30]. The final classification, semi-porous, is used for surfaces which fall somewhere in between porous and non-porous. Banknotes and magazine covers are prime examples of semi-porous substrates, which will tend to absorb water-soluble components at a slower rate than porous substrates [30,34]. The bulk of the lipid-soluble residue will remain on the surface for significantly longer than on porous surfaces (i.e. several days) and, similarly, a small developable amount will endure for extended periods [30].

### *1.3.2 Optical techniques*

Optical techniques utilise some form of light source for the visualisation of latent fingerprints, which can then be documented by photography [30]. As such they are non-destructive and can always be followed by additional techniques if sufficient detail is not revealed. Techniques range from simple white light exposure to more complicated methods for absorption, emission and diffused reflection of light [30]. As with most development techniques, the key is providing contrast between the print and the substrate background. Development of bloodied fingerprints is a common absorption based technique since a characteristic of dried blood is the strong absorption of light at a wavelength of 415nm [44]. For clear development the background surface must sufficiently reflect light at this wavelength to provide contrast. Diffused reflection techniques, which expose fingerprint heterogeneity on shiny surfaces (e.g. metal, plastic, glass, etc.), are also geared for producing contrast (light ridges against a dark background and vice versa) [45]. Ultraviolet (UV) light sources are another part of the electromagnetic spectrum that have been used for latent visualisation and these techniques essentially rely on a combination of absorption and diffuse reflection [30,46]. Other methods for fluorescence (light emission through

electromagnetic radiation) of fingermarks include high intensity single-wavelength light sources, or lasers [47]. Laser based development and optical techniques in general are typically more useful for augmenting the visualisation of a physical or chemical technique; however, due to their passive nature a development sequence for any latent fingermark should begin with an optical examination [30]. Examples of common routine physical and chemical techniques will be discussed in the following sections.

### *1.3.3 Dry & wet powders*

Broadly speaking, physical techniques usually rely on some form of particulate adhesion or deposition onto the latent fingermark residue. The classic example, powder dusting, is one of the oldest and most consistent of any kind of technique [48]. Powders have been used to develop fingermarks for over a century and during this period a great number of formulas have been developed, which follow the general blueprint of a pigment component (e.g. metal oxides, sulphates and carbonates) for contrast and a resinous component (e.g. rosin, corn starch and gum arabic) for adhesion to moist and oily fingermark residues [34]. Powder application is through dusting with a fine haired brush made from synthetic, natural or glass fibres; a method which is simple yet potentially destructive to fragile marks. Variations on the traditional model have included fluorescent powders, which are useful on surfaces where contrast is an issue, and magnetic powders, which are applied with a magnetic wand, eliminating the possibility of brushing destruction [30]. Powder dusting methods are most effective on smooth, non-porous substrates and despite the longevity as a technique, these are now typically restricted to surfaces that cannot be removed from a crime scene for more sensitive laboratory development [30].

More recently, the use of wet powder techniques have become increasingly popular for development on non-porous surfaces [12,49,50]. These consist of a fine insoluble powder suspended in an aqueous surfactant and the primary advantage of such a system is that the pre-wetting of a surface does not preclude development. The term small-particle reagent (SPR) is often used to collectively describe all powder suspension techniques [30]; however, there are a number of key differences between the standard molybdenum disulphide SPR and other wet powder suspensions. While

both techniques use a detergent, such as Kodak Photo-Flo, to help maintain the suspension, SPR uses a much lower detergent concentration in the final solution, which also has a far higher detergent to powder ratio [8,51]. For example, a typical SPR working solution may comprise a concentration solution (500ml water, 7.5ml 10% surfactant and 50g MoS<sub>2</sub>) mixed with 4.5 litres of water, whereas a typical wet powder suspension working solution may comprise 20g iron oxide, 100ml water and 20ml stock detergent solution (250ml surfactant, 350ml ethylene glycol and 400ml water). Additionally, SPR application is through a dipping procedure or spraying, whereas wet powder suspensions are typically made to a paste consistency and brushed onto the deposition surface [8]. The use of conventional powders in suspensions originated as an effective alternative to Sticky-side Powder™ for developing fingerprints on the adhesive side of tapes [51,52]. Contrast is achieved by suspending powders of different colours, such as carbon (black) and titanium dioxide (white) and this is an advantage over standard SPR, which is limited to the dark grey colour of molybdenum disulphide. The exact mechanisms behind how fine powders in suspension adhere to sebaceous fingerprint residues is still unclear, however, certain physical properties of the powder (size, structure and coating) have been shown to influence development efficacy [53].

#### *1.3.4 Physical developer & multi-metal deposition*

The utilisation of metal ion deposition for developing latent fingerprints has proved a very sensitive and versatile option since two techniques were successfully adapted from their original purposes in the late 60's and early 70's [30]. Physical developer (PD) is modified from a technique for developing photographic films in which silver ions (Ag<sup>+</sup>) are the active component. PD works preferentially on porous surfaces and, like powder suspensions, it is a water based technique that develops lipid-soluble fingerprint components, thereby being particularly useful for wetted porous surfaces [30]. The aqueous solution also includes ferrous ions (Fe<sup>2+</sup>) to reduce the silver ions to silver metal (Ag<sup>0</sup>), ferric (Fe<sup>3+</sup>) ions to prevent the formation of colloidal silver from the reduced ions and solution stabilisers in the form of citric acid and a surfactant [30,34]. Silver slowly deposits on the fingerprint residue as the sample is soaked in PD solution and ridges are left as dark grey against a light grey background, the preferential nature of this process is not fully understood [30]. Multi-metal deposition

(MMD), originating almost 20 years later, is a derivative of PD that involves pre-immersion of the sample in a colloidal gold solution followed by treatment with a modified PD solution [48]. The negatively charged gold particles deposit on organic residues with positive functional groups and then contrast is greatly improved by the subsequent PD step [48].

### 1.3.5 Vacuum metal deposition

Selective deposition of evaporated metals under a vacuum to create contrast between fingerprint marks and deposition surfaces was first described in 1968 [54]. The process, referred to as vacuum metal deposition (VMD), works on the basis that an initial gold layer deposits uniformly across the sample surface, including penetration into fingerprint ridges. This leaves exposed gold only in off-ridge and background areas and so the second evaporation with a metal (e.g. zinc), which preferentially deposits on gold, produces the desired contrast (Fig. 1.9) [30]. Normal VMD is an example of negative development, whereby the undeveloped areas represent fingerprint detail, however, a well documented reverse development phenomenon that results in the opposite occurring has been a continued source of intrigue for researchers [11,55,56]. The influence of surface type has been shown to have a significant effect on reverse development [11,55] and this is indicative of how post-deposition factors can be interpreted for improved development choices. VMD is typically used for non-porous substrates and has been shown to work well in combination with cyanoacrylate fuming [56,57]. Due to cost issues the technique is generally reserved for high profile investigations, although the high level of sensitivity that can be achieved is also often beneficial for otherwise difficult substrates, such as banknotes [30].

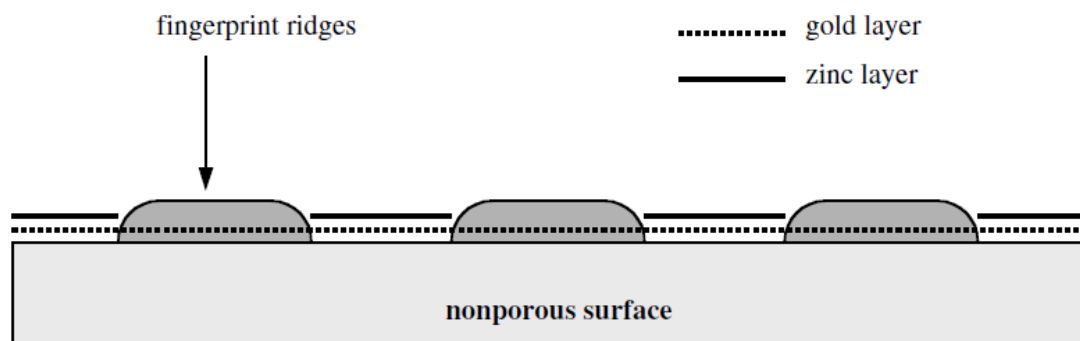


Figure 1.9 – A cross-sectional representation of the physical processes involved with normal VMD development. (Source: Champod *et al.* (2004) [30])

### 1.3.6 Ninhydrin

Chemical reagents that react with specific components of fingerprint residues have been manipulated and utilised to visualise latent fingerprints for a number of decades. A prime example is a compound called ninhydrin, which in the early part of the 20<sup>th</sup> century was shown to form a dark purple product (Ruhemann's purple) in the presence of primary and secondary amides (e.g. amino acids and proteins), and has been used to develop fingerprints since 1954 [58]. Ninhydrin reacts indiscriminately with amino acids and since these eccrine deposits remain relatively stable in porous surfaces the technique has become very popular for such substrates, particularly with very old marks [30]. The compound can be applied by dipping, spraying or brushing after being prepared in a solution with acetic acid (for optimum pH conditions) and various stabilising and carrier solvents [30]. In optimum conditions (i.e. sufficient amide availability, contrasting background and minimal background reaction) the technique is very effective, however, these are rarely present operationally and so a great number of ninhydrin analogues and contrast enhancement steps have been proposed since the compound was first used for fingerprint development [59]. One common alternative to ninhydrin is the compound diazafluorenone (DFO), which has an advantage of greater sensitivity through the strong room temperature luminescence of its reaction product without the need for any further treatment [59]. Though DFO is not a direct analogue of ninhydrin, it is functionally similar and because it is also more selective, the two techniques are commonly used in combination to good effect on porous surfaces [34].

### 1.3.7 Cyanoacrylate fuming

A widely used chemical technique for non-porous surfaces involves the selective polymerisation of cyanoacrylate (CA) ester monomers (i.e. superglue) on fingerprint residues. The process, which was conceived by the Japanese National Police Agency in 1978, typically requires an isolated and controlled environment (or fuming chamber) for application and involves heat induced vaporisation of CA liquid in the presence of the deposition surface [48]. These conditions result in initialisation and spread of solid white polycyanoacrylate across the fingerprint. A fuming chamber can be improvised from any sealed environment with a heat source; however, relative humidity has been reported to be important in development effectiveness, so specially

built commercial units that can finely control environmental conditions are preferred for forensic applications [30,60]. On surfaces where the white coloured development product presents a contrast issue, marks can be enhanced with an optical technique or stained with a coloured or luminescent dye before optical enhancement. The exact fingerprint components required to initiate CA polymerisation and then carry out good quality development are still poorly understood [34,60,61]. For example, microscopic morphology of the polymerised structures has been shown to differ with fingerprint type (sebaceous or eccrine) and age, which in turn influences visualisation of the polymerised ridges [60,62]. Rather than single component involvement, this suggests a complex process with multiple physical and chemical dependant steps [60-63]. CA development is also generally less effective on fingerprints over 2 weeks old and this is one reason why water is frequently cited as a critical component for initiation, however, studies have shown that amines and carboxylic acid alone are sufficient for polymerisation to occur [61].

#### *1.3.8 Development sequencing*

A systematic approach to fingerprint development is vital to ensure the maximum quantity and quality of evidence is acquired from each exhibit. This includes consideration for any further forensic examinations that may be required. For example, bloodied fingerprints are often a crucial source of DNA and any technique applied to firearms should not preclude subsequent gun shot residue analysis [30]. In the UK, development protocol tables offering guidelines as to the optimum technique sequence for a given situation are issued to police forces by the Home Office. Primarily these are based around three fundamental surface properties (material type, porosity and texture) and any knowledge of fingerprint exposure to water, or they deal directly with certain exceptional surfaces and conditions (adhesive surfaces, bloodied surfaces, human skin, firearms, etc.) [8]. Once these assessments are made protocols then function to recommend a development technique sequence that is likely to be the most efficient and effective for those conditions. As described earlier, all examinations begin with an optical development attempt since all other techniques can follow. Subsequently, if optical development is unsuccessful, a single technique can be sufficient for development or a combination of techniques in the correct order may be required. PD, for instance, is always applied at the end of a porous surface

sequence since it is complimentary to DFO/ninhydrin and no techniques are known to be effective after PD application [30].

It is important to recognise that protocol tables are only a guideline, and successful development is largely dependent on the skills and experience of the examiner. For example, judgements with regard to the age of a mark can often influence development technique selection. CA fuming is generally preferred for fresh marks (less than 2 weeks old) on non-porous surfaces, while powder suspensions can be successfully applied in situations where the mark is older [34]. Also, ordinarily optimum techniques can sometimes suffer the effects of subtle surfaces variations within protocol classification. One clear example of this is ninhydrin development on banknotes. The more effective techniques for porous (ninhydrin, DFO, etc.) and non-porous (CA, VMD, etc.) surfaces are typically applied to specific semi-porous surfaces based on prior knowledge and research [8,30]. Ninhydrin can be a very effective technique for banknote development; however some types of banknote paper are known to react in a similar way to amino acids with the reagent, causing complete destruction of any fingerprint evidence [30]. Such experience is built up from macroscopic observations and caution is subsequently taken for development in those specific circumstances. However, understanding the cause of, and mechanisms behind why certain similar surfaces (e.g. different types of banknote) behave differently following the same development treatment remains important for several reasons, including anticipation of related issues with other surfaces, improvement of protocol choices and development of more effective techniques. Research at micro- and nanoscopic scales is being successfully utilised for these purposes. Continuing with the banknote example, Azoury and colleagues (2004) [10] conducted a detailed examination of two sets of counterfeit US \$100 bills, one of which responded positively to the routine application of amino acid sensitive techniques and the other negatively. It was discovered that differences in surface free energy between the two sets of notes contributed heavily towards their development disparity and the report concludes that thorough investigations of paper properties should be performed prior to fingermark development in high profile cases [10].

## **1.4 Summary & research objectives**

Latent fingermarks are an invaluable source of evidence for police agencies across the world and this is based on their inherent ability to provide human individualisation and identification. This ability is underpinned by two particular properties of friction ridge skin patterns, uniqueness and permanence, which have been recognised and utilised for well over 100 years. During this period the level of knowledge relating to the composition of fingermark residue and targeting of development agents towards specific components has steadily evolved, such that a large number of highly effective techniques are now available to examiners for the purpose of visualising and recording latent marks. Despite these advances, an enormous amount of potential variable factors that can influence development mean no technique is universally effective and protocol specificity with regard to substrate classification remains a major issue [8-12]. The negative effects of subtle variations in surface properties (chemistry, physics and topography) that exist between members of the same classification have been shown in a diverse range of studies [10-12,55,64]. Such attempts to develop an understanding of the three way interaction between development agents, fingermark residues and deposition surfaces are important for enhancing protocol specificity and ultimately increasing the efficiency of the entire fingerprinting process. Furthermore, any improvements to technique and protocol that result from empirical scientific research are more likely to build confidence in the validity of fingerprint evidence within an environment of unprecedented social scrutiny towards criminal forensics.

This project focuses around an operationally relevant subset of ‘CAST’ polymers. Formica, polyethylene (PE) and unplasticised polyvinyl chloride (uPVC) are all classified under current development protocols as smooth, non-porous plastics and have recently been reported to exhibit significantly varied development effectiveness with iron oxide powder suspension based on micro- and nanoscale differences in surface topography [12]. This work will centre on the effects linear topographic surface features on CA development, as well as how the chemistry of polymer additives can also selectively influence the usefulness of routine techniques. Through direct collaboration with the Centre for Applied Science and Technology (CAST, part



of the UK Home Office) it is hoped that any significant observations can help inform protocol refinements that will more accurately represent development efficiency dependant surface properties. A number of high resolution imaging and powerful analytical tools will be applied to the three CAST surfaces and any additional relevant surfaces in order to achieve the levels of sensitivity and specificity required for such mechanistic investigations. The principles of each of these techniques and their respective merit for this approach to fingerprint development research will be discussed in the following chapter.

**IMAGING & ANALYSIS****2****2.1 Scanning electron microscopy (SEM)**

SEM technology represents one of the most powerful characterisation tools available to any field of scientific research or industry today. The use of an electron beam for imaging purposes was born out of a fundamental limitation of light microscopy and the natural human inclination towards deeper levels of understanding. As first described by the German physicist Ernst Abbe in 1873, the relationship between the resolving power of a microscope and the wavelength of its illuminating source can be written as follows

$$d = \frac{0.612\lambda}{n \sin \alpha},$$

where  $d$  is the resolution,  $\lambda$  is the wavelength of the illuminating source and  $n \sin \alpha$  collectively represents the numerical aperture or light collecting capability of the optical lens [65]. Given that the wavelength of light is between 400 and 700nm, the resolving power of a conventional light microscope is limited by the manufacturing quality of the lens to a maximum of ~200nm, which restricts magnification to below x2000. Higher resolving power requires smaller wavelengths and the discovery that negatively charged electrons can be accelerated through large potential differences for increasingly smaller wavelengths, as described by

$$\lambda = \frac{1.22}{\sqrt{V}},$$

led to the development of the first electron microscopes during the 1930's [65]. These original instruments were transmission electron microscopes (TEM), which are designed to produce images based on information contained in the electron beam once it has passed through a sample. However, by nature this technique requires samples that are thin enough to transmit an electron beam and is therefore restricted to sectional based imaging. The development of commercial SEM technology around 30 years later, which images a sample surface by probing it with the electron beam in a

raster motion and analysing the products of beam-sample interactions, has allowed for far more diverse applications of electron microscopy.

### 2.1.1 Instrumentation

Figure 2.1 is a schematic representation of a standard SEM setup featuring two main areas, the electron column and specimen chamber [66]. The electron beam source or electron gun is situated at the top of the electron column, in modern SEM systems these are typically either thermionic or field emission guns [67]. Two common examples of thermionic emission guns, which vary based on the cathode electron source, are tungsten filament and lanthanum hexaboride. Electron emission is achieved by heating the cathode filament to provide enough kinetic energy for electrons to escape [65]. Lanthanum hexaboride sources are more widely used since they have a lower work function than tungsten filaments, which means less kinetic energy is required for emission and results in a longer cathode lifespan [68]. Field emission guns produce very high intensity beams without the need for any thermal input [67]. This is achieved by passing a high electric field through the source (e.g. sharp tungsten crystal) and results in a beam that is not only brighter than thermionic guns, but has more stable emission and can be focused into smaller spot sizes for higher resolution [67,69]. The drawback with field emission beams compared to the thermionic kind is a higher sensitivity to atmospheric ions and therefore a specialised high vacuum instrument environment is required.

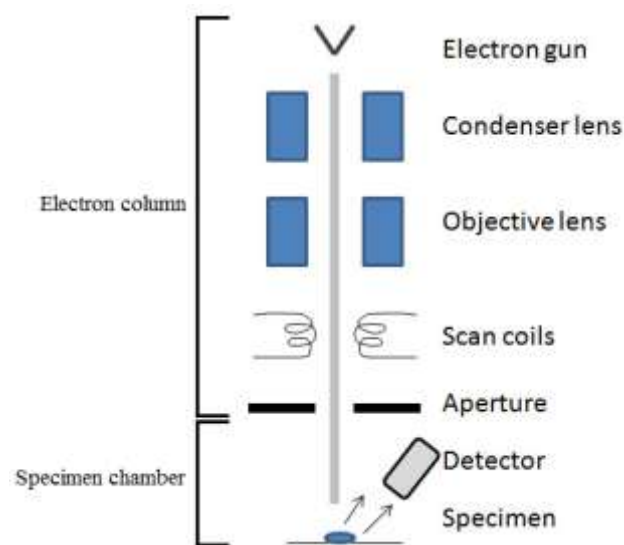


Figure 2.1 – A schematic representation of a typical SEM setup, including features within the two main areas: the electron column and specimen chamber. (Source: cnx.org [66])

Once the beam has left the source it travels down the electron column on an optical path determined by a number of electromagnetic lenses. These consist of two condenser lenses, which demagnify the beam, and an objective lens to focus it down to the final probe spot size [67]. The lenses function by selectively deflecting the electron beam based on changes in their magnetic field across the column. This effectively creates variable focal lengths for each lens that on modern systems are digitally controlled by the SEM software to bring the beam into focus on the sample [65]. Before reaching the sample, the electrons pass through a final aperture, which can be adjusted to limit any beam divergence. Within the objective lens are two pairs of scanning coils that provide the deflection system to achieve a raster scanning motion of the beam over the sample surface [67]. At each point of scan the signal emitted by the sample is collected by a detector, amplified, and used to create the image. These points directly correlate with picture points on the monitor screen and SEM magnification is therefore determined by the ratio of this linear size to the linear size of the scan area [67].

The specimen chamber houses a stage on which samples are mounted and typically this has remote XYZ-tilt-rotation operations to provide a comprehensive range of sample movement. Whereas the entire electron column area must be constantly kept under high vacuum conditions to ensure beam stability, systems equipped with variable pressure (VP) technology are compartmentalised and can allow for controlled leaking of gases (e.g. nitrogen) into the specimen chamber [69]. For principle imaging modes the specimen chamber is also kept under high vacuum and non-conducting samples must be coated with a thin layer of a conductive metal (e.g. gold or platinum) to avoid negative charging induced damage. This type of preparation may conceal relevant surface detail or preclude subsequent analysis of the sample; by creating a VP environment, which causes gas-beam interactions and produces neutralising positive ions, non-conducting samples may also be imaged without the need for pre-coating treatment. Unless imaging with VP or a similar environmental SEM, all samples must be free from moisture and stable enough to cope with the hostilities of vacuum conditions before SEM imaging.

### 2.1.2 Image generation

The versatility of SEM comes from the variety of signals produced following sample-beam interaction. These include primary backscattered electrons (BSE) and secondary electrons (SE) for the two principle imaging modes, and a number of other characteristic emissions (Fig. 2.2a) [65]. Each type of interaction occurs at regular distributions within the sample surface (Fig. 2.2b). The depth, area and amount (or coefficient) of emission at each probe site are influenced by the incident beam accelerating voltage, which usually ranges from 1-40kV [67]. BSE emission occurs when negatively charged electrons from the incident beam enter close proximity to positively charged atomic nuclei of the sample without colliding and are deflected back out of the surface [70]. This is an example of elastic scattering, since a significant amount of electron energy is retained [65]. Inelastic scattering, where kinetic energy is not conserved, describes SE emission. Here the incident electrons collide with, and dislodge loosely bound electrons from sample atoms [71]. The ejected SEs are substantially lower in energy than the incident electrons and can therefore only escape from close to the surface [67].

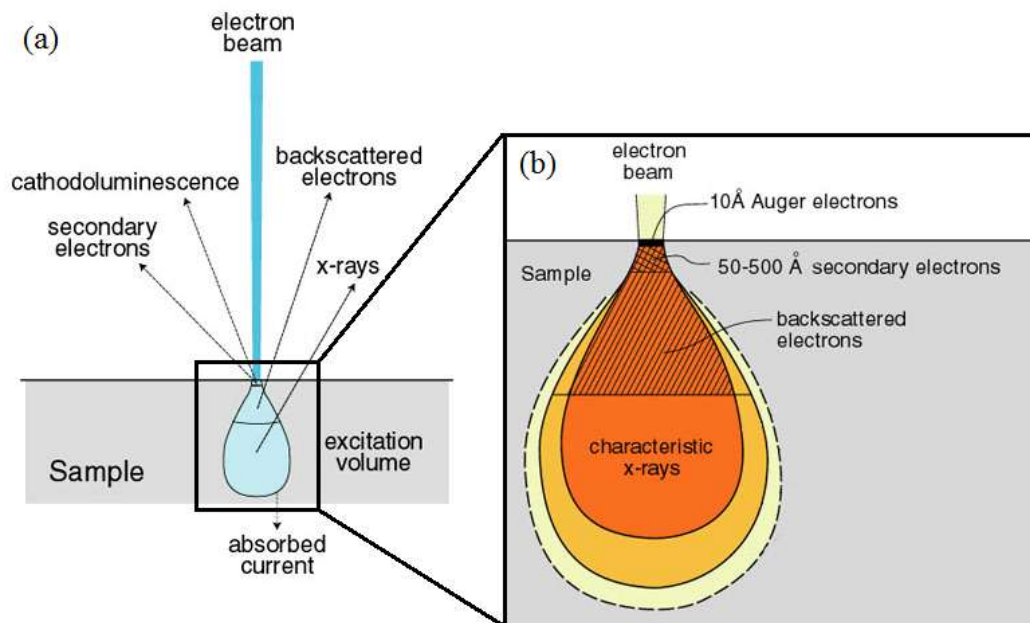


Figure 2.2 – Emission signals and their distribution following electron beam-sample interaction. (Adapted from source: nau.edu [104])

The most common type of electron detector in SEM systems is the Everhart-Thornley (E-T) scintillator detector. Its main function is to attract low energy SEs to a positively charged collector grid (+250V) and accelerate them through a scintillator potential difference of between +10 and +15kV for conversion into detectable photons [67]. E-T detectors can be selectively biased towards BSE collection by reducing the collector grid voltage to a negative potential (-50V) and repelling low energy SEs, although most modern systems are equipped with independent specialised BSE detectors.

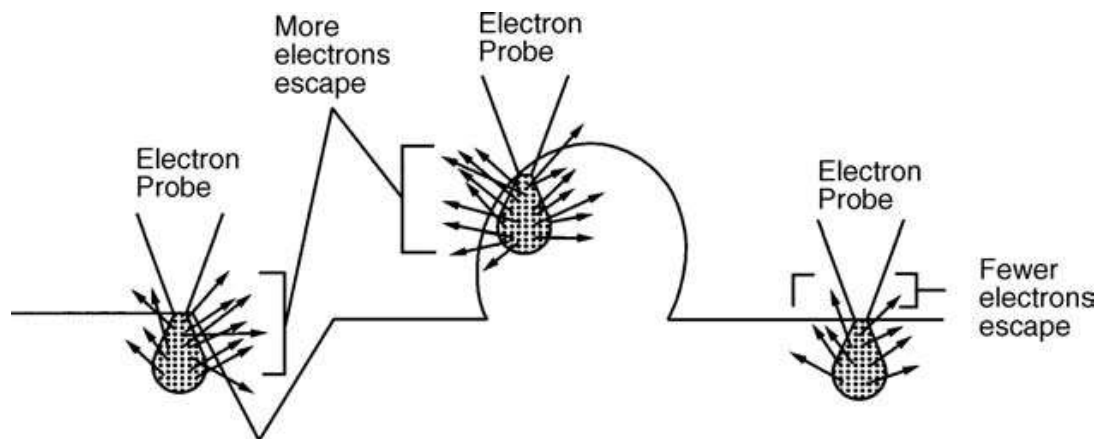


Figure 2.3 – The effects of surface topography and tilt angle on the surface area available for electron emission. (Source: Leng 2008 [67])

### 2.1.3 Contrast & resolution

Primary sources of contrast for SEM imaging are topographic and compositional (atomic number). Variations in these features across the surface will quantitatively affect how the beam interacts with the sample, which is displayed in the image as signal intensity. For example, as the tilt angle between the incident beam and the sample increases (i.e. with raised or recessed surface features), more surface area for electron emission is available (Fig. 2.3) [67]. Similarly, atomic number ( $Z$ ) will affect the amount of electrons released. SE and BSE emissions both produce topographical and compositional contrast; however, SE is the primary topographic signal due to a high emission coefficient with tilt angle and BSE is the primary compositional signal due to a high emission coefficient with increasing  $Z$  [67].

The two most important SEM attributes are spatial resolution and depth of field. Resolution can be described as the ability to separate two distinct entities and with SEM this is determined by the diameter of the incident beam at the sample contact point [65]. Smaller beam sizes can be achieved with smaller apertures and by reducing the distance between the aperture and the sample (i.e. the working distance (WD)). Theoretically, according to the Abbe solution for resolving power, electrons accelerated to 20kV have the potential to separate structures up to  $\sim 0.005\text{nm}$  apart. In practise, this is limited to  $\sim 1\text{nm}$  by three optical aberrations: chromatic, spherical and astigmatism [67,72]. Depth of field, the range of positions for which sharp sample focus can be maintained, is inherently related to resolution. An SEM image is at its sharpest focus at the crossover point between electrons coming from the extreme sides of the aperture opening, here the beam diameter ( $d$ ) is at its smallest and resolution is optimised (Fig. 2.4) [65]. As the beam moves across raised or recessed areas in the sample,  $d$  increases and resolution is reduced, however, because beam diameter changes ( $\alpha$ ) across these distances are so small, any effects are negligible and even

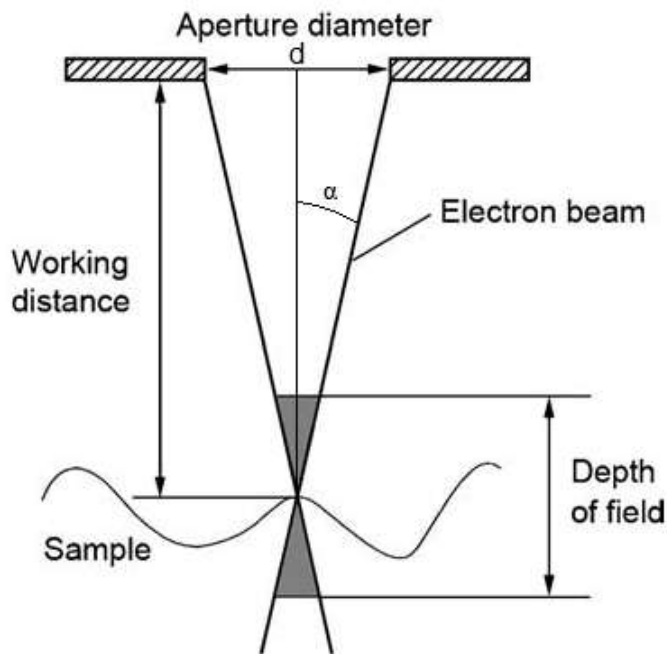


Figure 2.4 – The effects of aperture size and working distance on SEM depth of field. (Adapted from source: Leng (2008) [67])

very rough surfaces can be resolved (Fig. 2.4) [65]. Such depth of field capabilities can be improved by optimising certain operational conditions (e.g. increased WD and decreased aperture size) and they provide a 3-dimensional appearance to SEM images.

#### 2.1.4 Energy dispersive X-ray (EDX) analysis

The final layer of emission shown in figure 2.2b

represents a significant asset for SEM technology. When high energy particles, such as those from the SEM incident beam, collide with and eject electrons from inner atomic shells, those atoms become ionized. In order to quickly return from this excited state back to a stable state, an outer shell electron will fall and fill the vacancy [73]. The energy generated from this transition results in the emission of either a characteristic X-ray photon or a characteristic free electron (Auger electron) [73]. By introducing EDX spectroscopic detectors into the specimen chamber, it is possible to simultaneously image and qualitatively analyse the chemical composition of a sample. The spectral peaks produced represent a chemical fingerprint for the atoms in that area of the sample since each individual shell transition from each element produces X-ray photons with a unique energy and emission coefficient [73]. The qualitative distribution of elements across a selected sample area can also be mapped by point to point EDX analysis.

#### *2.1.5 Applications in dactyloscopy*

SEM is an extremely versatile surface analysis technique and due to the importance of surface characteristics for fingerprint development, applications for research in this field are vast. At the levels of magnification that can be achieved it is possible to directly visualise how development techniques, fingerprints and deposition surfaces are interacting with each other, as well as any external factors. Complimentary EDX analysis also provides compositional information on surfaces and the development agents to help investigate the mechanisms behind any interactions. Examples in the literature have included substrate effects on development [12], environmental effects on development [60,62], effects of technique sequencing [57,74], development agent mode of action [56,60,61], composition of development agent [53,75,76] and new technique efficacy [75,76].

## **2.2 Time-of-flight secondary ion mass spectrometry (ToF-SIMS)**

This technique analyses the mass of secondary ions following bombardment of a sample surface with primary ions for the purpose of chemical characterisation. When energised heavy ions (e.g.  $\text{Ar}^+$ ,  $\text{Cs}^+$ ,  $\text{Ga}^+$  or  $\text{In}^+$ ) impact on a solid surface a large



variety of neutral and charged species are ejected (sputtered) from that surface [69]. These may include atoms, clusters of atoms and molecular fragments, a small proportion of which is ionised during the process and carries an extremely sensitive chemical fingerprint of the sample surface [67]. The origins of modern SIMS technology date a long way back into the 1900s when the effects of ion bombardment were beginning to be experimented with and improved vacuum systems were being developed. Despite this, it took a number of decades for the technique to be regarded with a similar analytical credibility as related techniques, such as Auger electron spectroscopy (AES) and X-ray photoelectron spectroscopy (XPS) [77]. This results from the complex processes involved with sputtering and ionisation of a solid surface, which are enormously changeable based on primary ion choice and sample material type, and are still poorly understood [67,77]. The first commercial SIMS instruments were developed in the 1960s and were based on magnetic sector analysis systems, the original mass spectrometry analysers [67]. These systems were an example of dynamic SIMS, whereby a high flux of primary ion bombardment removes numerous atomic layers from the sample surface for elemental distributions in a depth profile [67]. Static SIMS, which was developed at the end of that decade and uses low flux primary ion bombardment for monolayer compositional analysis, is, by comparison, a non-destructive technique [78]. This method uses time-of-flight mass analysers and comes with two significant surface science advantages: elemental detection sensitivity in the order of parts per million (ppm) and a nominal depth resolution of ~2nm [67].

### *2.2.1 Instrumentation*

An ultra-high vacuum (UHV) environment is required for ToF-SIMS in order to prevent any disturbance to the flight path of secondary ions. Figure 2.5 shows a schematic of the components contained within this UHV environment, which can be divided into the primary ion system and the mass analysis system [67]. At the head of the primary ion system is the source gun, which can take the form of electron bombardment, plasma ion, liquid metal ion or surface ionisation sources [67]. Once the ion beam has been produced and accelerated to the required energy, typically between 3 and 30 kV, it is filtered by mass (Wien filter) and then focused onto the sample surface by a series of electrostatic lenses and two apertures [69]. A deflection system, similar to that found in SEM technology, functions to raster the beam over the

desired scanning area. The positive charging of non-conducting samples is an inherent issue with ion bombardment. To cope with this problem ToF-SIMS instruments are fitted with flood guns that irradiate the insulating sample with electrons, thus preventing the build up of positive charge.

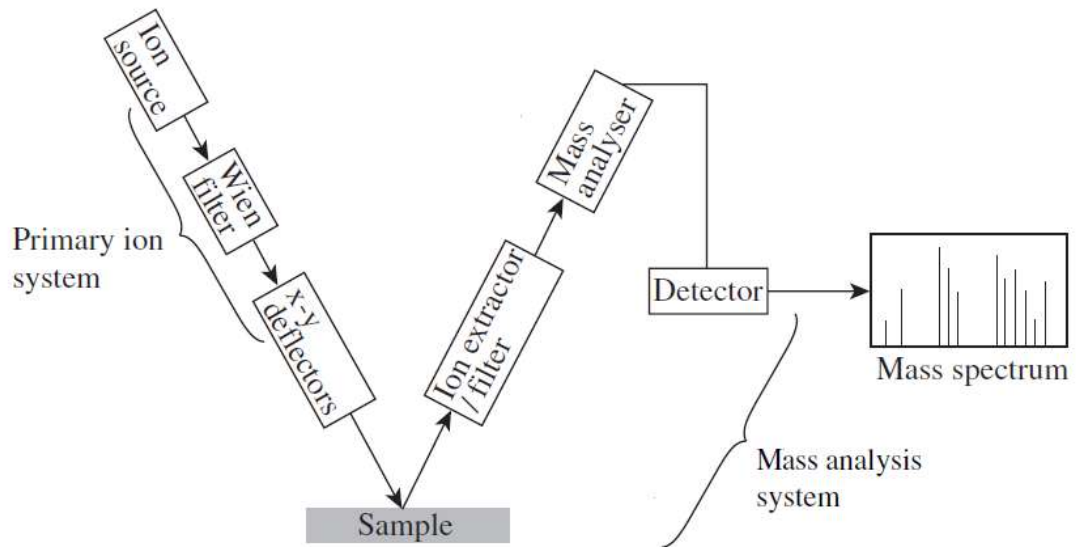


Figure 2.5 – A schematic representation of a typical SIMS setup, including the two main systems: primary ion and mass analysis. (Adapted from source: Leng (2008) [67])

Following beam-sample interaction the secondary ions are collected then separated based on their mass to charge ratio ( $mz^{-1}$ ) and detected to produce a digital spectral signal by the mass analysis system [67]. Secondary ions are immediately removed from the interaction site by an extraction or immersion lens. At this stage the mass range for analysis is determined and scattered primary ion species are removed from the analyte [67]. In modern systems collection can also be biased for positively or negatively charged ions in accordance with user preference. ToF analysers are the most commonly used form of ion separation for static SIMS due to higher levels of sensitivity and mass resolution than other analysers [80]. As the name suggests, this separation is based on the time taken for the ions to travel a particular distance, which increases with mass. Flight time analysis requires a finely tuned pulse period of primary ion bombardment; this can be as short as 0.5ns and allows for the production of the entire mass spectrum simultaneously with ion separation [67]. Mass resolution, or the ability to separate closely related peaks, increases with shorter pulse timing. To account for differences in velocity between secondary ions of the same  $mz^{-1}$ , which

may affect resolution, ToF analysers use a mirror system of wire rings under incrementally increased electric fields to ensure ions of the same  $mz^{-1}$  all arrive at the detector at the same time [67]. Most modern SIMS instruments are equipped with a number of detectors, which function to amplify the ion signal for the electronic conversion of flight time into  $mz^{-1}$  and to ultimately provide spectral output [81].

### 2.2.2 Spectral interpretation

SIMS can detect elements ranging from hydrogen to uranium, as well as distinguish between different isotopes of the same element. The spectrum produced for a particular sample contains numerous peaks from the fragmented sample species and in the absence of calibration standards their intensities are primarily a representation of relative sensitivity to the technique rather than the quantity of a particular species [67]. This sputtering yield is a function of both the sample material (matrix effect) and the primary ion beam properties (type, energy and incident angle) [80]. The highly sensitive nature of ToF-SIMS can be a problem with regard to interpretation of the spectra produced, since information can be obscured by signal abundance [82]. This also relates to the complexity of SIMS yield, which, as described previously, may include atoms, clusters of atoms or molecular fragments and makes quantitative analysis difficult. The high level of sensitivity is an additional consideration in terms of sample handling since even contact with plastic specimen bags can leave detectable contamination on sample surfaces [67]. These and additional environmental contaminants, such as a build up of adventitious carbon, can be removed by sputtering the sample for a period prior to analysis [79]. However, caution with vulnerable samples is required with such preparation methods due to the destructive nature of the sputtering process. Maximising the useful data achieved from ToF-SIMS experimentation relies heavily on a correct choice of operational conditions for the particular investigative circumstances. This may be as simple as selecting for positive/negative secondary ion signal (electronegative elements give intense negative ion peaks and electropositive elements give intense positive ion peaks) or it may require a more complicated trade off between spatial resolution and mass resolution, which are determined by aperture size, pulse method and pulse timing [67,82].

Material chemical composition can be established directly from  $mz^{-1}$  spectral information or by referring to known sources such as a model compound or a SIMS library of spectra [82]. In certain circumstances a peak of interest may overlap with some exogenous component or be out of position due to charging or operational conditions. To ensure accurate conclusions, care should always be taken to calibrate spectra with known or expected peaks, such as those resulting from implanted primary ions. Higher levels of chemical heterogeneity with regard to structure and composition produce increasingly complicated spectra. For example, an inorganic compound such as sodium nitrate may produce ion peaks from unbound associated molecules in addition to fragments of the molecule itself [67]. This will result in a more complicated spectrum than, say a homogenised metallic surface, while still being substantially less complex than those from polymeric substrates [67]. In each case a correct interpretation requires instrumental experience and knowledge of materials.

### 2.2.3 Imaging maps

With the addition of X-Y deflection systems to ToF-SIMS instruments it is possible to raster the primary ion beam over a defined area of the sample surface. An elemental distribution image can then be created by collecting spectra at pre-defined scanning intervals (or pixels) and then selecting one or a combination of  $mz^{-1}$  bands to map. Liquid metal ion sources are able to provide primary ion beams that can be focused to the diameters required for SIMS imaging. Typically this ranges from 200nm to 1 $\mu$ m, with higher spatial resolutions achieved at smaller beam diameters [67]. Reductions in beam diameter also reduce signal intensity and increase noise; however, one way to combat this problem, at the expense of higher scanning times, is to increase the number of scans per pixel or the number of scan frames.

### 2.2.4 Applications in dactyloscopy

The most significant attributes of ToF-SIMS for fingerprint research are its extremely high surface sensitivity and encompassing elemental detection range. Together with mapping capabilities this allows not only detailed compositional information regarding the precise interface at which fingermarks are deposited, but also chemical and imaging analysis of the fingermark itself. One application in particular that takes

advantage of these benefits is the determination of deposition sequence events by ToF-SIMS analysis. It can be of significance, for example in cases of fraud, whether a fingerprint was deposited on a document before or after the written or printed application of ink, since that sequence may establish if an individual had been exposed to its contents or merely handled the blank paper. The extreme surface sensitivity of this technique has been utilised to demonstrate detectable fingerprint ridge signal when deposition occurs after ink application and obscured signal when deposition occurs before ink application [83]. Other notable applications have included the trace detection of contaminants in fingerprints [84,85] and the potential of ToF-SIMS imaging for identification purposes based on visualisation of sufficient minutiae detail [84,85].

### **2.3 Fourier transform infrared (FTIR) spectroscopy**

Molecular analysis by infrared (IR) radiation is the most commonly used type of vibrational spectroscopy. The principle behind this technique relates to inherent bonding properties between atoms and within molecules. These bonds can be thought of as elastic springs that are under constant motion in some form of stretching, bending, twisting, scissoring, rocking or wagging action [65]. The more bonds there are in a molecule, the more complex the patterns of vibration will be, however, each has its own characteristic frequency or wavelength [65]. If an input source of the same wavelength is exposed to a particular bond, the two waves will interfere constructively (i.e. resonate) or destructively, which effectively absorbs the input source in a characteristic fashion. IR radiation has wavelengths that range from 700nm to 1mm, which places it between visible light (380-700nm) and microwaves (1mm-1m) in the electromagnetic spectrum. In terms of wave number or the number of waves per unit distance, 4000 to 400  $\text{cm}^{-1}$  represents the most important analytical range for molecular vibration and this falls squarely within the IR spectrum [65].

The development of FTIR resulted from the limitations of conventional dispersive IR spectroscopy, which separates (or disperses) the output signal into individual frequencies before measurement [86]. Here, the input IR beam must be a continuous

wavelength range containing all of the wave numbers of interest and, following sample interaction, this is separated into its individual frequencies and measured one at a time [65]. A fundamental problem with this system is the time taken measure individual frequencies. With FTIR, however, an interferometer converts the polychromatic input beam into an interference wave (or interferogram) that has every IR frequency encoded within it and can therefore provide information at each wavelength simultaneously [65]. This not only dramatically reduces scanning times, but also introduces more energy to the incident beam, which together result in significantly higher quality spectral output (i.e. higher signal-to-noise ratio) [86].

### 2.3.1 Instrumentation

The basic setup for an interferometer is shown in figure 2.6 and at the heart of its functionality is the moving mirror. The primary IR beam is directed towards the beam splitter, which is designed to transmit half of the radiation and reflect the other half in the direction of the fixed mirror. The transmitted half carries on straight towards the moving mirror, which is in a back and forth motion at a constant velocity [86]. As the beams from the fixed and moving mirrors recombine in the direction of the sample, an interference pattern is created that is a function of the difference between the two optical paths; F and M (Fig. 2.6) [65]. The full range of partial and total beam

interference is achieved both constructively and destructively; as a consequence the interferogram contains the complete range of IR frequencies [86]. Another significant advantage of FTIR instruments over dispersive instruments is the lack of external calibration requirements. Because the velocity of the moving mirror is under the control of a laser

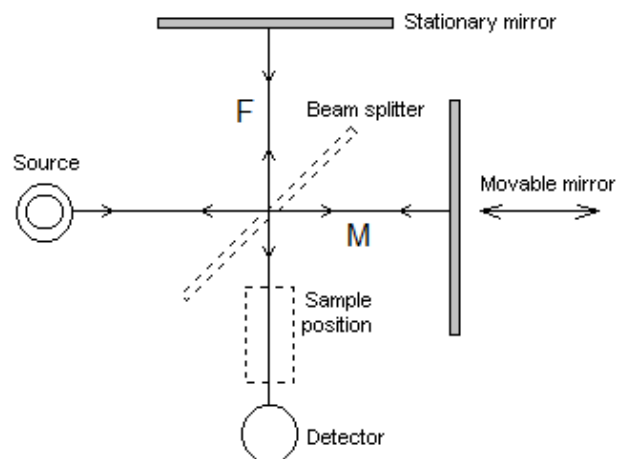


Figure 2.6 – A schematic representation of FTIR interferometer equipment and functionality. (Adapted from source: teaching.shu.ac.uk [105])

with a constant wavelength, all FTIR data can be automatically calibrated to this known value [86].

When the interferogram beam has interacted with (i.e. transmitted through or reflected at) the sample surface, a proportion of its signal has been absorbed and it is the remainder that is detected and converted into a digital spectrum of the sample's molecular composition. There are two types of FTIR detector, thermal and semiconductor, which produce an electric signal from the output IR beam [67]. Thermal detectors, of which deuterated triglycine sulphate (DTGS) is an example, can operate at the entire 4000 to 400  $\text{cm}^{-1}$  range and are simple and inexpensive compared to semiconductor detectors [67]. The most commonly used semiconductor detector is composed of mercury cadmium telluride (MCT); these are more sensitive than DTGS detectors, however, they analyse within a smaller wave number range (4000 to 700  $\text{cm}^{-1}$ ) and require liquid nitrogen cooling to operate [67]. The electrical signal produced following detection requires a mathematical process of decoding, known as Fourier transformation, before it can be interpreted in the form of a spectrum [65]. In modern systems these calculations are performed automatically by the instrument computer.

### 2.3.2 Spectral interpretation & experimental modes

Since the vast majority of FTIR systems are designed to operate in atmospheric conditions, the detected beam signal represents information from the sample and the background. It is always necessary to take a background reading prior to sample analysis using as many, or more scan counts than intended for the sample analysis. This background scan will contain any superfluous information from the instrument hardware and the surrounding environment. It can then be subtracted from any subsequent sample acquisitions by the computer software, provided operational conditions are not altered [67]. The ability to perform in non-vacuum conditions has the significant advantage of sensitivity for volatile compounds. Spectra are initially generated with transmittance (T) intensity plotted on the y-axis against wave number ( $\text{cm}^{-1}$ ) on the x-axis. This produces 'upside down' peaks, which can be converted, again automatically via the computer software, into a traditional looking spectrum of

absorbance (A) against wave number by taking the negative  $\log_{10}$  of each data point [86]. An example of a typical FTIR absorbance spectrum is shown in figure 2.7; subsequent material characterisation is achieved through prior knowledge of characteristic bonding peak locations or by comparing to libraries of known compounds. FTIR is a very powerful analytical technique for organic compounds and certain inorganic compounds, however, it is not able to provide any elemental characterisation and metallic surfaces cannot be analysed in transmittance as they strongly reflect electromagnetic radiation [67].

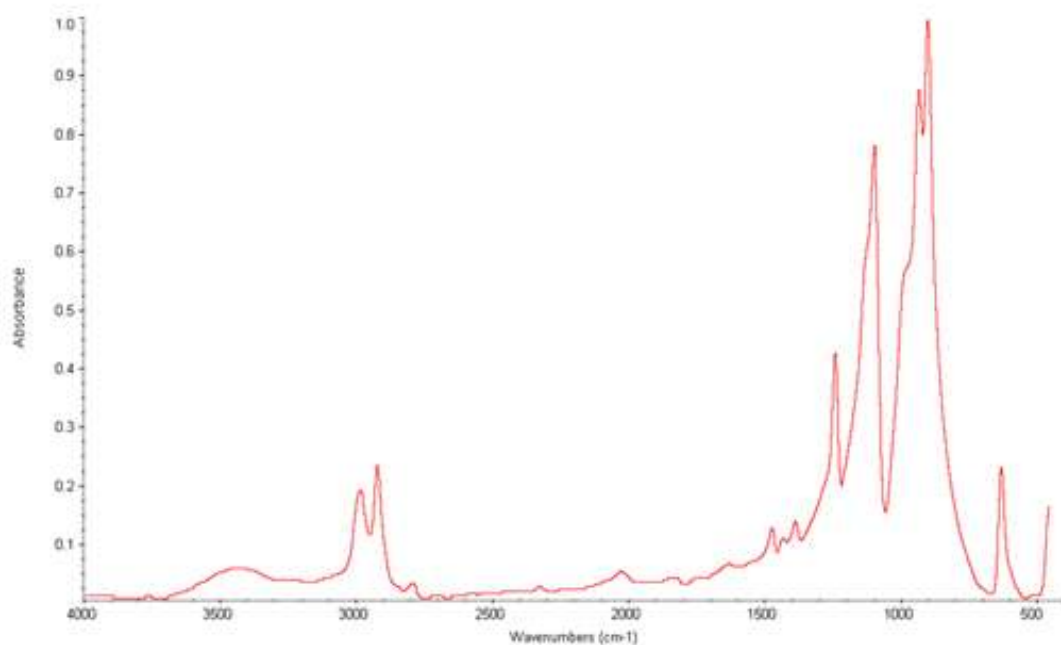


Figure 2.7 – An absorbance FTIR spectrum of polyoxymethylene, an engineering thermoplastic. (Source: semlab.com [106])

The two main FTIR operating modes are transmittance and reflectance. For transmittance the sample specimen must be either IR transparent or thin enough to transmit the IR beam. As a result, any non-IR transparent materials over  $\sim 20\mu\text{m}$  thick cannot be considered for transmittance analysis without some form of sample preparation, since a sufficient signal will not be achieved [67]. Such solid samples are typically prepared into thin films or powders, while liquids and gases can be analysed following encapsulation in specimen cells [67]. Reflectance experimentation is particularly useful for solid samples that cannot easily be ground into a powder or require non-destructive analysis. This method is better suited to very flat surfaces that



can cleanly reflect the incident IR beam; however, specialised optical arrangements can be implemented to collect the diffused reflection from rougher samples [67]. One of the main disadvantages to reflectance spectroscopy is the lack of surface sensitivity resulting from penetration depths of between 1 and 10µm [67]. Additionally, the extra steps required to collect the output IR beam have the effect of reducing signal-to-noise ratio. These limitations can be alleviated by using a separate reflective method known as attenuated total reflectance (ATR). Here the sample (solid, liquid or gas) is placed in contact with an optically dense crystal that has a high refractive index at a certain angle [87]. When the IR source is passed through the crystal an evanescent wave is created that protrudes a small distance (0.5-5µm) above and along its surface [87]. The IR signal is characteristically altered by any material close enough to contact the wave and this signal is significantly amplified across the length of the crystal until it exits towards the detector.

All modes of FTIR experimentation can be augmented through the addition of microscope technology. Micro-FTIR instrumentation can effectively be retrofitted to standard FTIR equipment by introducing a visible light source and allowing for detection from both transmitted and reflected beams [67]. The principles of the technique remain the same for micro-FTIR, however, analysis is at microscopic scales and chemical composition can be spatially resolved by mapping spectra over a scanned area.

### *2.3.3 Applications in dactyloscopy*

Micro-FTIR for imaging and trace detection has the most widespread appeal for fingerprint research; secondary to this is substrate material characterisation applications. In a similar manner to ToF-SIMS mapping, Micro-FTIR has been suggested in a number of publications as a tool for non-invasive development of latent fingerprints due to the potential for highly resolved, minutiae detailed images [88-90]. A major benefit to this type of enhancement is the preservation of trace contaminants such as cosmetics and drugs, which can also be analysed simultaneously [91,92]. Micro-FTIR has been used extensively in combination with research regarding the biochemistry of latent fingerprints, particularly to study the differences between child and adult deposits [93-95]. The potential to extrapolate this type of data back as a

biometric gauge for age has also been reported [42,93]. The operation of micro-FTIR in atmospheric conditions is a significant attribute for the study of latent fingerprints since compositional or morphological changes can be observed in evidential circumstances as a function of time and environmental conditions. For example, it may be prudent to understand the concentrations and breakdown of illegal drugs following deposition to establish if they are an excreted metabolite or have been handled, either directly or through secondary contact. The effects of environmental conditions during certain development techniques (e.g. CA and VMD) can also be investigated.

#### **2.4 Atomic force microscopy (AFM)**

The measurement of atomic forces for surface imaging falls under the more general classification of scanning probe microscopy (SPM), which utilises extremely fine solid probe tips to physically scan or ‘feel’ the surface of a sample and provide an interaction based 3-dimensional profile (topographic, electronic, magnetic, chemical, thermal, etc.) at sub-nanoscale scales [65]. The first AFM instrument was reported in the literature as recently as 1986 by Binnig *et al.* [96]. They introduced the technique as an application for the scanning tunnel microscope (STM) concept, which was designed by the same group just 5 years earlier to measure local electronic properties on conducting surfaces. The first AFM was designed to investigate atomic topography of insulating surfaces by detecting van der Waals interactions; however, it quickly became apparent that the technique would have much more far reaching applications [65,96]. Original AFM technology operated only in contact mode, since then two other commonly used modes (non-contact and intermittent contact) have been developed and an extensive range of secondary imaging modes that utilise varying probe properties and scanning techniques are available to investigate material, chemical and biological samples [97,98]. It is now possible to not only image these samples in ambient, vacuum and liquid environments, but also utilise probes for the structural and functional manipulation of surfaces at an atomic scale [65].

### 2.4.1 Instrumentation

The two most important components in AFM equipment are the probe and the scanner (Fig. 2.8). The probe, which sits on the end of a  $\sim 225\mu\text{m}$  long,  $\sim 38\mu\text{m}$  wide and  $\sim 7\mu\text{m}$  thick flexible cantilever, consists of an extremely sharp, typically silicon-based tip  $\sim 10\text{-}15\mu\text{m}$  in height and is the point of interface with the sample

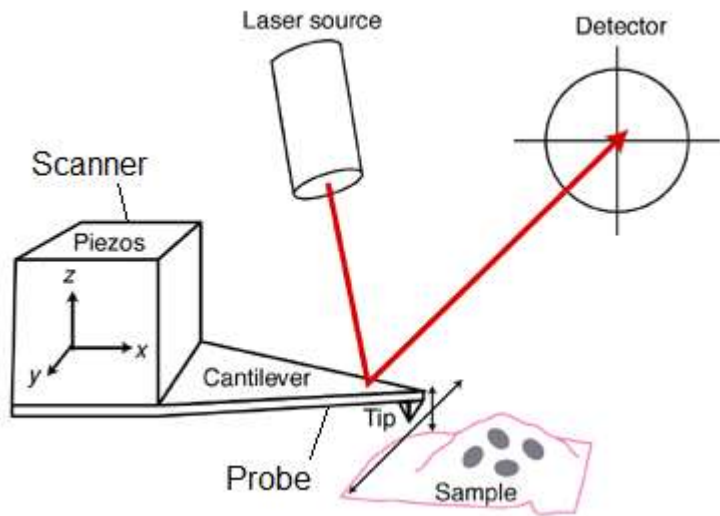


Figure 2.8 – A diagrammatic representation of a typical AFM setup, including the two principal components: probe and scanner. (Source: Petri *et al.* (2000) [107])

[98]. The position of the tip relative to the sample is controlled by a piezoelectric scanner operating laterally ( $x, y$ ) and vertically ( $z$ ). Piezoelectric materials, such as the synthetic ceramics used for AFM, expand or contract when a potential difference (voltage) is applied to them [99]. Such materials are ideally suited for AFM due to the scale of these geometric changes ( $\sim 0.1\text{nm}$  per volt) [99]. Samples are mounted on a stage that has a large range of XYZ movements to cope with macroscopic sized samples, however, the area of surface that can be imaged at any one time is limited by the piezoelectric scanner range to  $\sim 25\mu\text{m}$  vertically and  $\sim 400 \times 400\mu\text{m}$  laterally.

Image formation by the detection of atomic forces and topographic variations is achieved using either an ‘error signal’ or a ‘feedback loop’ [98]. In both cases changes to the position of the tip (i.e. attraction towards/repulsion away from the surface or encountering a topographic feature) or the resonant frequency of its cantilever oscillation, are measured by a laser that is bounced off the back of the tip towards a photodiode detector and this signal is digitally converted into the image. The use of cantilever oscillation detection is dependant on the mode of operation and will be discussed in the following subchapter. An error signal is the measured difference between a predetermined ‘setpoint’ (i.e. sample-tip distance or cantilever oscillating

frequency) and any new tip position caused by sample variations as the tip scans the surface in a raster motion [98]. Conversely, a Z feedback signal is generated by applying a potential difference across the probe and measuring the voltage required to maintain the predetermined setpoint [98]. The Z feedback can be turned on or off at the users preference, with Z feedback off the image is generated by the error signal, which is faster due to the negated need for piezoelectric  $z$  movement, although not practical for rougher surfaces [98]. For standard AFM, which measures at ‘short-range’ distances, van der Waals forces are the dominant interaction [100]. In order to detect such weak forces, the cantilever force constant must be sufficiently low. Modern microscopes have cantilevers with force constants lower than  $0.1 \text{ N m}^{-1}$  and can detect forces in the sub-nanonewton range, which is “...*about 10,000-100,000 times lower than the force of gravity induced by a fly (1 mg) sitting on a surface*” [65]. Such force scales allow for extremely precise measurements, however, they also render AFM instruments sensitive to external vibrations and so the scanning stage must be isolated from the building in which it is housed by some type of dampening system.

The resolutions that can be achieved with standard AFM are dependant on the roughness of the sample surface and the sharpness of the probe tip. These variables have a large effect on lateral resolution capabilities ( $\sim 0.1\text{-}1\text{nm}$ ), whereby rougher surfaces display decreased resolutions due to limitations regarding the tip curvature radius ( $\sim 8\text{nm}$ ) and aspect ratio [65]. Despite sophisticated modern etching techniques that create ultra sharp silicon probes there will always be a degree of rounding at the tip extremity. When the tip encounters surface features that are smaller than the diameter of this curve, their size will either be overestimated or they will be unresolved [65]. These limitations have a negligible effect on the vertical resolution capabilities, which can reach  $0.01\text{nm}$  [65].

#### 2.4.2 Modes of operation

There are three primary modes of operation for conventional AFM: contact, non-contact and intermittent contact. These methods differ primarily in relation to the range at which they operate away from the sample surface; however, each is used to provide highly resolved topographic information in 3-dimensions. A great variety of

additional surface properties can also be imaged using secondary AFM modes; one example is scanning Kelvin probe microscopy (SKPM), which detects changes in the surface potential across a sample and will be discussed here based on its relevance to this project.

*Contact mode* – This is the original and most simple form of AFM, whereby the probe can be considered in perpetual contact with the sample and any changes in topography are directly measured by cantilever deflection [99]. Rather than directly touching the sample surface, however, the tip is generally at a separation distance of  $<0.5\text{nm}$ . At this range the probe is pulled towards a contaminant layer of adsorbed gases that covers solid surfaces in atmospheric conditions and the predominant sample-tip interactions are repulsive van der Waals forces [65,100]. Imaging based directly on cantilever deflection has the advantage of rapid scanning times, however, the level of proximity between the sample and the probe during contact mode can cause a number of issues relating to lateral forces, including sample or tip damage and loss of resolution [99,100].

*Non-contact mode* – In this form of AFM the tip is set to hover at  $\sim 0.5\text{-}1.5\text{nm}$  from the surface and attractive van der Waals forces are the predominant interaction [65]. At this range such forces are so weak that in order to be detected the cantilever is piezoelectrically set to oscillate and image formation is achieved by measuring minute changes to the amplitude, phase or frequency of oscillation that are induced by sample heterogeneities [65]. One major drawback to this method is that closer range van der Waals force detection is required for high resolution imaging and these do not extend beyond the layer of adsorbed gaseous contamination, which can disrupt cantilever oscillation [65]. The use of UHV conditions can significantly enhance non-contact mode imaging; however, these systems are expensive additions to AFM equipment.

*Intermittent contact mode* – Also known as TappingMode<sup>TM</sup>, this method combines the positive aspects of contact and non-contact modes to provide the most versatile and commonly used form of AFM imaging. Here the cantilever is set to oscillate at, or near its resonant frequency [100]. High resolution images are achieved by periodically bringing the vertically oscillating probe into contact with the sample (i.e. tapping).

Because contact is brief and oscillations are of sufficiently high amplitude the likelihood of lateral force damage is dramatically reduced and the influence of adsorbed contaminants is negated [65,99]. Again, image formation is achieved by detecting sample induced changes to the oscillating properties of the cantilever and this can be measured using either the error signal or the Z feedback loop. The ability to simultaneously map cantilever oscillation phase shifts in high resolution with topographic imaging is a powerful tool for intermittent contact mode AFM, which can provide contrast based on other sample properties, such as composition, adhesion, friction and viscoelasticity [67].

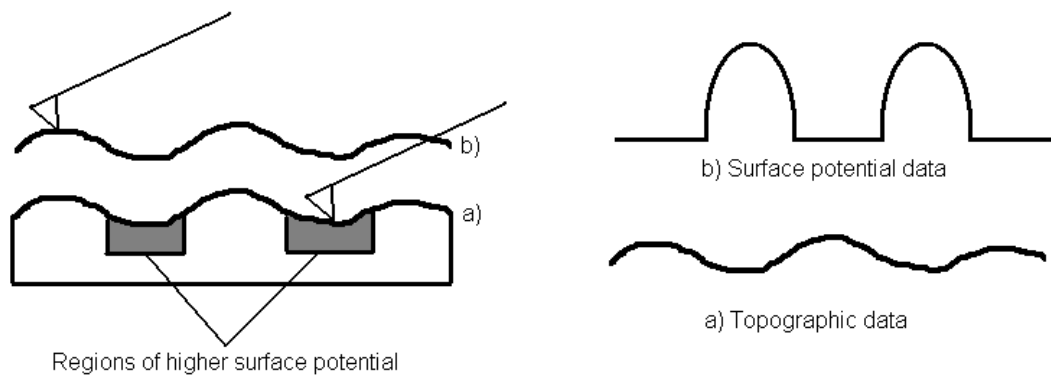


Figure 2.9 – A diagrammatic representation of the detection of variations in sample surface potential by SKPM analysis.

*SKPM* – This secondary method is a derivative of intermittent contact mode AFM that uses specialised conducting tips to map the electrostatic potential across the sample surface [98]. A number of techniques have been designed for producing surface potential sensitive tips, including the removal of native oxides from silicon tips by etching or ion bombardment and the coating of silicon tips with a metal or metal alloy (Au, Cr, Pt/Ir, etc.) [101]. Surface potential images are generated by performing an initial intermittent contact mode AFM retrace scan, followed by raising the probe a set distance (~50nm) and performing a second retrace scan along the same contours of the first scan, whilst detecting variations in potential (Fig. 2.9). This patented LiftMode method is referred to as a nullifying technique, whereby during the second scan, at any point where the surface potential and the tip potential differ, a voltage is applied to the cantilever to neutralise this discrepancy [102]. As a result, sub-

nanometer surface potential contrast maps can be created simultaneously with topographic images at precisely the same surface location.

#### *2.4.3 Applications in dactyloscopy*

Of the four techniques discussed in this chapter, AFM has had the least direct influence on fingerprint research. However, as a surface imaging and analysis technique AFM is very powerful for investigating various properties of deposition surfaces, which can then be related to development effects with a combinational technique approach. For example, the effects of nanoscopic scale surface topography variations on development have been characterised using combined AFM and SEM analysis [12]. The physical nature of probing a surface makes directly imaging developed or undeveloped fingerprint difficult due to the malleable nature of these residues. However, utilisation of ‘long-distance’ scanning Kelvin force microscopy techniques has shown promise as a tool for fingerprint visualisation [108] and more recently the possibilities for electrostatic fingerprint imaging have also been reported [109].

## THE EFFECTS OF POLYMER PIGMENTATION ON FINGERMARK DEVELOPMENT TECHNIQUES 3

### 3.1 Introduction

Final product plastics are rarely the pure form of a polymer; most are sold with the addition of various fillers that generally fall into two categories, reinforcing and non-reinforcing [110]. The latter may simply be added to reduce costs; however, usually they are pigments, such as titanium dioxide ( $\text{TiO}_2$  or titania) and calcium carbonate ( $\text{CaCO}_3$ ), which provide colour or opacity and inevitably affect polymer chemistry [110]. The use of conventional black and white powders in suspensions as so called ‘wet powders’ originated as an effective alternative to Sticky-side Powder<sup>TM</sup> for developing fingermarks on the adhesive side of tapes [51,52]. The technique is now widely applied for development on smooth and non-porous surfaces such as plastics, particularly when the substrate has been wetted or the fingermark is considered too old for CA fuming [49,60,111]. Such progressions in technique or designs of novel or alternative development processes have historically been made through macroscopic comparisons and examiner experience, whereby substrates and techniques are variable factors and the most effective combination for development is observed. However, no technique is universally effective within substrate classifications and macroscopic comparisons may not reveal the mechanisms involved where two similar substrates behave differently [8-12]. Micro- and nanoscale analysis techniques, including SEM, SIMS and SKPM, have been used to investigate how development is influenced by variations in polymer additives on the three CAST polymers (Formica, PE and uPVC) and a selection of other polymers within the smooth, non-porous classification. Analysis will include carbon powder suspension (CPS), cyanoacrylate (CA) fuming and molybdenum disulphide ( $\text{MoS}_2$ ) both as small particle reagent (SPR) and wet powder (powder suspension) development techniques.

### 3.2 Experimental

#### 3.2.1 CAST polymers

Fingermarks were collected at the Centre for Applied Science and Technology (CAST, part of the UK Home Office) from two donors and deposited on three



surfaces classified as smooth, non-porous plastics under current protocols [8]. Formica, polyethylene (PE) and unplasticised polyvinyl chloride (uPVC) were chosen by CAST for their operational relevance and are referred to here as CP1, CP2 and CP3 respectively. In order to remove any water soluble or fat soluble contaminants each sample substrate was washed with warm water and detergent, cleaned with ethanol and subsequently left to dry in air prior to deposition. To produce natural latent fingerprints, donors were asked to not wash their hands for 30mins before deposition and no loading with sebaceous or eccrine secretions was performed. Immediately prior to deposition donors lightly rubbed their fingertips together to minimise variability and then marks were deposited on two samples for each of the three surfaces. All pre-imaging and analysis procedures (cleaning, deposition and development) on the CAST polymers were performed at CAST before transferring the samples to Brunel.

### *3.2.2 Sample development*

Fingermarks were left to age in ambient indoor conditions for 18h and then developed at CAST using either CPS, CA fuming, MoS<sub>2</sub> SPR or MoS<sub>2</sub> PS. Pre-mixed Wet Powder™ Black was used for CPS development and applied with a standard, dampened squirrel hair brush. Sample surfaces were pre-wetted prior to suspension application, which consisted of a light brushing of the solution across the surface and a 10 seconds exposure time, followed by rinsing under a running tap to remove any excess and a period of time to dry at room temperature. CA fuming was carried out using an MVC 5000 fuming cabinet with ‘Cyanobloom’ superglue. Environmental conditions were room temperature and 80%RH. An SPR ‘working solution’ was prepared using 432ml of tap water, 75ml of 1% detergent solution and 50g of MoS<sub>2</sub>. Immediately prior to use the working solution was shaken vigorously and deposited into a beaker at a depth of at least 50mm. Samples were held at the bottom of the beaker for 30 seconds and then removed before being drawn across the surface of clean water to remove excess MoS<sub>2</sub> and left to dry at room temperature. A MoS<sub>2</sub> powder suspension formulation was made up by mixing 10g MoS<sub>2</sub> with 15ml of detergent solution (25% triton X-100, 35% ethylene glycol, 40% deionised water (by volume)). This was applied to pre-wetted samples with a squirrel hair brush and left on the surface for 1min, before rinsing under a running tap to remove any excess. A

number of extra samples of the three substrates were also studied; these were cleaned as above without performing the fingerprint deposition or development steps and are referred to here as ‘blank’ samples.

### 3.2.3 Brunel polymers

A total of 12 additional polymers, 6 used (UP, approx. 20 years old) and 6 new (NP) samples of polymer based household products, were sourced internally to assist with studies on the CAST polymers based on similar properties. Each one is therefore also classified as a smooth, non-porous plastic under current protocols. Cleaning and development procedures for all UPs and NPs, where appropriate, were performed internally and in accordance with the methods described above for CAST polymers.

### 3.2.4 FTIR polymer characterisation

The samples were scanned on a Perkin Elmer Spectrum One Fourier Transform Infrared (FTIR) spectrometer, using a Specac Golden Gate Single Reflection ATR accessory, consisting of a Diamond crystal at a fixed incidence angle of 45°. Spectra were collected over the 4000  $\text{cm}^{-1}$  to 650  $\text{cm}^{-1}$  wavenumber range, at a resolution of 4  $\text{cm}^{-1}$  and 100 accumulations were collected for each sample.

### 3.2.5 SEM analysis

Imaging of all samples was conducted using a Zeiss Supra 35VP field emission SEM operating in high vacuum mode. Samples were mounted on microscope receptive aluminium stubs using pressure sensitive conducting adhesive. Due to the non-conducting nature of the polymers, each was sputter-coated with a thin, conductive layer of gold prior to SEM analysis to prevent beam induced charging effects that lead to substrate damage and poor quality images. All samples were coated using a Polaron-SC7640 for 60 seconds at a target voltage of 2kV and a current of 20mA to achieve coats of 12nm nominal thickness. Secondary electron and backscattered electron images were collected at various magnifications using a broad range of accelerating voltages (2-20kV) in order to highlight surface sensitive topological features (low kV) and generate subsurface elemental contrast (high kV). Qualitative elemental characterisation, in the form of spectra and distributional maps, was also

conducted at accelerating voltages of 12-20kV with an Oxford Instruments INCA energy EDX analysis system integrated with the microscope.

### 3.2.6 ToF-SIMS analysis

Secondary ion mapping studies were performed on three areas of a blank Formica sample with a Kore Technology Ltd. time-of-flight secondary ion mass spectrometer (ToF-SIMS), using a 25KeV Indium primary ion source (FEI Liquid Metal Ion Gun) operating at 1  $\mu$ A current. Secondary ions were analysed in a reflectron mass spectrometer and detected with a dual microchannel plate assembly. Flight times were recorded with a 0.5 ns time-to-digital converter. Spectra were taken from an area of approximately 250 micrometres square. The sample was selectively coated with gold, leaving one small area for analysis uncoated, in order to reduce the effects of charging. In accordance with a previous study [79], the first two areas were sputtered prior to analysis for 30 seconds (area A) and 15 seconds (area B) respectively to ensure the removal of adventitious carbon and achieve a sufficient signal. To test whether a signal could be achieved without sputtering and gain more surface sensitive information, a third area was mapped four times successively without prior sputtering (area C). Maps are presented from positive secondary ion detection and peak areas selected for investigation were determined following preliminary acquisitions.

### 3.2.7 SKPM analysis

Surface potential analysis was performed on a blank Formica sample using a Digital Instruments Dimension 3100 scanning probe microscope. Primary intermittent contact (tapping) mode and secondary LiftMode were performed laterally with a TAP300E electric mode probe operating at a resonant frequency of approximately 300 kHz in order to image surface morphology features directly alongside surface potential variations. Scanning areas ranged from 2.5 x 2.5 $\mu$ m to 50 x 50  $\mu$ m, topographic images are shown after first-order plane subtraction and surface potential images are shown after first-order plane subtraction and ‘flattening’. Scanning sites were chosen based on SEM imaging of surface features in proximity to patches of titania that could be subsequently located using the AFM’s light microscope. Since gold coating the blank samples would affect SKPM analysis, these sites were imaged using variable pressure (VP) SEM with nitrogen at pressures between 20 and 40 Pa. Image quality is

often reduced using this method for non-conducting samples, however, it remained sufficient to locate patches of titania.

### 3.3 Results & Discussion

#### 3.3.1 Titanium dioxide pigment

Macroscopic analysis of the CPS developed fingerprints on Formica indicates prints with good detail quality and good contrast (Fig. 3.1, inset); however, initial SEM imaging of these samples reveals patchy areas of overdevelopment both on and off ridge. Figure 3.1a shows four CPS developed fingerprint ridges separated by three off ridge sections; multiple randomly distributed patches of over development are visible in the image as whiter areas. By progressively increasing magnification on these areas the overdevelopment becomes clearer and evidence for an associated feature within

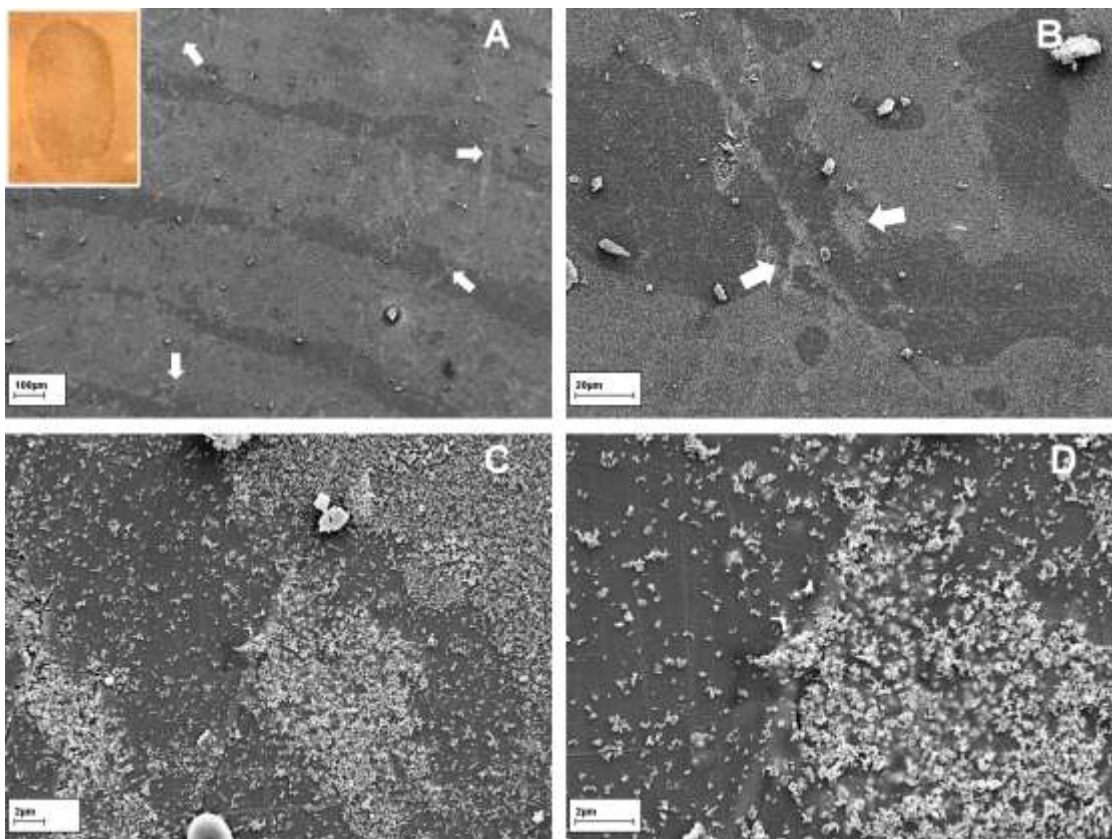


Figure 3.1 – (a) Low magnification SEM image of four fingerprint ridges developed with CPS suspension on the Formica surface. White patches of overdevelopment are visible on and off ridge. (b) Increased magnification SEM image from the centre of (a). (c,d) Two more increases in magnification, revealing a feature within the Formica surface and its association with overdevelopment.

the surface appears (Fig. 3.1b,c,d). Of the other fingerprint development techniques examined as part of this study, MoS<sub>2</sub> powder suspension displays a similar overdevelopment association, while MoS<sub>2</sub> SPR and CA fuming display no associated overdevelopment with these features (Fig. 3.2). For comparison purposes all developed fingerprint images presented are from a single donor, however, studies on additional samples have demonstrated the observations are not donor specific.

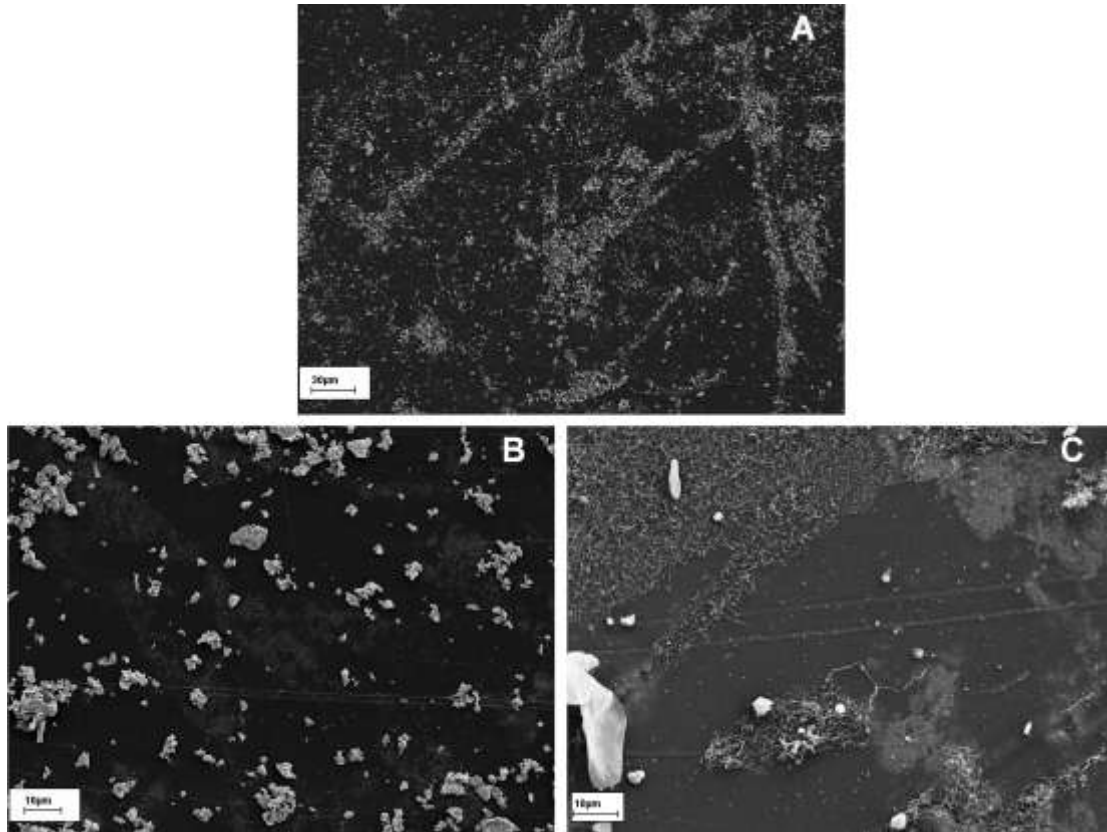


Figure 3.2 – (a) SEM image of an MoS<sub>2</sub> powder suspension developed fingerprint on Formica showing a level of association between overdevelopment and the presence of a surface feature. (b,c) SEM images of MoS<sub>2</sub> SPR (b) and CA (c) developed fingerprint on Formica showing no association between overdevelopment and the same surface feature.

Subsequent SEM imaging of a blank Formica sample has shown the existence of two very distinct types of feature within the polymer surface, which are localised in randomly distributed patches (Fig. 3.3). EDX analysis identified the larger ‘flake’ shaped structures as aluminium and silicon based (Fig. 3.3, region 3), and the smaller ‘particulate’ patches as titanium based (Fig. 3.3, region 2). Cross-referencing with the developed fingerprint images suggests an involvement for the titanium features rather than the aluminium-silicon features. This was confirmed by developing a blank

Formica sample with Wet Powder™ Black and utilising a combination of SEM imaging modes. Figure 3.4a shows an area of increased development compared to its surroundings; the image was generated at a low accelerating voltage using secondary electron detection to allow surface sensitive imaging. Figure 3.4b is an image of the same area generated by a high accelerating voltage using backscattered electron detection in order to increase penetration depth and highlight elemental contrast; it acutely demonstrates that overdevelopment is associated with the titanium features and not the aluminium-silicon features. Observing the same overdevelopment effects on the blank sample also ensures the rejection of the hypothesis that superfluous development is caused by one or more component of the fingerprint being attracted to titanium-containing surface locations and then developed normally by CPS; the phenomenon is fingerprint-independent.

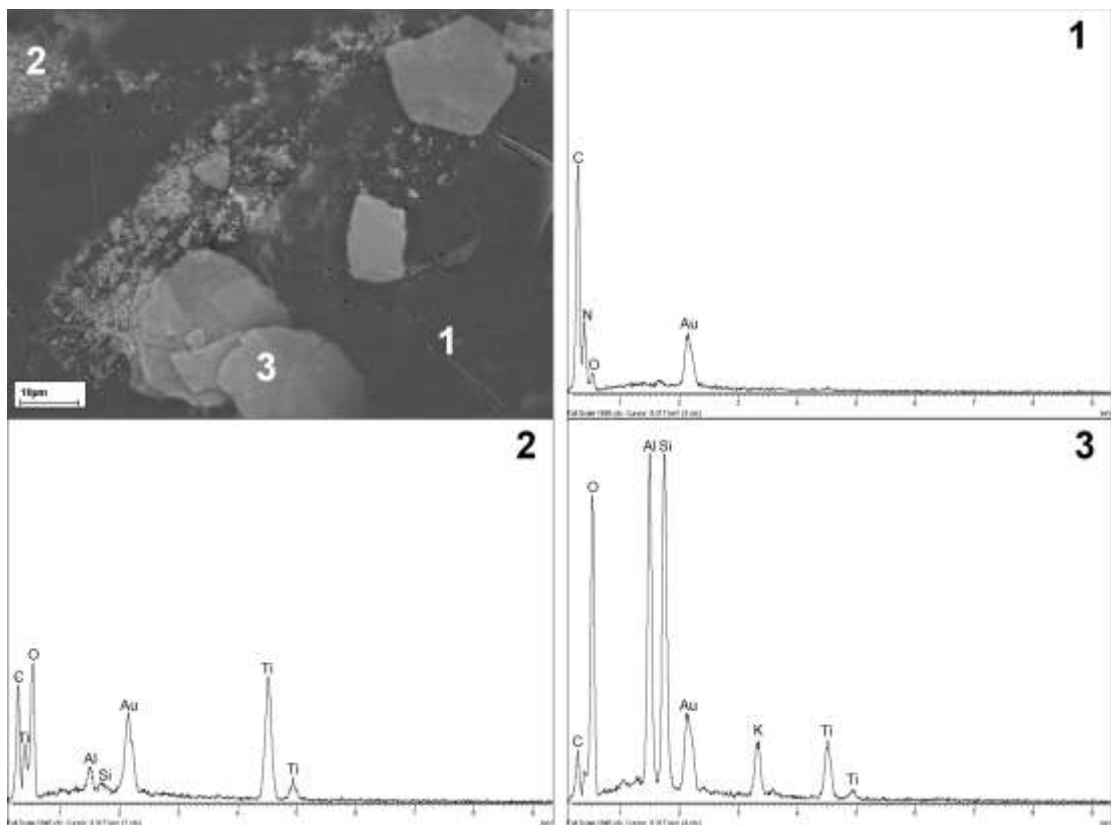


Figure 3.3 – An SEM image of an area of Formica containing two distinct surface features., associated with EDX spectra from a location away from both surface features (1), a location containing only the small ‘particulate’ feature (2) and a location containing only the large ‘flake’ shaped feature (3).

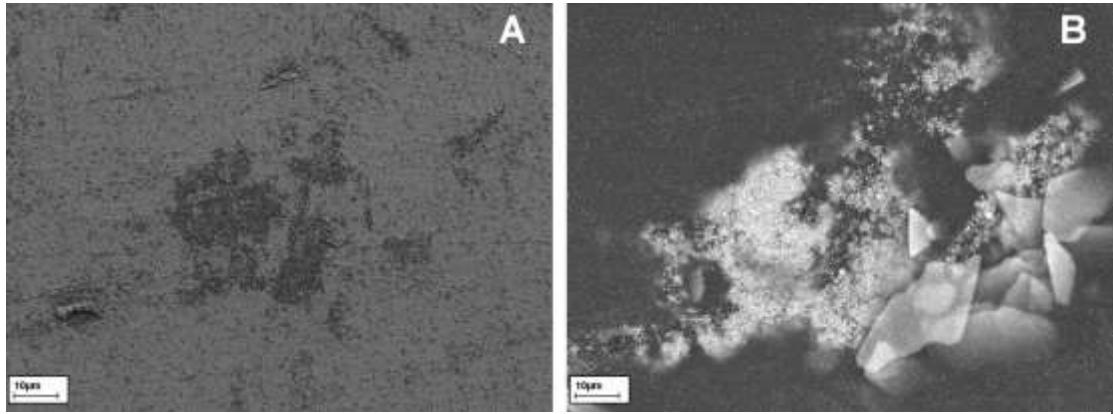


Figure 3.4 – A low kV SEM image (a) of a blank Formica sample developed with CPS alongside an increased kV, backscattered electron detection SEM image of the same area (b). While overdevelopment is clearly associated with titania, not all areas of the compound exhibit this effect.

The third CAST polymer (uPVC), sourced from material used to make window frames, was subsequently shown using EDX analysis to also contain titanium within its surface. Unlike Formica, however, SEM imaging does not present clearly defined patches of the element and EDX analysis shows the presence of at least one other filler (calcium carbonate). The remaining CAST polymer, PE, is not discussed in this chapter as SEM analysis showed it to contain no titanium. By mapping EDX spectra over areas of the Formica and uPVC surfaces it is possible to demonstrate their relative distributions of the element titanium with a nominal spatial resolution of  $1\mu\text{m}$ . As shown in figure 3.5, titanium has a localised random distribution within the Formica surface and is spread ubiquitously within the uPVC surface. When imaging CPS developed fingerprints on uPVC it is very difficult to differentiate between on-ridge and off-ridge areas (Fig. 3.5c). This reduction in contrast is due to heavy background staining across the surface and may result from the ubiquitous presence of titania and a similar overdevelopment effect as described on Formica. However, without any titanium-free areas in the uPVC surface it is difficult to isolate its effect on overdevelopment from those that could be occurring due to an inherent property of the polymer or the presence of another filler. In an attempt to establish a connection between titanium in uPVC with surface wide overdevelopment a second uPVC sample containing no titanium was sought for analysis. Figure 3.6a shows extremely sparse carbon coverage following CPS development on a blank transparent uPVC surface (NP5) that showed no titanium content following EDX analysis, as compared to heavy carbon coverage following the same development on a blank white uPVC

(CP3) sample containing ubiquitous titanium (Fig. 3.6b). This observation supports idea that titanium overdevelopment effects are not Formica specific, however, ATR-FTIR spectra for the two uPVC samples are only 51% similar and therefore their development disparity may be related to polymer type.

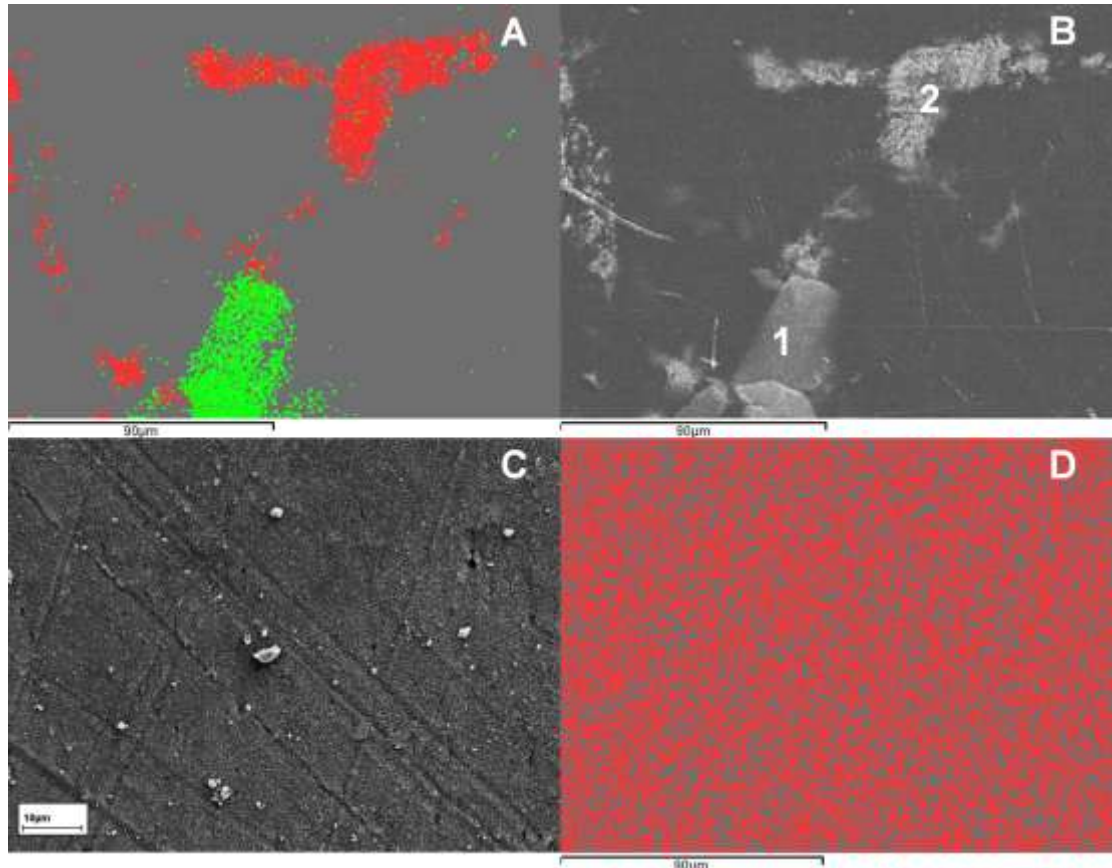


Figure 3.5 – (a) An EDX map of a blank Formica sample (green-aluminium, red-titanium) alongside an SEM image of the corresponding area (b), illustrating two frequent subsurface structures (1-aluminosilicate, 2-titanium dioxide) and a localised spread of titanium. (c) An SEM image of a CPS developed uPVC surface highlighting the problems with ‘blanket’ development and ridge-boundary contrast (boundary running from bottom left to top right). Alongside is a representative EDX map of a blank uPVC sample (d), showing a ubiquitous spread of titanium (red).

The two forms of distribution of titanium within Formica and uPVC (CP3) pose individual problems to the evidential value of fingerprints on such surfaces. Heavy background staining on uPVC (CP3) reduces contrast between on ridge areas and off ridge areas, however, as long as donor conditions are such that there is sufficient adhesion to the fingerprint residue this may not cause significant loss of detail. The random and patchy background development on Formica has the potential cause more significant issues by interfering with fingerprint detail. Theoretically, this could result in the false exclusion of matches and false positives during the identification process.



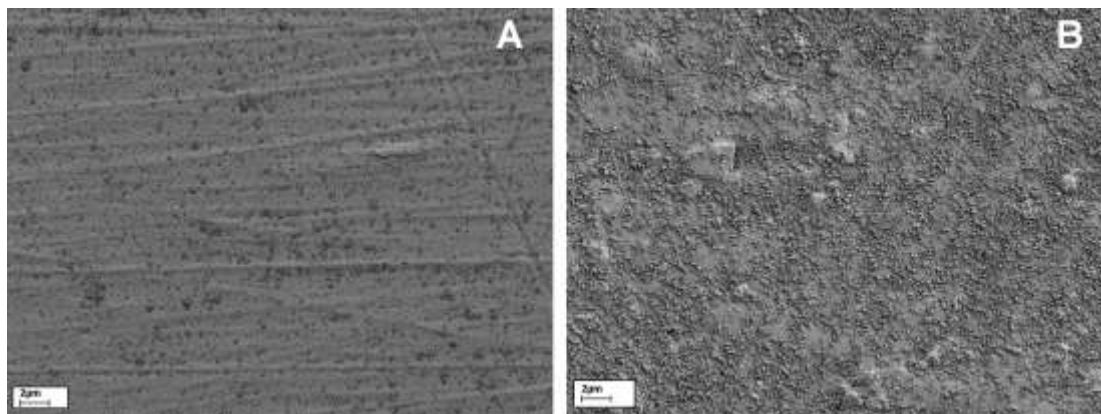


Figure 3.6 – A comparison between CPS development on a blank transparent uPVC surface containing no titanium (a) and a blank white uPVC surface (CP3) containing surface wide titanium (b). The level of carbon powder adhesion is significantly higher on the titanium containing substrate.

Table 3.1 lists all CAST and Brunel polymer samples analysed in this study along with information on their origins, polymer characterisation and elemental constituents. The presence of titanium in 12 out of 15 samples is indicative of the prevalence of titania as a pigment in the plastics industry and represents the potential extent of the problem for fingerprint development on plastics. Titania is a commodity due to being one of the whitest compounds on earth and having the highest refractive index of any white pigment [112]. Furthermore, the compound has strong UV stabilising and photocatalytic capabilities, which can augment materials with numerous beneficial properties (UV protection, self cleaning, antibacterial, deodorising, depollutant, etc.) [112,113]. This level of versatility sees the use of titania in a vast array of industries other than plastics, and consequently its global market was estimated to exceed a capacity of 5 million metric tonnes in 2011 [114]. Such prevalence, together with the observation of increased oxygen EDX signals over titanium patches (Fig. 3.3, region 2) compared to non-titanium areas (Fig. 3.3, region 1) in Formica, links titania specifically with the overdevelopment effects described above.

Table 3.1 – An overview of all primary and secondary polymers used during this study.

| Name | Polymer                   | Colour              | FTIR characterisation           | Elemental constituents       |
|------|---------------------------|---------------------|---------------------------------|------------------------------|
| CP1  | Formica (kitchen worktop) | Beige               | Melamine formaldehyde           | Al, C, N, O, Si, Ti          |
| CP2  | Polyethylene (generic)    | Translucent         | HDPE                            | C, O                         |
| CP3  | uPVC (window frame)       | White               | uPVC                            | C, Ca, Cl, O, Ti             |
| UP1  | Pendant light fitting     | White               | Urea formaldehyde               | C, Cl, N, O, Ti              |
| UP2  | Collet light fitting      | White (discoloured) | Unknown                         | Al, C, Ca, Cl, O, Si, Ti, Zn |
| UP3  | Socket casing             | White               | Urea formaldehyde               | C, Cl, K, Na, O, Ti, Zn      |
| UP4  | Ariel casing (large)      | White               | Acrylonitrile butadiene styrene | Al, C, O, Ti                 |
| UP5  | Ariel casing (small)      | White               | Polystyrene                     | C, Ca, O, Ti                 |
| UP6  | Wire junction unit        | White               | PVC                             | C, Cl, O, Ti                 |
| NP1  | Wall blank                | White               | Urea formaldehyde               | C, Ba, N, O, S, Zn           |
| NP2  | Melamine faced chipboard  | White               | Melamine formaldehyde           | Al, C, N, O, Si, Ti          |
| NP3  | Toilet seat               | White               | Isotactic polypropylene         | C, O, Ti                     |
| NP4  | Rectangular ducting       | White               | PVC                             | C, Ca, Cl, O, Si, Ti         |
| NP5  | uPVC (generic)            | Transparent         | uPVC                            | C, Cl, O, Ni                 |
| NP6  | Cladding                  | White               | uPVC                            | C, Ca, Cl, O, Ti             |

All surfaces in table 3.1 that have been shown to contain titanium with EDX analysis display high levels of CPS staining following development on blank samples. However, only one of the Brunel polymers (NP2) has localised patches of titania (similar to Formica) that allow for direct development comparisons between areas that contain the pigment and areas that do not. Figure 3.7a,b demonstrates similar titania related CPS overdevelopment on NP2 by comparing low kV and BSE images of the same surface location. Overdevelopment with large surface topographical features is also evident in the top left hand corner of figure 3.7a, which is a clear indication that

multiple surface factors can influence development and these must be considered alongside pigment chemistry. This was duly taken into consideration following an attempt to produce a custom titania containing epoxy resin, which exhibited very localised but also very rough patches of the pigment (Fig. 3.8a,b). Overdevelopment was clear in these areas; however, this observation could not be isolated from the topographical effects (Fig. 3.8c,d)

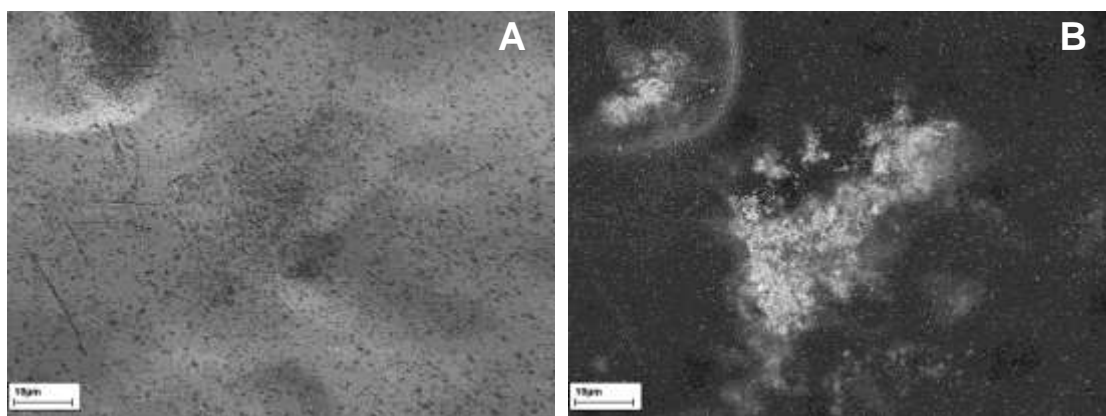


Figure 3.7 – A low kV SEM image (a) of a blank NP2 sample developed with CPS alongside an increased kV, backscattered electron detection SEM image of the same area (b). Overdevelopment in the central region is associated with underlying titania, however, a large patch of overdevelopment is also associated with a topographic feature in the top left corner of the images.

### 3.3.2 Interaction mechanisms

The discovery of a correlation between the presence of titania pigments in two polymers and overdevelopment with CPS on those surfaces was followed by an investigation into the possible mechanisms behind these observations. Enhanced attraction and adhesion of carbon powder to regions of titania in the substrate may be the result of direct chemical bonding; titania-induced changes to surface conditions such as surface potential, hydrophobicity, or surface energy; or titania-induced changes to the polymer structure. For example, the overdevelopment effect is seen with MoS<sub>2</sub> in powder suspension form, but not in SPR form. SPR formulations have reduced particle concentration and reduction in levels of surfactant component, both of which affect the surface tension of the liquid. Localised variations in substrate surface energy, together with these liquid properties, may therefore be affecting wetting behaviour on the substrate surface and consequently facilitating overdevelopment in these regions.

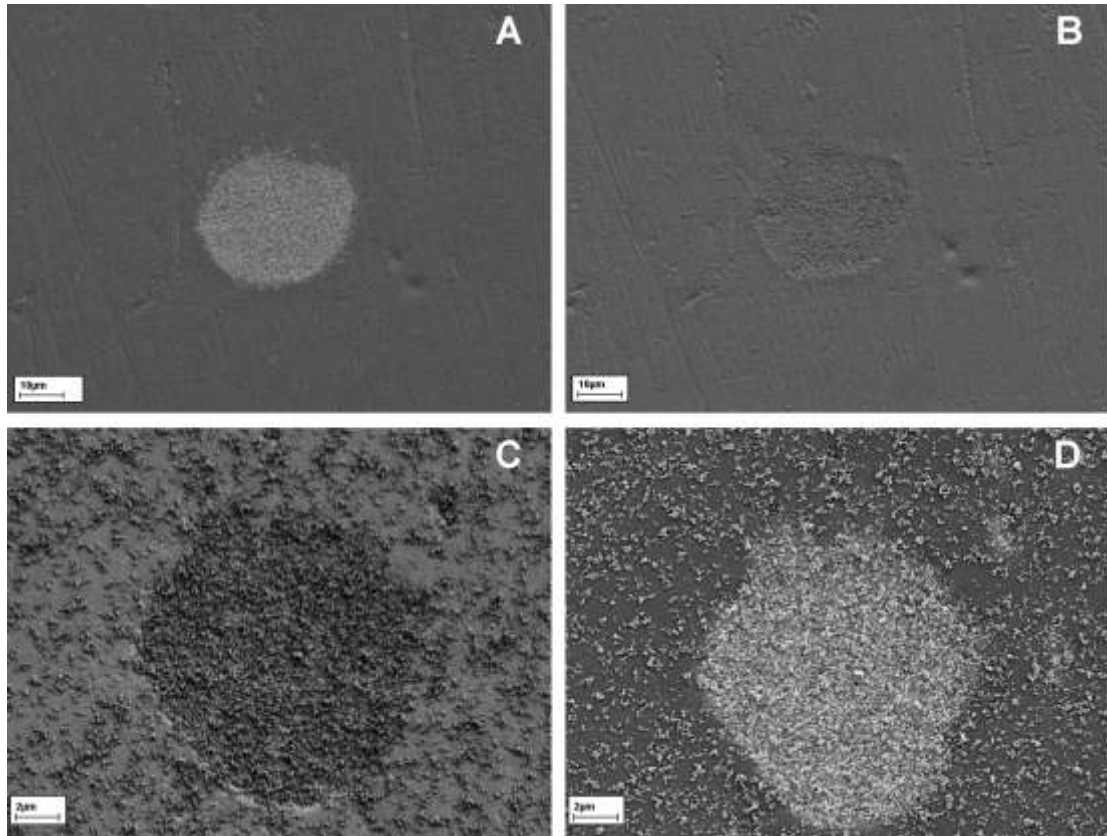


Figure 3.8 – A high kV SEM image (a) of a titania doped epoxy resin alongside a low kV image of the same area (b). Localised patches of titania are significantly rougher in texture than the surrounding areas, which may explain increased levels of powder adhesion over these patches when this surface is developed with CPS (c,d).

Similarly, a previous study [12] has shown that iron oxide based powder suspension (IOPS), with significantly larger particle size and partially conducting powder content, does not display titania induced overdevelopment. This indicates that a property of the suspended powder can be sufficient to prevent interaction despite being within a similar formulation. Due to electrical property disparity between IOPS, which is partially conducting, and CPS, which is non-conducting, a possible involvement for titania induced surface potential changes was investigated using SKPM. This technique was able to demonstrate significant differences in signal between areas of the surface containing titania and areas of the surface completely away from the pigment (Fig. 3.9). Despite significantly more surface potential contrast in titania areas, the areas of increased potential did not conclusively match up with underlying patches of titania following subsequent imaging of the same areas with SEM (Fig. 3.9a). However, the complete lack of contrast in titania-free areas may suggest that either surface potential is not involved in the overdevelopment

interaction or it is only partially involved. Future work, with the addition of known standards to test the accuracy of surface potential observations, could help clear up this issue. Another explanation for the iron oxide powder suspension observations in comparison to carbon and MoS<sub>2</sub> powder suspensions is disparity in the powder suspension formulations. It may be possible to test this by manually producing identical powder suspension formulations, varying the powder component and using each to develop the Formica surface. If the iron oxide powder suspension remained unaffected by titania it could be concluded that some component or property of this

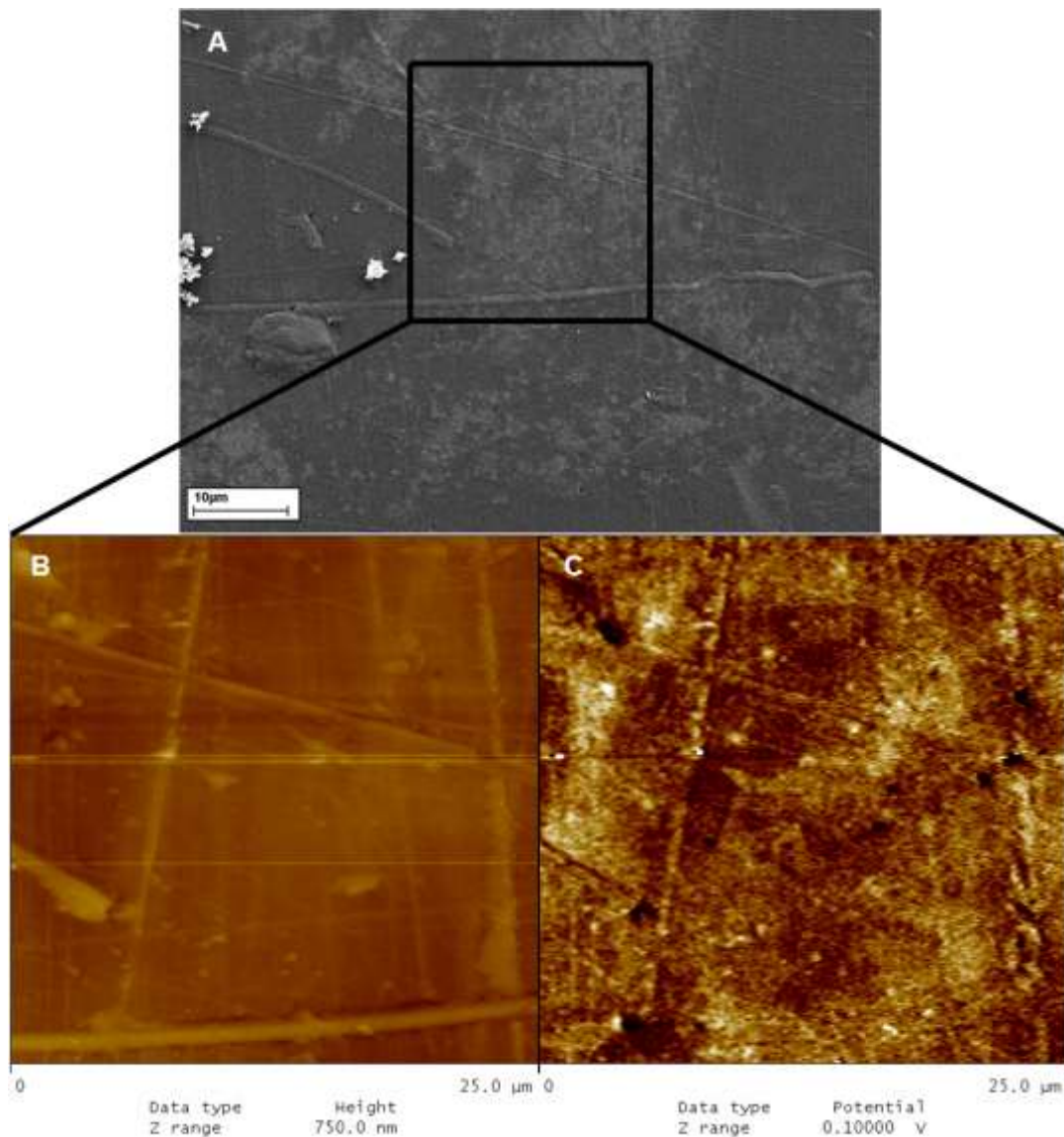


Figure 3.9 – An area of Formica with patchy titania as imaged using secondary electron SEM (a), tapping mode AFM (b) and SKPM (c). Significant variation in surface potential in this small area is visible as contrast in image C; however, this does not correlate entirely with titanium dioxide localisation as seen in image A.

powder is preventing interaction. Similarly, isolating the change in formulation responsible for the observed difference between SPR and powder suspensions could be investigated by varying relative particle and surfactant concentrations with a constant powder component.

Information on the depths at which titania is present within the Formica surface is a further guide to determining the mechanism of interaction. The surface sensitivity of SEM imaging relates directly to the accelerating voltage of the electron beam and very low kV acquisitions are capable of generating a high level of surface detail. However, in order to excite secondary electrons from titanium atoms at the surface and distinguish these from atoms of the polymer itself, the accelerating voltage must be significantly higher. This results in beam penetration, and therefore imaging, at greater depths ( $\sim 1\mu\text{m}$ ) within the surface. ToF-SIMS mapping analysis was employed to gather information on the surface of Formica with a far reduced surface penetration ( $\sim 2\text{nm}$ ).

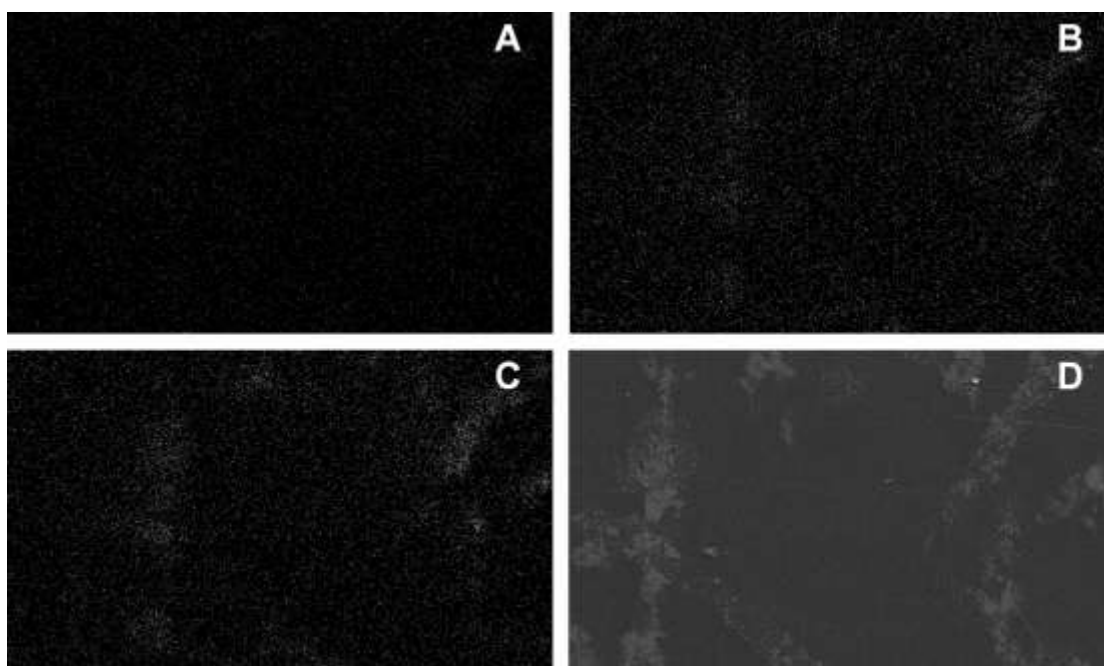


Figure 3.10 – Maps of the 2<sup>nd</sup> (a), 3<sup>rd</sup> (b) and 4<sup>th</sup> (c) successive ToF-SIMS acquisitions from area C, showing localised titanium signal by the 3<sup>rd</sup> acquisition. Alongside is a retrospective SEM image of the same area (d) - larger patches of titanium are visible here, owing to the greater penetration depth of the technique.

Initially two sample areas were mapped following incrementally decreasing periods of sputtering (areas A & B). A significant titanium signal was obtained and mapped in both areas; however, it is difficult to accurately estimate the depth of titania in these areas due to little information regarding sputtering coefficients, which vary significantly with material. A third sample area was mapped four times successively without any prior sputtering (area C) and a significant titanium signal can be seen after the third acquisition (Fig. 3.10). The need for a period of ion beam exposure to stimulate secondary ion emission and remove environmental contaminants such as adventitious carbon has been described previously [79] and may account for the lack of titanium signal in the first area C map. The observations, however, suggest that no significant amount of titanium is exposed at the surface of untreated Formica and therefore a direct chemical bonding mechanism is not possible. Based on a nominal sensitivity of 2nm and allowing for variations due to scanning parameters and substrate disparity, it is estimated that significant amounts of titanium are situated within the top 30nm of the Formica surface. Retrospective SEM imaging of the mapped area also indicates that the depth of titanium within Formica is not uniform; extra patches of the element are visible in the SEM and the patches visible with SIMS mapping appear to cover a greater area when imaged with SEM (Fig. 3.10d). It is possible that the effect of titania on CPS decreases as its depth within the surface increases and this may explain why overdevelopment does not always cover patches that are visible with SEM imaging as demonstrated in figure 3.4. SIMS analysis also confirmed the titanium based feature as titania.

Aluminium and silicon peaks were also selected for detection in all maps based on their trace presence in the previously described characterisation of titanium patches in Formica (Fig 3.3). Figure 3.11 shows these maps alongside the titanium map from area B and a localised correlation between all three elements is clearly visible. These results suggest an aluminosilicate coating around the pigment, which may correspond to powder dispersion and UV stabilising properties that have previously been described [53,115]. In particular, it is thought that the ability of alumina and silica in titania coatings to accept electrons and clear free radicals is crucial in preventing UV induced degradation of the polymer [115].

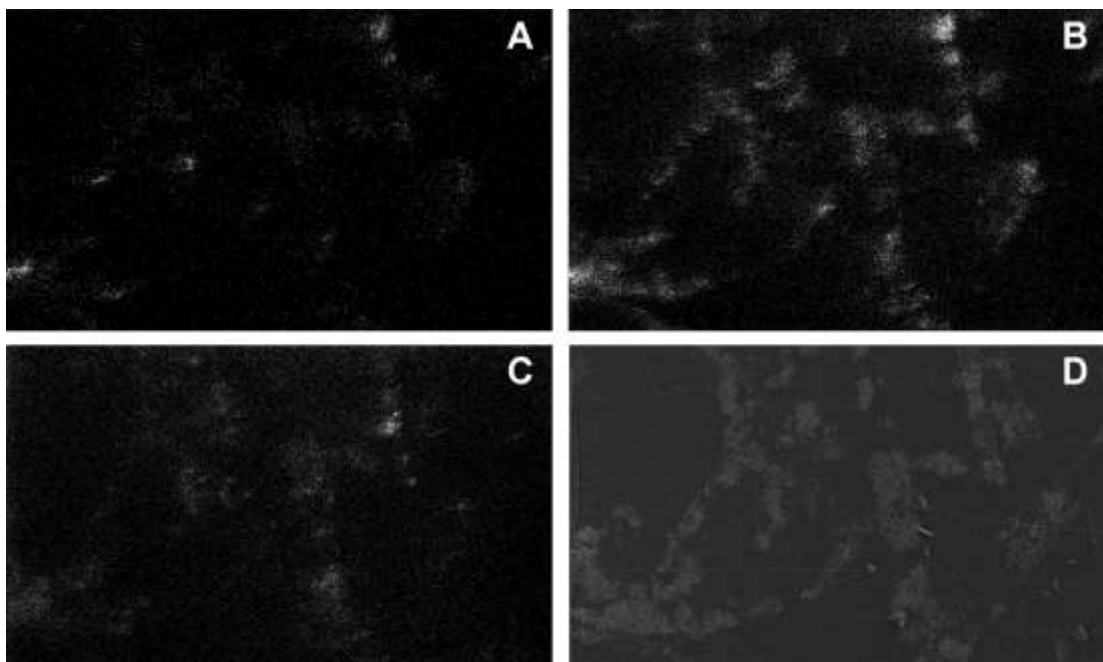


Figure 3.11 – Distribution of titanium (a), aluminium (b) and silicon (c) in the surface of Formica, as demonstrated by maps from area B and compared to a retrospective SEM image of the same area. Co-localisation of the three elements suggests a coating around the titania pigment.

Titanium and aluminium also correlate on maps from area C; however, a significant silicon signal is not present. This observation could be due to a number of reasons, including lower instrument sensitivity for silicon ions, poorly resolved silicon peaks due to sample charging or a less abundant presence in the coating. Alumina and silica coatings are known to be added to titania based white development powders in order to improve their performance by altering chemical properties (e.g. oleophobicity and hydrophobicity) of the formulation [53]. Similar chemical effects may be occurring on the Formica surface due to a coating around the titania pigment and may have a role in the mechanism for CPS overdevelopment. If overdevelopment is influenced or governed by the presence of a coating it is possible that the effect may be less widespread in titania-containing polymers as a class, due to potential inter-surface variations in coating properties such as thickness, morphology and composition [53]. However, the titania prevalence and associated overdevelopment observed for white polymers highlighted in table 3.1 suggests that either this is not the case or any coating effect is universal.



### 3.4 Conclusions

Slight variations in chemistry within a single surface classification (smooth, non-porous plastics) have been shown to exert a considerable effect on the performance of fingerprint development techniques. Specifically, the presence of titania in Formica and other polymers causes fingerprint-independent overdevelopment with powder suspension formulations based on carbon or MoS<sub>2</sub> powders. This is detrimental to the quality of the developed mark either through reduction in contrast or interfering with print detail, depending on how titania is localised within the surface. The extent of the problem has also been highlighted by illustrating the amount and range of use for titania in the plastics industry, particularly as a white pigment. Combined ToF-SIMS mapping and SEM imaging has provided evidence to suggest that the mechanism for pigment-CPS interaction is not a direct chemical bonding but that it may be occurring over a nominal distance of 30nm with the effect decreasing with separation. Possible mechanisms include variation of surface energy or potential induced by the presence of the titania pigment or associated aluminosilicate coating.

Operationally, many light coloured plastic surfaces contain titania pigment which may lead to overdevelopment if treated with carbon powder suspensions. CA fuming or MoS<sub>2</sub> SPR are demonstrated here as viable alternatives, dependent on environmental aging considerations and other factors. Since previous work [12] has shown that an iron oxide based powder suspension does not display the same titania induced overdevelopment as CPS, it may be possible to further investigate the mechanisms of these effects by treating Formica with manually produced suspensions that vary with either formulation or powder component.

## THE EFFECTS LINEAR SURFACE FEATURES IN POLYMERS ON FINGERMARK DEVELOPMENT TECHNIQUES 4

### 4.1 Introduction

In addition to chemical effects, variations in surface topography can also selectively influence the effectiveness of fingerprint development techniques. Figure 4.1a [116] demonstrates an overdevelopment phenomenon that has been observed on two of the three CAST polymers (PE and uPVC), whereby cyanoacrylate (CA) polymerisation occurs along linear surface features into off-ridge areas. A previous study utilising AFM has shown characteristic topographical features in both surfaces [12]. PE is defined by short, sharp ridges that are parallel to and within large wave like features. Imaging demonstrates that the CA overdevelopment is occurring in the valleys of the larger surface features and is unaffected by the smaller ridges (Fig. 4.1a). The uPVC surface is significantly smoother than PE with an average roughness of  $83 \pm 6\text{nm}$  compared to  $319 \pm 60\text{nm}$  [12]. However, it is defined by heavy, random scratches and these features cause a similar CA overdevelopment problem (Fig 4.1b). There are three main processes that could account for these observations:

- a) CA development occurring normally on migrated fingerprint residue;
- b) CA development occurring normally on trapped environmental residues;
- c) CA development occurring abnormally (i.e. initiating on-ridge and tracking into off-ridge areas).

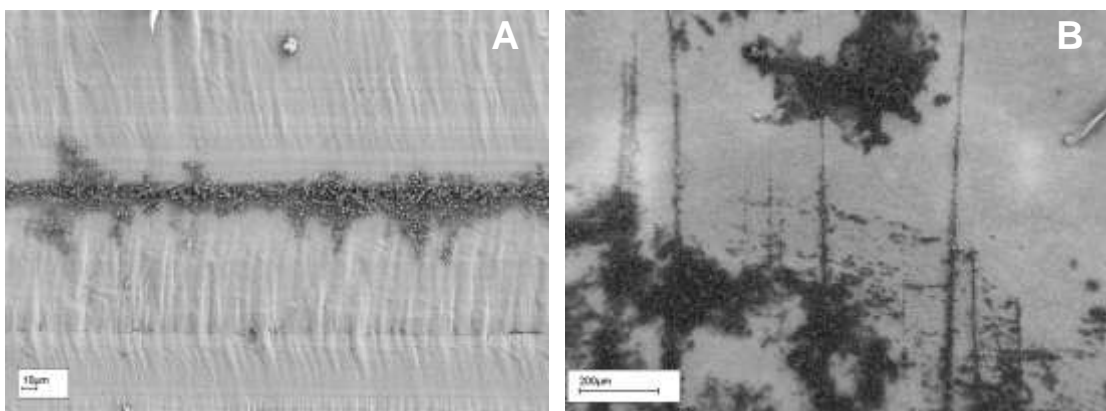


Figure 4.1 – CA overdevelopment into off-ridge areas following development of fingerprints on PE (a) and uPVC (b). Overdevelopment is associated with large wave-like surface features and sharpe scratches respectively. (Source: Jones (2011) [116])

This study attempts to isolate which process is responsible for the observed overdevelopment effects using FTIR microspectroscopy to track print residues over a 48hr period. A silicon wafer model system has been used as the substrate for this investigation, which provides a clean view of any residue movement due to infra-red transparency of the substrate material. Natural latent fingermarks are used here as oppose to those that have been sebaceous or eccrine loaded due to a better representation of crime scene conditions [36]. Additionally, the mechanisms behind CA polymerisation are still very unclear and although water is generally considered as an important polymerisation initiator, it is likely that a number of fingermark residue components are involved [61-63]. Preferentially loading the donor fingermarks with one type of secretion and consequently obscuring the other might therefore be detrimental to a study directly related with CA development.

## **4.2 Experimental**

### *4.2.1 Model preparation*

Silicon wafer tiles were prepared to approximately the same size as the CAST polymer samples as described in chapter 3. Four horizontal scratches were made with a diamond tip pen at approximate intervals of 3mm across the width of the silicon tiles. Natural latent fingermarks were placed over the scratched area. Pre-deposition sample cleaning and natural fingermark production procedures can be found in chapter 3.2.1. A small square of transparent adhesive tape (Sellotape®) was placed in close proximity to the mark as a stable material for normalisation purposes. Areas of scratched and non-scratched silicon were reserved on the opposite side of the tape as negative control regions. All model sample procedures in this chapter were performed internally at Brunel in accordance with CAST technique.

### *4.2.2 AFM scratch analysis*

Prior to fingermark deposition, topographic imaging and analysis of the diamond pen induced scratches was conducted using a Digital Instruments Dimension 3100 scanning probe microscope (SPM) operating in intermittent (tapping) mode. Scanning was performed over areas of  $50\mu\text{m}^2$  with an LTESP-50 Silicon-SPM-Sensor probe at

a resonant frequency of ~155 kHz. Scratch depth and width information was used to help determine the relevance of the model system to PE and uPVC surface features.

#### 4.2.3 FTIR microspectroscopy

Imaging was performed on natural latent fingermarks from two donors, A & B (both male aged 25-40). Each fingermark was analysed twice over a period of four days with 48 hours in between to allow for any residue migration. As such, donor A deposited on day 1 was analysed on days 1 & 3, and donor B deposited on day 2 was analysed on days 2 & 4. Micro-FTIR spectra were taken on a Perkin Elmer Spotlight FTIR Imaging System. Micro FTIR spectra were collected over the  $4000\text{ cm}^{-1}$  to  $700\text{ cm}^{-1}$  wavenumber range, at a resolution of  $8\text{ cm}^{-1}$ , using a focal plane array (FPA) detector consisting of mercury–cadmium–telluride IR arrays, and beam diameters of  $25\mu\text{m}$  and  $6.25\mu\text{m}$  determined by corresponding aperture sizes.

### 4.3 Results & Discussion

#### 4.3.1 Silicon model relevance

The smooth and non-porous properties of silicon wafer, together with its infra-red transparency, made this substrate sufficiently similar to PE and uPVC while allowing for FTIR microspectroscopy in the preferred transmission mode. The main variable factor with this model system was the production of scratches along the silicon surface, although a degree of control was afforded by the smoothness of the model substrate. Each scratch was scribed manually with the aid of a ruler to produce straight lines and by applying the same amount of pressure to minimise variability. Figure 4.2 shows a representative cross section of a scratch on the donor A substrate sample, average horizontal (H) and vertical (V) values were calculated from four separate areas on each of the four scratches at approximately  $12 \pm 3\mu\text{m}$  and  $1.5 \pm 0.5\mu\text{m}$  respectively. The structures created by this diamond pen inscribing method give a model that is more analogous to the scratched uPVC surface than the large wavy features that characterise PE. In contrast to the uPVC scratches, which are relatively smooth and homogeneous, the scratches created in silicon displayed high levels of roughness and heterogeneity due to the brittle nature of this surface. Another notable feature of the silicon scratches is their raised profile compared to the rest of

the surface. Figure 4.2 shows slopes either side of the main scratch valley that fall progressively to a flat surface; this architecture is consistent across all of the scratches and results from the physical stresses (Hertzian contact stress) of the scratching process [117]. Water contact angle measurements were performed on the model surface and the two CAST polymers to compare hydrophobicity. The silicon wafer at  $34.39^\circ$  has less than half the contact angle of both PE ( $90.77^\circ$ ) and uPVC ( $80.81^\circ$ ), which makes it a far more hydrophilic surface and more receptive to the spread of liquids across its surface. However, this observation does not necessarily account for non-water fingerprint components (e.g. lipids) and since a number of other model surface scratch –properties (roughness, heterogeneity and raised profile) are



Figure 4.2 – A representative cross-sectional view of one area from one scratch on the donor A sample substrate. Slopes either side of the scratch opening, caused by physical stresses during scratching, are clearly evident.

anticipated to make it less conducive to fingerprint residue migration than the PE and uPVC surfaces, any such observations can also be expected to occur on the operationally relevant CAST polymers with respect to linear feature structure.

#### 4.3.2 Residue migration

Microspectroscopic imaging with FTIR, as reported previously [88-90], provides non-destructive visualisation of individual fingerprint residue components with microscopic spatial resolutions. Crucially, the technique functions in atmospheric conditions and therefore any changes to these residue components are able to be mapped as a function of time. To ensure the atmospheric conditions were having no bearing on fingerprint residue observations and to assess whether CA overdevelopment is due to the trapping of environmental residues in surface features, a negative control region was scanned in addition to a fingerprint region; these

included scratched and non-scratched areas of the substrate. A second consideration regarding operation in atmospheric conditions relates to potential variable performance of the instrument on separate scanning days. For reliable comparisons of scans taken 48 hours apart, adhesive tape was placed in proximity to, and scanned simultaneously with fingerprint and control regions. As a stable material, any changes

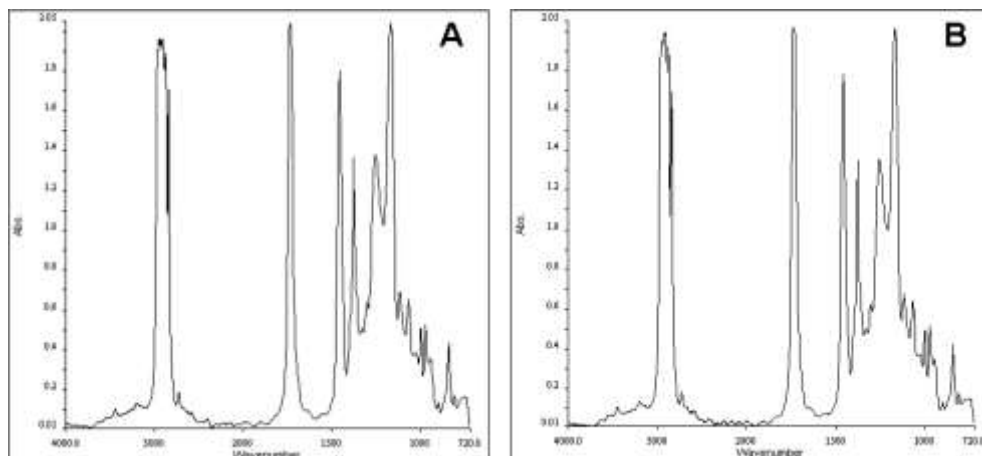


Figure 4.3 – FTIR absorbance spectra taken from the same area of tape on the donor A (donor B is not shown, however, can be represented by these spectra) sample substrate from day 1 (a) and day 3 (b). The high levels of similarity are sufficient to allow comparisons between over the 48hr period for all scans.

to the spectra taken in the tape areas could only be due the performance of the instrument and all other spectra would then require normalisation by a factor of the difference. The spectra for single tape locations on donor A and donor B samples are indistinguishable between day 1-3 and day 2-4 respectively (Fig. 4.3, donor A only), and so all maps from fingerprint areas and control areas were deemed directly comparable over the 48 hour period. Mapping was performed for the following bands in fingerprint and control regions: hydroxyl groups (water), fatty acids/triglycerides, sugars/phospholipids, hydrocarbons and proteins (Table 4.1).

The locations of these bands within a representative spectrum from donor A are shown in figure 4.4. Figure 4.5 is a

Table 4.1 – Wave bands selected for micro-FTIR mapping of fingerprint residue components [118-120].

| Compounds                | Wave number band (cm <sup>-1</sup> ) |
|--------------------------|--------------------------------------|
| Hydroxyl groups          | 3598-3115                            |
| Fatty acid/triglycerides | 1790-1700                            |
| Sugars/phospholipids     | 1180-975                             |
| Hydrocarbons             | 2994-2827                            |
| Proteins                 | 1697-1542                            |

light microscope image of the donor A sample prior to analysis, highlighting the scanned fingerprint and control regions for both aperture sizes (25 $\mu\text{m}$  and 6.25 $\mu\text{m}$ ). With the larger aperture size scanning times are lower, which enabled large regions to be mapped, and spectra have higher signal-to-noise ratio. In contrast, the smaller aperture produces more highly resolved maps; however, spectra are noisier and only small regions could be mapped due to higher scanning times. For comparison purposes all subsequent results presented are from donor A, however, studies on donor B have demonstrated the observations are not donor specific.

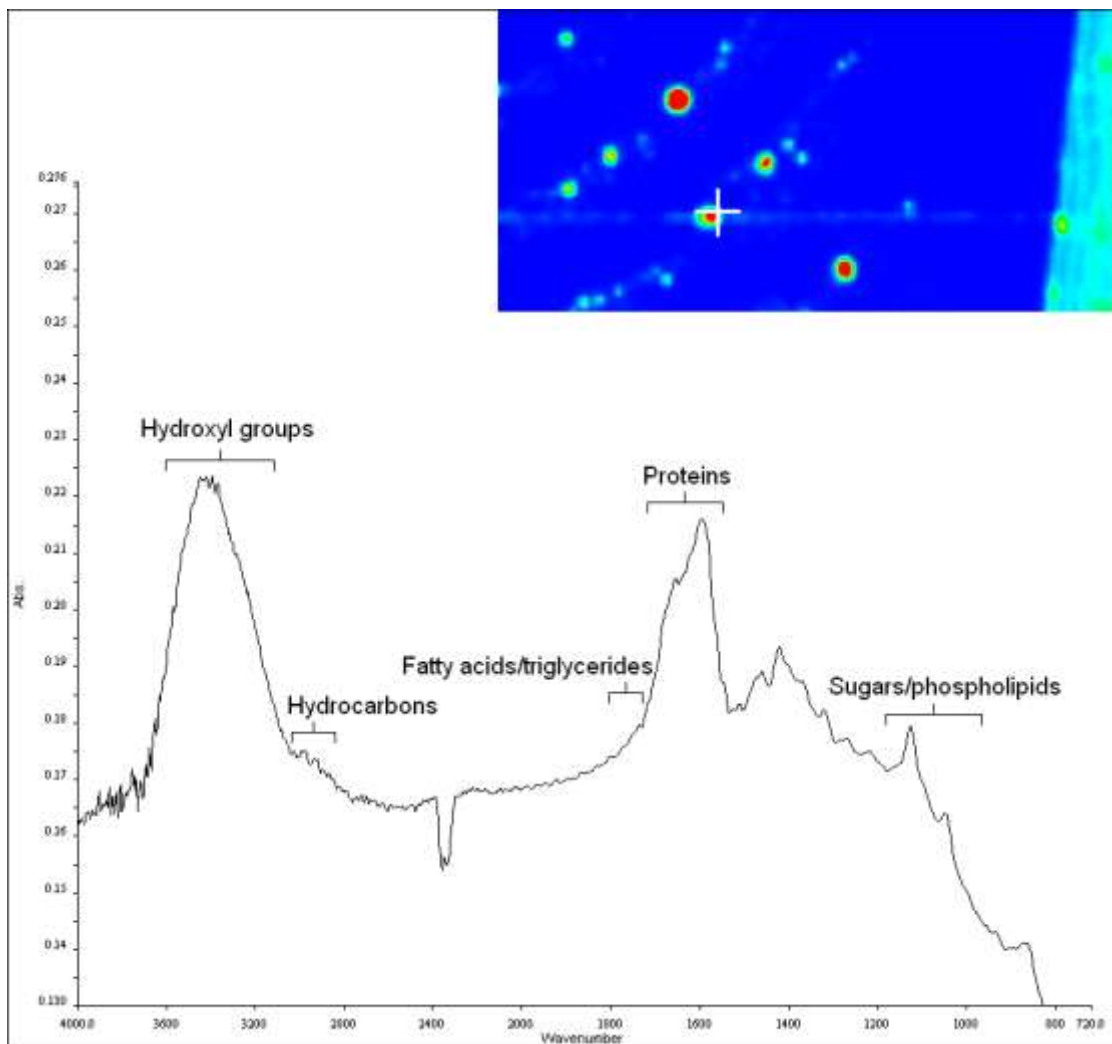


Figure 4.4 – An FTIR spectrum from a Donor A fingerprint residue location (indicated by the cross on a representative micro-FTIR hydroxyl group map image) showing the functional groups to be mapped.

Hydroxyl group maps from fingerprint and control regions at both apertures and on both days are shown in figures 4.6 (25 $\mu\text{m}$ ) & 4.7 (6.25 $\mu\text{m}$ ). The image absorbance

colour scales are the same where the aperture size is the same, allowing direct comparisons over the 48 hour period and between fingerprint and control regions. Low to high intensities, i.e. from blue to red colours, represent relative abundance of the mapped functional group. A lack of any significant contrast in the hydroxyl group control maps demonstrates that there is no significant amount of water in this region at any period of analysis and therefore any changes that are seen in the fingerprint

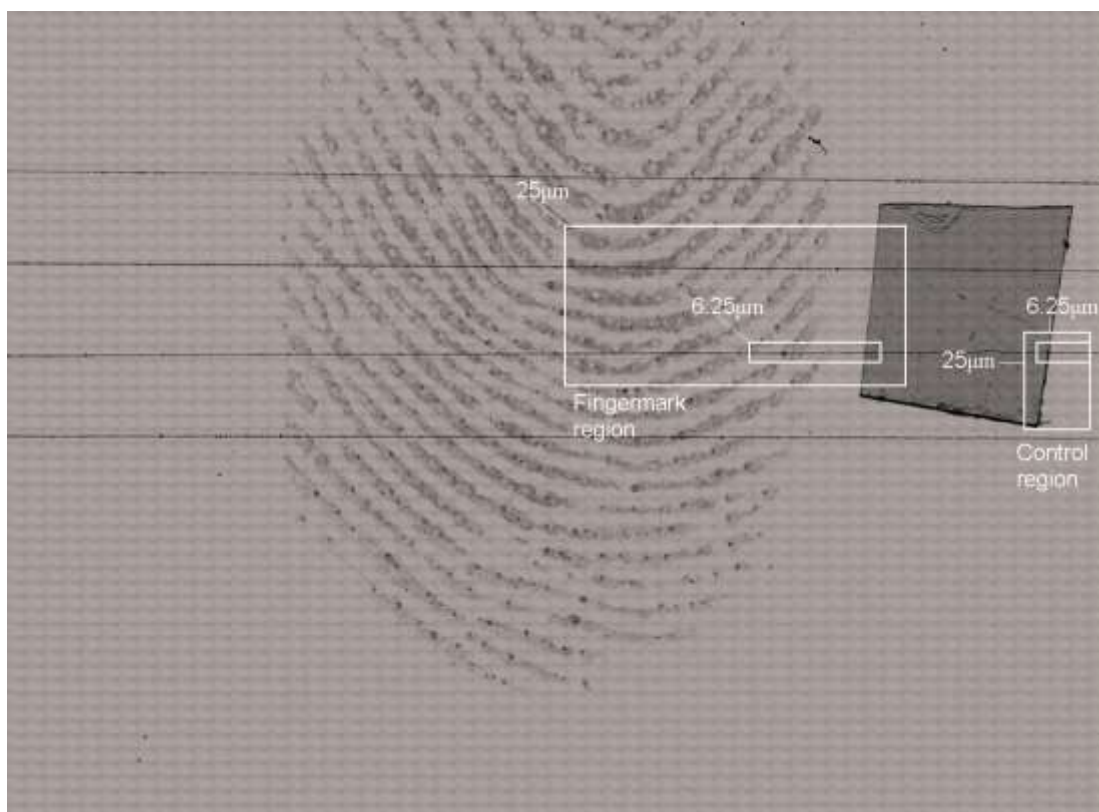


Figure 4.5 – A light microscope image of the donor A sample, including each area chosen for micro-FTIR mapping

region cannot be due to environmental contamination. It is evident in the fingerprint region 25µm maps, based on increases in green colour area and brightness that more water is occupying the scratches off ridge after the 48hr period has elapsed. Since this cannot be due to environmental contamination or instrument disparity, it must be the result of migrated residue. This effect is even clearer with the increased resolution provided by a 6.25µm aperture. Here the circular residue droplet is seen to dramatically reduce in size while filling up the scratch either side of its original position. Referring back to the 25µm map, every other droplet of similar or larger size is positioned away from the scratches and such reductions do not occur. Figure 4.8



shows maps of the  $6.25\mu\text{m}$  scanned area for each of the other relevant residue groups (fatty acids/triglycerides, sugars/phospholipids, hydrocarbons and proteins), where absorption colour scales are the same within each group but not comparable between groups (see appendix A for  $25\mu\text{m}$  maps). Control region maps are not shown for these residue groups since they all display equal to or less contrast as shown for hydroxyl groups in figure 4.6. The same reduction in droplet size and tracking of residues into the scratch is evident in each case. Hydrocarbons and sugars/phospholipids, in particular, also display a certain amount of tracking in the time from fingermark deposition to the day 1 scans ( $\sim 2\text{hr}$  for  $6.25\mu\text{m}$  scans), which may be due to a higher mobility for these residues.

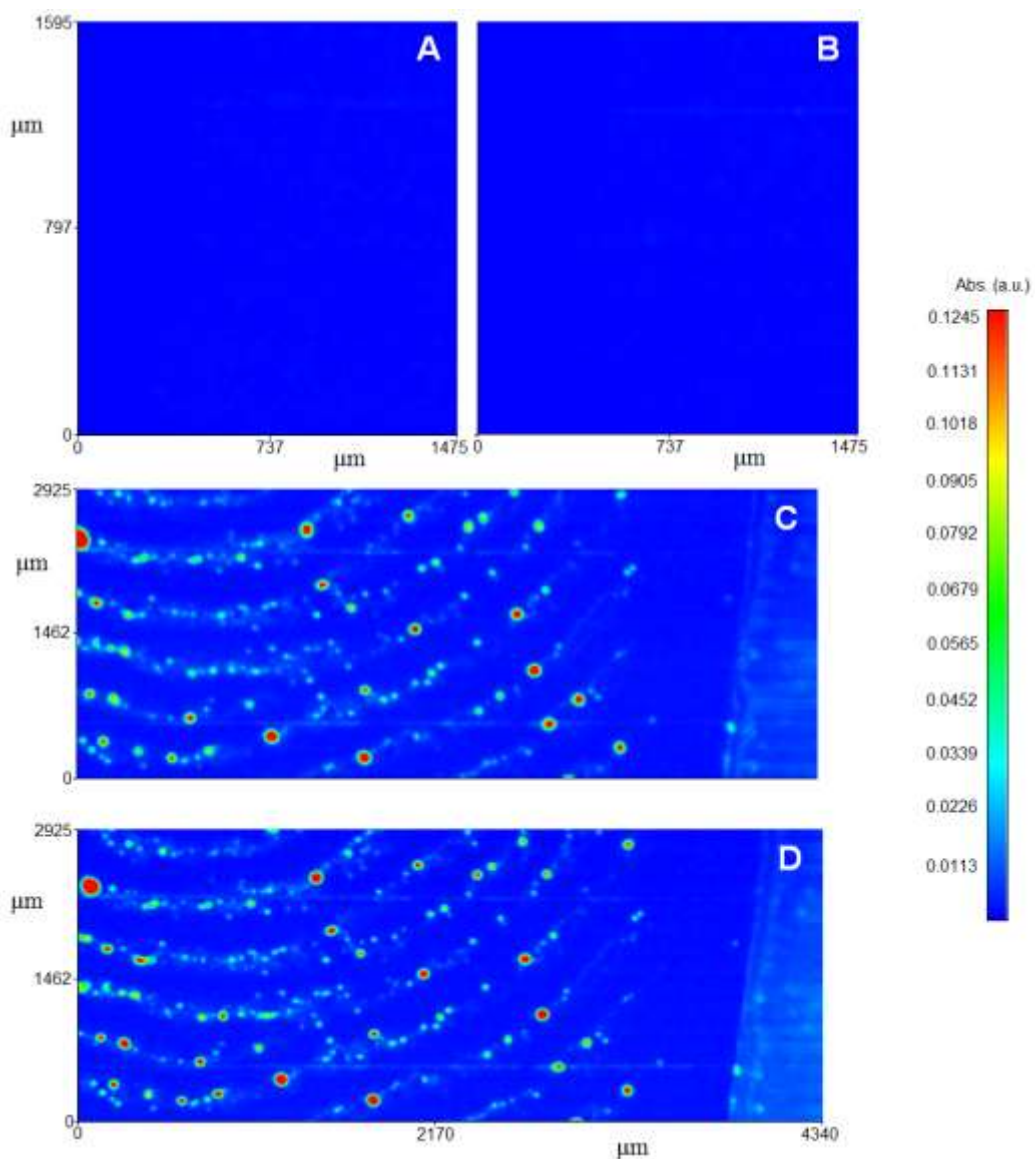


Figure 4.6 – Control region hydroxyl group maps taken with a  $25\mu\text{m}$  aperture on day 1 (a) and day 3 (b) showing no significant contrast along the scratch line (situated approximately a quarter from the top of the images). Fingermark region maps taken with a  $25\mu\text{m}$  aperture on day 1 (c) and day 3 (d) showing residue movement and droplet size reduction associated with scratch lines (situated approximately a quarter and three quarters from the top of the images).

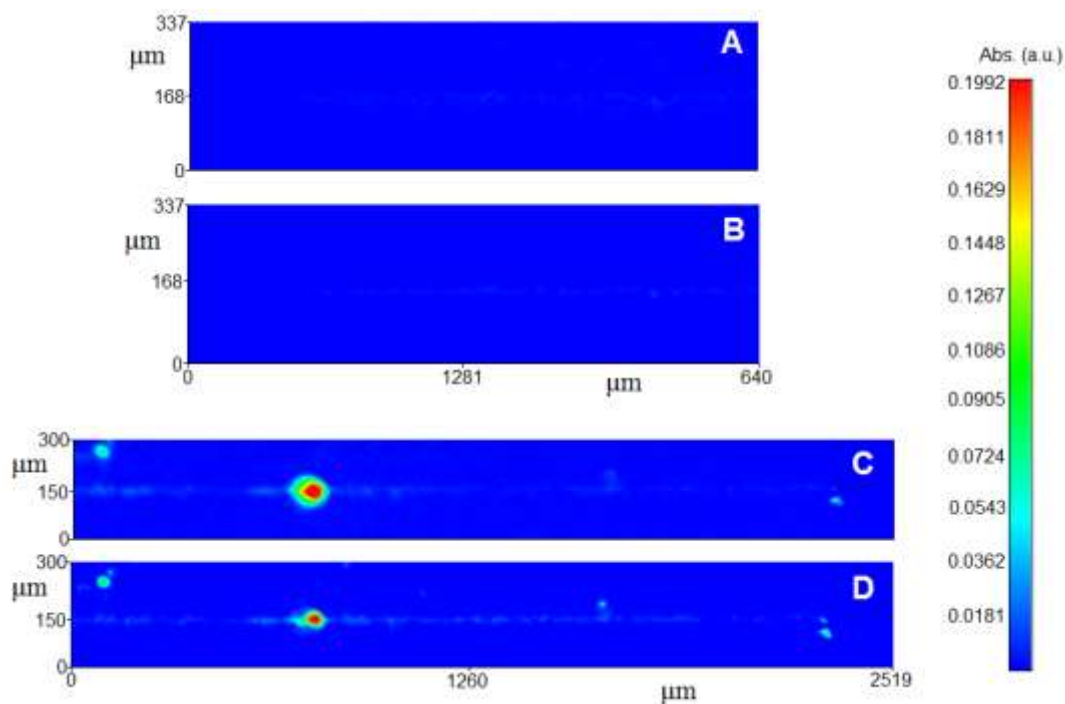


Figure 4.7 – Control region hydroxyl maps of the scratch line from figures 4.5a,b taken with a 6.25 μm aperture on day 1 (a) and day 3 (a) showing no significant contrast. Fingermark region maps of the bottom scratch line from figures 4.5c,d taken with a 6.25 μm aperture on day 1 (c) and day 3 (d). The increased resolution provided by a smaller aperture highlights scratch associated residue migration and droplet size reduction.

FTIR microspectroscopic imaging is able to clearly map the migration of a number of key fingermark residues along the linear features of a silicon model substrate. Based on current knowledge of the CA polymerisation mechanism for fingermark development [61-63], the demonstration of hydroxyl group (water) movement across linear features is an important observation. Operationally this may take on increased significance if the migrated residues on the model surface can subsequently be demonstrated to develop with CA under operational standard conditions, however, based on CAST polymer overdevelopment observations (Fig. 4.1b), the distance of residue migration (i.e. from ridge to ridge) is comparable. Such investigations have not been performed here due to a lack of access to the appropriate equipment; however, following repeat FTIR analysis this experimental stage would be possible. In terms of protocol implications, if CA polymerisation could be demonstrated on migrated residues, it would be difficult to suggest changes to technique since development is performing normally. Furthermore, CA fuming is generally preferred for rougher, non-porous substrates since the brushing action of certain alternative techniques can be detrimental to print quality on these surfaces. However, this issue is

more specifically related to linear surface features and so any protocol refinements could be implemented to possibly tighten the ‘smooth’ classification. The observed migration of all the analysed residue groups also renders possible alternative techniques (e.g. those that target amino acids) as ineffective solutions.

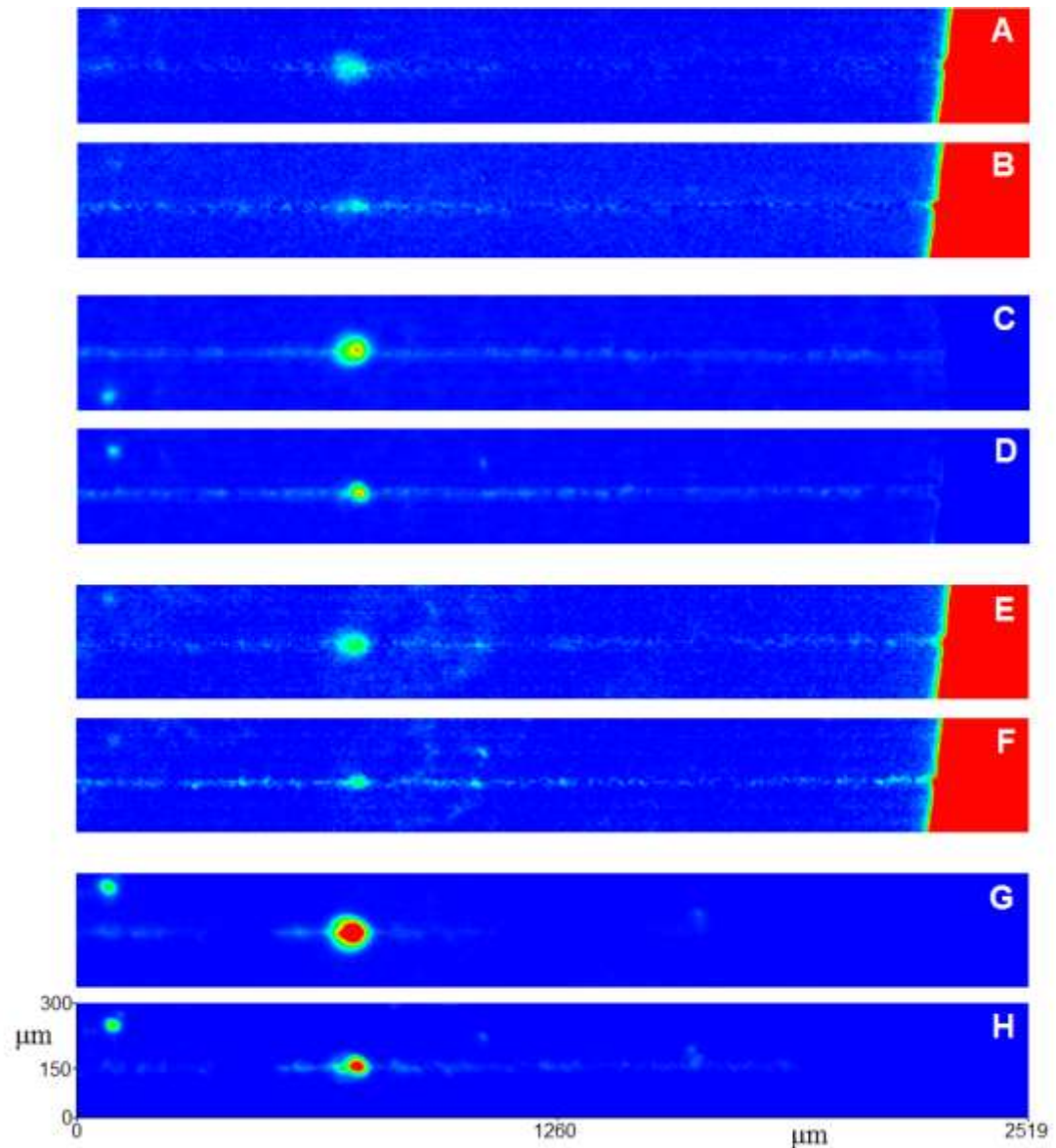


Figure 4.8 – Residue migration and droplet size reduction demonstrated with 6.25µm maps for the remaining residues, including fatty acids/triglycerides (a,b), sugars/phospholipids (c,d), hydrocarbons (e,f) and proteins (g,h), on days 1 and 3 respectively. (Note: Arbitrary colour scales are comparable between the two analysis days, but not between individual residue types)

An additional benefit to performing operational CA development following FTIR analysis is to monitor the effects of humidity. It is entirely possible that migrated residue alone may not be sufficient to cause overdevelopment into off ridge areas and

moisture created by an atmosphere of 80% relative humidity, which is required for optimal CA development, could be trapping in the linear surface features. Any CA polymerisation in scratches of the control regions would support this theory.

#### **4.4 Conclusions**

It has been shown that a number of key fingerprint residues migrate along linear surface features created in a silicon model system, which may account for an observed overdevelopment phenomenon occurring in similar features on PE and uPVC. Despite the drawbacks of using a model to represent operationally relevant surfaces, the silicon substrate features are expected to be less conducive to residue migration than both operationally relevant substrate features. A lack of any significant residue build-up in control regions discounts the possibility that linear surface features are trapping moisture or contamination from the environment, which is subsequently being developed. It is possible, however, that an environmental condition during development, namely relative humidity, is partially or fully responsible for the observed overdevelopment effect. Police force standard CA development of samples following FTIR analysis will shed more light on this theory and ultimately help determine the operational significance of observed fingerprint residue migration on the silicon model. Due to the importance of CA development as an alternative method to brushing techniques for rough, non-porous surfaces it would be difficult to re-grade surfaces with abundant linear features as ‘rough’, however, these could feature as a sub-category of the smooth classification for protocol purposes.

**SUMMARY****5**

The merits of combining highly sensitive and specific analytical and imaging techniques to research how latent fingerprints, deposition surfaces and development agents interact with each other are well understood and have been explained previously in this report. Firstly it is important to recognise that the data acquired over the course of two individual investigations that comprise this project lends further weight to these empirical benefits. Macroscopic and low resolution microscopic (see figure 3.1, inset) analysis of CPS developed fingerprints on a Formica substrate reveals well defined prints with good levels of contrast. However, this work demonstrates through the integration of high resolution imaging and powerful chemical analysis that a specific compound, randomly distributed in microscopic patches within this surface, has the potential to create erroneous print detail, which may negate the macroscopic quality.

Titania is widely used in the polymer industry, primarily as a white pigment and also due to a number of beneficial photocatalytic properties. As well as isolating titania from aluminosilicate (a second commonly occurring pigment within the Formica substrate) in terms of active involvement in the CPS overdevelopment interaction, SEM and EDX analysis has demonstrated its prevalence in a selection of used and new household plastics. Additionally, titania has been shown to interact selectively with other powder suspensions (i.e. with MoS<sub>2</sub> PS, and not iron oxide PS) and a similar effect has been characterised on surfaces that display a ubiquitous distribution of the pigment, which is thought to cause detrimental reductions in contrast. An insight into the mechanism for how titania is interacting with these development agents has been gained through ultra surface sensitive ToF-SIMS analysis, which places significant quantities of the compound within the top 30nm and suggests a possible role for the pigment's aluminosilicate coating. Further investigations into the coating significance and how suspension formulation affects interaction could have potential benefits for developing analogous techniques that are unaffected by titania. However, current viable alternatives, such as CA fuming or MoS<sub>2</sub> SPR, can be recommended here for potentially problematic surfaces, such as light coloured polymers, depending on aging considerations and additional factors.

The chemical mapping of individual and developmentally relevant fingerprint residues with micro-FTIR analysis has demonstrated their significant mobility along linear surface features in a silicon model and provided an explanation for SEM observed CA overdevelopment into off-ridge areas on PE and uPVC. This has excluded the possibility that CA polymerisation is initialising in on-ridge areas and then developing abnormally into off-ridge areas. Instead, it indicates that CA development is occurring correctly, which renders any protocol refinements more challenging. Simply reclassifying overly scratched surfaces and those finished with linear features as ‘rough’ would not be an adequate solution due to the benefits of CA fuming in this classification. Additionally, the migration of several residue types suggests that certain alternative techniques, such as those that target amino acids, may also be affected. There is significant scope to build upon these findings for further characterisation of residue migration into linear features and for more general movement of residues across surfaces (e.g. influence of substrate and heavy prints on ‘empty’ VMD development [11]). These could range from basic expansions of experimental parameters (e.g. increased donor set, larger donor age variation, varying donor sex, etc.) to developing objective measurements of migration distance and time, both collectively and for individual residue types. Such data could have the potential to assist with development technique choices by creating mathematical models of residue movement.

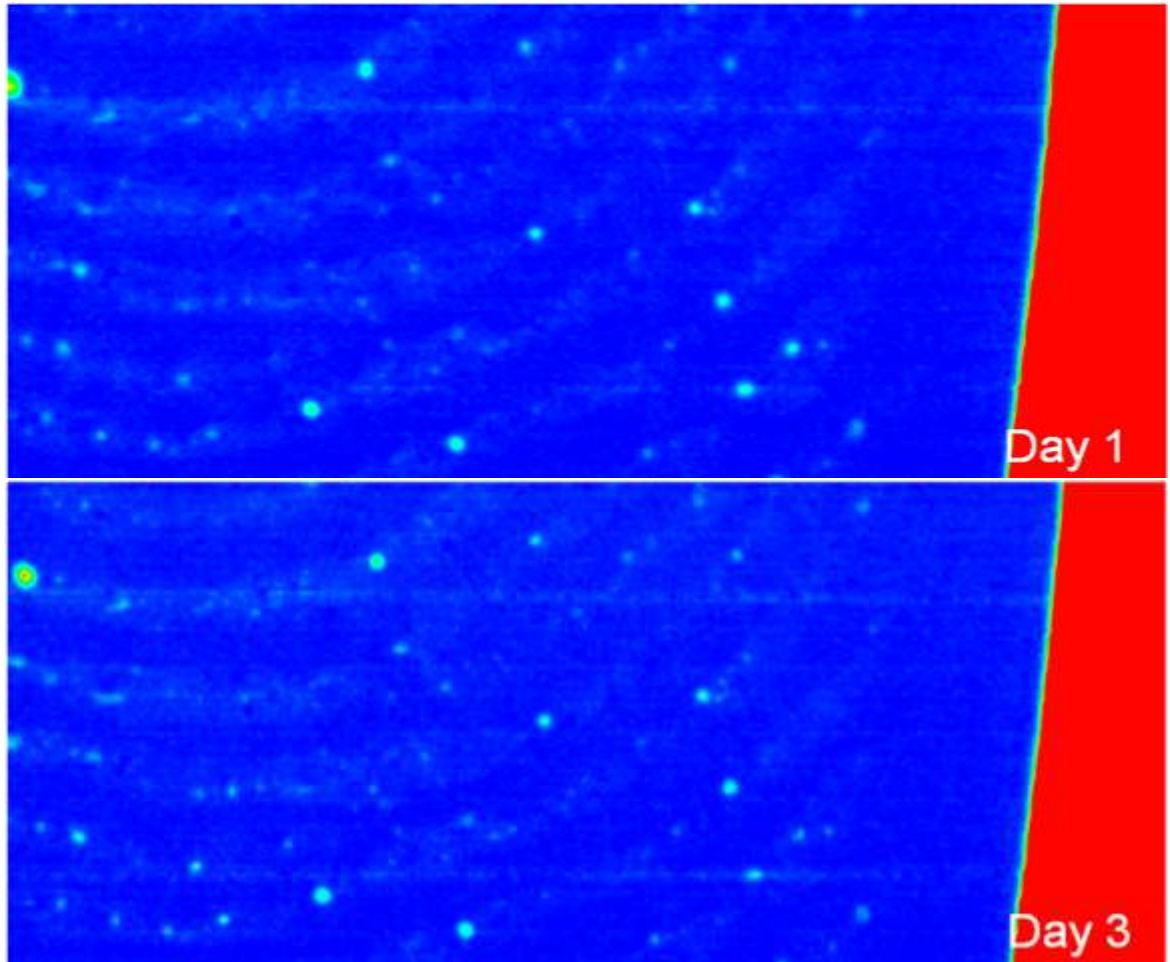
As a physical, topological and fingerprint dependant effect, the migration of residues into linear features is a fundamentally different problem mechanistically to interactions between powder suspensions and polymer additives. However, the relationship between combinational instrument experimentation and the characterisation of otherwise invisible intra-classification surface heterogeneities, which are detrimental to development, is directly comparable and evident here. This work demonstrates both fingerprint-independent and fingerprint-dependant detrimental development effects within a small subset of equally classified, operationally relevant polymers. In doing so it highlights the importance of understanding each element of the three way interaction between fingerprints, deposition substrates and development agents for improving the effectiveness of the

entire identification process. Such development effects are governed by very slight variations in surface properties that occur frequently within current protocol classifications. By characterising these effects and their mechanisms, in conjunction with research into development technique mode of operation and residue composition, it becomes possible to increase specificity in technique choice by recommending more effective options and developing new methods. Ultimately, this should function to increase the quantity and quality of usable prints from a given operational situation using the minimum necessary application.

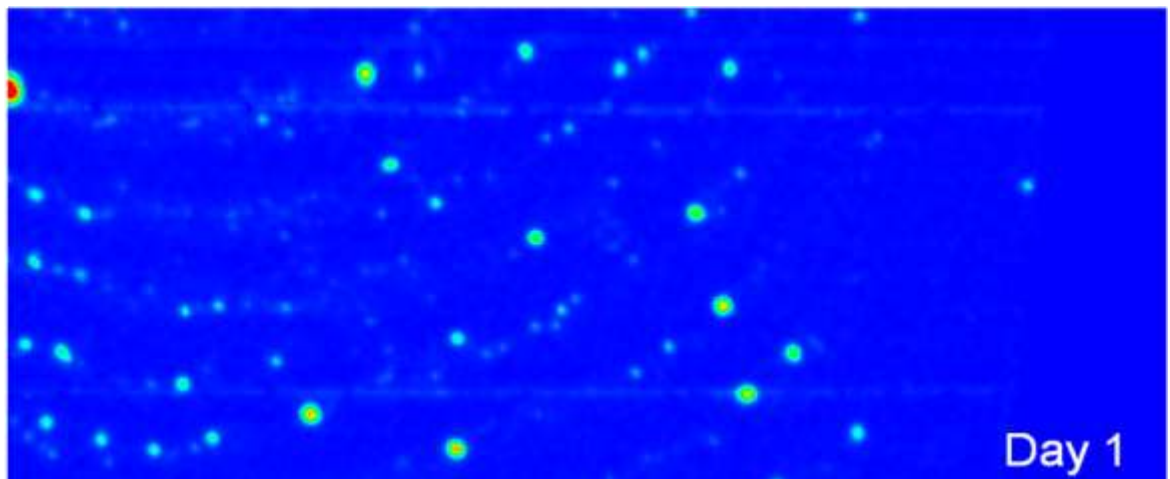
**APPENDIX A**

**Donor A 25 $\mu$ m Maps**

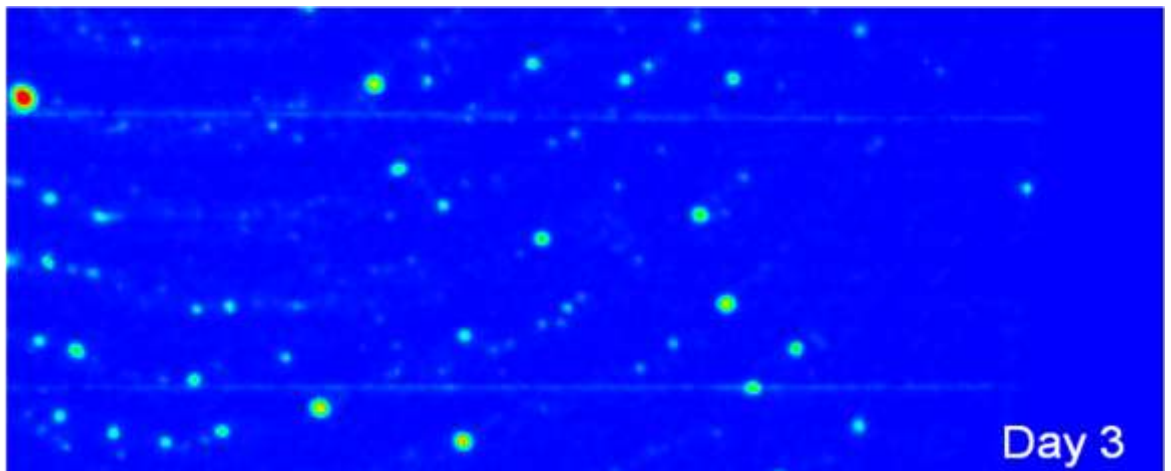
*Fatty acids/triglycerides*



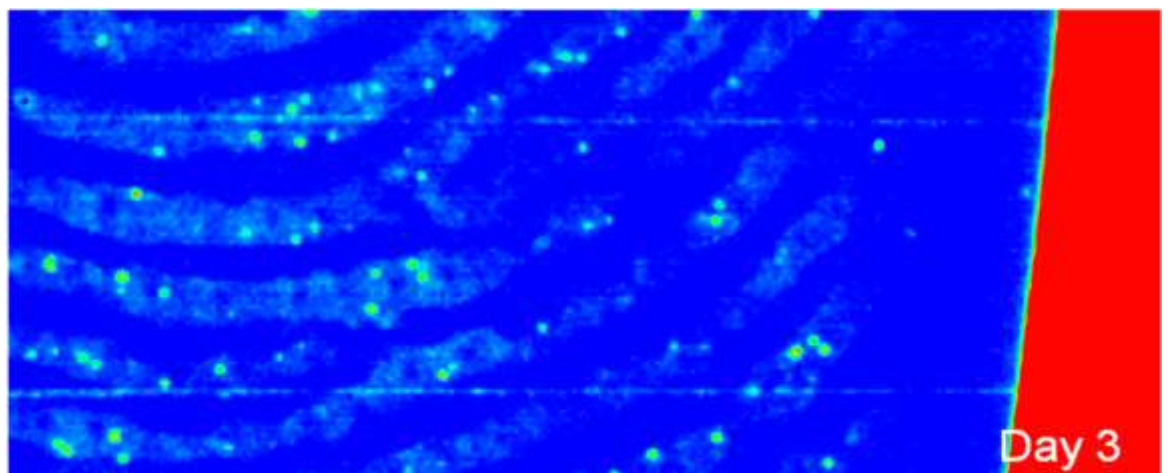
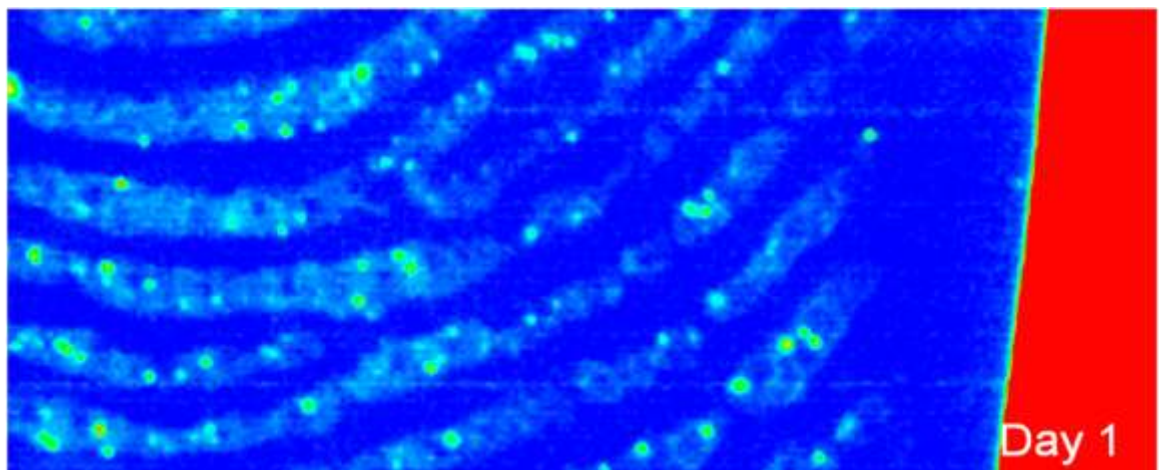
*Sugars/phospholipids*



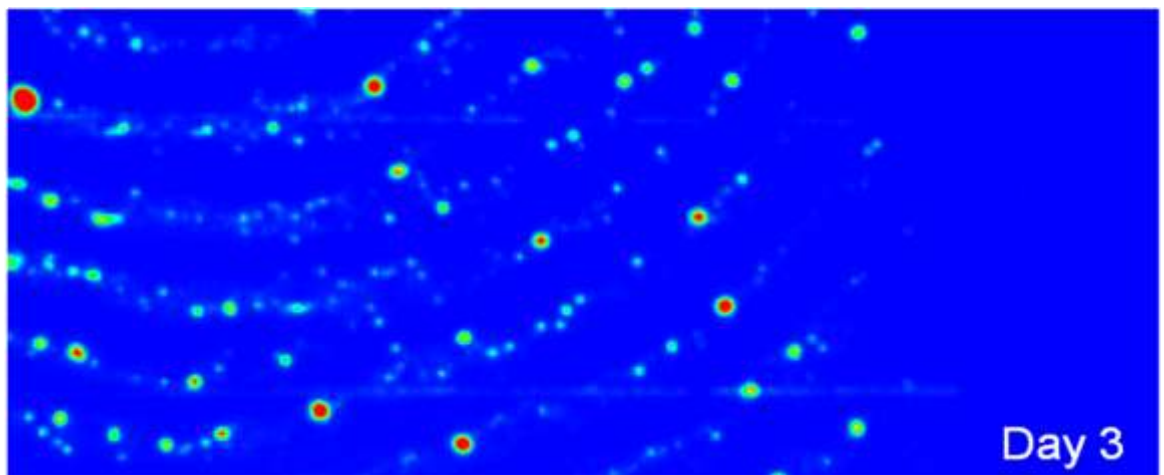
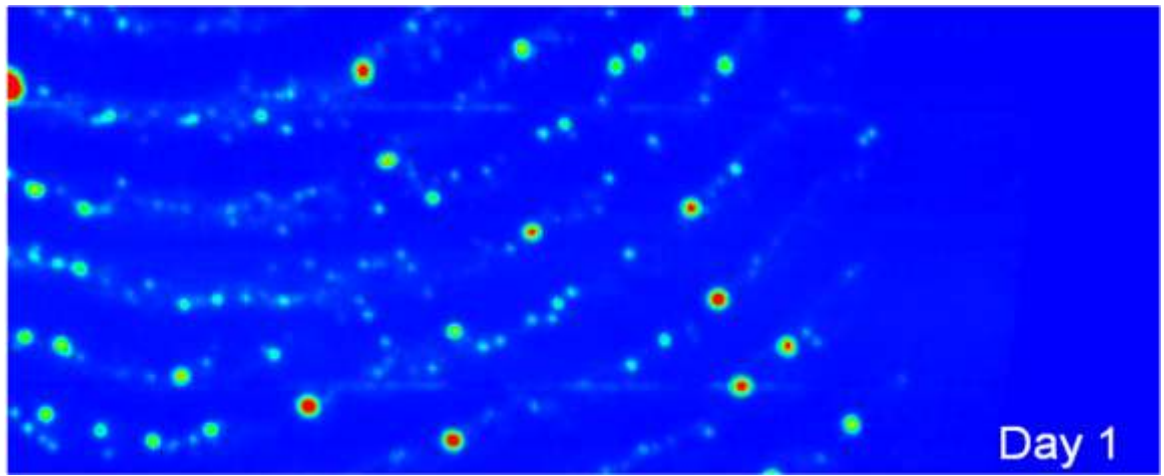




*Hydrocarbons*



*Proteins*



## APPENDIX B

A portion of the early work towards this project was presented by Dr Ben Jones at the University of Wolverhampton for the 36<sup>th</sup> Fingerprint Society Annual Conference in April 2011. The abstract, printed below under the title of Interactions Between Latent Fingerprints, Surfaces and Fingerprint Development Techniques, has subsequently been published in issue 37 of Fingerprint Whorld.

Jones B.J., Bacon, S. R., Downham, R., Sears, V. G., Interactions between latent fingerprints, surfaces and fingerprint development techniques, *Fingerprint Whorld* **37** (2011) 130-131:

“Latent fingerprint deposition and effectiveness of detection are strongly affected by the surface on which prints are deposited. Material properties, surface roughness, morphology, chemistry and hydrophobicity affect the usefulness or efficacy of forensic print development techniques such as dry powder, powder suspension, cyanoacrylate fuming or vacuum metal deposition. Lack of development agent adhering to deposited print as well as excess background staining can both be problematic. We investigate surface characteristics that adversely affect print development for a range of techniques to potentially enhance development algorithms.

We discuss a series of surfaces classified as smooth non-porous plastic; utilising atomic force microscopy (AFM), Fourier transform infra-red spectroscopy (FTIR) and scanning electron microscopy (SEM) to characterise the surfaces and to investigate the interaction between latent fingerprint, surface and development agent. Natural latent prints from a number of donors were developed with various powder suspensions, cyanoacrylate fuming or small particle reagent. Surfaces and prints were analysed on a range of scales from macro- to nano- to help to elucidate the mechanisms of fingerprint development. Differences between the surfaces have a strong effect, even within a single classification<sup>1,2</sup>. Surface texture, the average roughness, spatial variation, and topographical feature shape, as well as substrate and pigment chemistry, affect the development techniques in varying ways. This is related to the physical and chemical structure of the development agent and application or development process.

[1] BJ Jones, R Downham, VG Sears “Effect of substrate surface topography on forensic development of latent fingerprints with iron oxide powder suspension” *Surface and Interface Analysis* **42** (2010) 438

[2] BJ Jones, AJ Reynolds, M Richardson, VG Sears “Nano-scale composition of commercial white powders for development of latent fingerprints on adhesives” *Science and Justice* **50** (2010) 150”

**REFERENCES**

- [1] Maltoni, D., Maio, D., Jain, A. K., Prabhakar, S., *Handbook of Fingerprint Recognition*, 2<sup>nd</sup> ed., Springer, London, 2009.
- [2] Berry, J., Stoney, D. A., History and Development of Fingerprinting, in: Lee, H. C., Gaensslen, R. E. (Eds.), *Advances in Fingerprint Technology*, 2<sup>nd</sup> ed., CRC Press, Boca Raton, 2001, pp. 13-52.
- [3] Kücken, M., Newell, A. C., Fingerprint Formation, *J. Theor. Biol.* **235** (2005) 71-83.
- [4] International Biometric Group, *The Henry Classification System*, 2003. Accessed at <http://www.biometricgroup.com/Henry%20Fingerprint%20Classification.pdf> on 01/02/11.
- [5] Jain, A. K., Feng, J., Latent Fingerprint Matching, *IEEE T. Pattern Anal.* **33** (2011) 88-100.
- [6] Druce, J. F., Bristow, L. C., Latent Mark Development and Analysis Within a Modern Policing Environment, *Surf. Interface Anal.* **42** (2010) 343-346
- [7] Olsen, R. D., Lee, H. C., Identification of Latent Prints, in: Lee, H. C., Gaensslen, R. E. (Eds.), *Advances in Fingerprint Technology*, 2<sup>nd</sup> ed., CRC Press, Boca Raton, 2001, 13-52.
- [8] Bowman, V., Sears, V. G., Bandey, H., Bleay, S., Fitzgerald, L., Gibson, A., *Manual of Fingerprint Development Techniques: A Guide to the Selection and Use of Processes for the Development of Latent Fingerprints*, 2<sup>nd</sup> ed., Home Office Police Scientific Development Branch, Sandridge, 1998.
- [9] Bandey, H. L., *Fingerprint Powders Guidelines*, HOSDB Publication No. 09/07, 2007.
- [10] Azoury, M., Cohen, D., Himberg, K., Qvintus-Leino, P., Saari, T., Almog, J., Fingerprint Development on Counterfeit US Dollar Banknotes: The Importance of Preliminary Paper Examination, *J. Forensic Sci.* **49** (2004) 1015-1017.
- [11] Jones, N., Mansour, D., Stoilovic, M., Lennard, C., Roux, C., The Influence of Polymer Type, Print Donor and Age on the Quality of Fingerprints Developed on Plastic Substrates Using Vacuum Metal Deposition, *Forensic Sci. Int.* **124** (2001) 167-177.

- [12] Jones, B. J., Downham, R., Sears, V. G., Effect of Substrate Surface Topography on Forensic Development of Latent Fingerprints with Iron Oxide Powder Suspension, *Surf. Interface Anal.* **42** (2010) 438-442.
- [13] Fisher, J., *Forensics Under Fire: Are Bad Science and Duelling Experts Corrupting Criminal Justice?*, Rutgers University Press, New Jersey, 2008.
- [14] Pyrek, K. M., *Forensics Under Siege*, Elsevier Academic Press, London, 2007.
- [15] Page, M., Taylor, J., Blenkin, M., Uniqueness in the Forensic Identification Sciences – Fact or Fiction?, *Forensic Sci. Int.* **206** (2011) 12-18.
- [16] Spinney, L., The Fineprint, *Nature* **464** (2010) 344-346.
- [17] Ulery, B. T., Hicklin, R. A., Buscaglia, J., Roberts, M. A., Accuracy and Reliability of Forensic Latent Fingerprint Decisions, *PNAS* **108** (2011) 7733-7738.
- [18] Cummins, H., Ancient Fingerprints in Clay, *J. Crim. Law Crim.* **32** (1941) 468-481.
- [19] Penrose, L. S., The Medical Significance of Finger-Prints and Related Phenomena, *Brit. Med. J.* **2** (1968) 321-325.
- [20] Grew, N., The Description and Use of the Pores in the Skin of the Hands and the Feet. *Phil. Trans.* **14** (1684) 566-567.
- [21] Cummings, H., Kennedy, R. K., Purkinje's Observations (1823) on Finger Prints and Other Skin Features, *J. Crim. Law Crim.* **31** (1940) 343-356.
- [22] Barnes, J. G., History, in: *The Fingerprint Sourcebook*, 2011. Accessed at <https://www.ncjrs.gov/pdffiles1/nij/225320.pdf> on 27/10/11.
- [23] Herschel, W. J., Skin Furrows of the Hand, *Nature* **23** (1880) 76.
- [24] Faulds, H., On the Identification of Habitual Criminals by Finger-Prints, *Nature* **50** (1894) 548.
- [25] Henry, E. R., *Classification and Uses of Fingerprints*, Routledge, London, 1900.
- [26] Polson, C. J., Finger Prints and Finger Printing. An Historical Study, *J. Crim. Law Crim.* **41** (1950) 495-517.
- [27] Ramotowski, R. S., Composition of Latent Print Residue, in: Lee, H. C., Gaensslen, R. E. (Eds.), *Advances in Fingerprint Technology*, 2<sup>nd</sup> ed., CRC Press, Boca Raton, 2001, pp. 63-104.
- [28] Marieb, E. N., *Human Anatomy & Physiology*, 5<sup>th</sup> Ed., Benjamin Cummings, San Francisco, 2001.

- [29] Maceo, A. V., Anatomy and Physiology of Adult Friction Ridge Skin, in: *The Fingerprint Sourcebook*, 2011. Accessed at <https://www.ncjrs.gov/pdffiles1/nij/225320.pdf> on 27/10/11.
- [30] Champod, C., Lennard, C., Margot, P., Stoilovic, M., *Fingerprints and Other Ridge Skin Impressions*, CRC Press, Boca Raton, 2004.
- [31] Wertheim, K., Maceo, A., The Critical Stage of Friction Ridge and Pattern Formation, *J. Forensic Iden.* **52** (2002) 35-85.
- [32] Wertheim, K., Embryology and Morphology of Friction Ridge Skin, in: *The Fingerprint Sourcebook*, 2011. Accessed at <https://www.ncjrs.gov/pdffiles1/nij/225320.pdf> on 27/10/11.
- [33] Weyermann, C., Roux, C., Champod, C., Initial Results on the Composition of Fingerprints and its Evolution as a Function of Time by GC/MS Analysis, *J. Forensic Sci.* **56** (2011) 102-108.
- [34] Yamashita, B., French, M., Latent Print Development, in: *The Fingerprint Sourcebook*, 2011. Accessed at <https://www.ncjrs.gov/pdffiles1/nij/225320.pdf> on 27/10/11.
- [35] Weyermann, C., Ribaux, O., Situating Forensic Traces in Time, *Sci. Justice* (2011) doi:10.1016/j.scijus.2011.09.003.
- [36] Croxton, R. S., Baron, M. G., Butler, D., Kent, T., Sears, V. G., Variation in Amino Acid and Lipid Composition of Latent Fingerprints, *Forensic Sci. Int.* **199** (2010) 93-102.
- [37] Cuthbertson, F., *The Chemistry of Fingerprints*, AWRE Report No. 013/69, Atomic Energy Authority, UK, 1969.
- [38] Coltman, C. A., Rowe, N. J., Atwell, R. J., The Amino Acid Content of Sweat in Normal Adults, *Am. J. Clin. Nutr.* **18** (1966) 373-378.
- [39] Hadorn, B., Hanimann, F., Anders, P., Curtius, H. C., Halverson, R., Free Amino Acids in Human Sweat from Different Parts of the Body, *Nature* **215** (1967) 416-417.
- [40] Knowles, A. M., Aspects of Physicochemical Methods for the Detection of Latent Fingerprints, *J. Phys. E: Sci. Instrum.* **11** (1978) 713-721.
- [41] Archer, N. E., Charles, Y., Elliot, J. A., Jickells, S., Changes in the Lipid Composition of Latent Fingerprint Residue with Time After Deposition, *Forensic Sci. Int.* **154** (2005) 224-239.

- [42] Hemmila, A., McGill, J., Ritter, D., Fourier Transform Infrared Reflectance Spectra of Latent Fingerprints: A Biometric Gauge for the Age of an Individual, *J. Forensic Sci.* **53** (2008) 369-376.
- [43] Sodhi, G. S., Kaur, J., Fingermarks Detection by Eosin-blue Dye, *Forensic Sci. Int.* **115** (2001) 69-71.
- [44] Stoilovic, M., Detection of Semen and Blood Stains Using Polilight as a Light Source, *Forensic Sci. Int.* **51** (1991) 289–296.
- [45] Bullock, K. M., Harris, J. S., Latumus, P. L., Use of a Simple Coaxial Lighting System to Enhance Fingerprint and Handwriting Evidence, *Can. Soc. Forensic Sci. J.* **27**, 69-80.
- [46] Bramble, S. K., Creer, K. E., Wang, G. C., Ultraviolet Luminescence from Latent Fingerprints, *Forensic Sci. Int.* **59** (1993) 3-14.
- [47] Dalrymple, B., Duff, J. M., Menzel, E. R. (1977): Inherent Fingerprint Fluorescence Detection by Laser. *J. Forensic Sci.*, **22**, 106–115.
- [48] Lee, H. C., Gaensslen, R. E., Methods of Latent Fingerprint Development, in: Lee, H. C., Gaensslen, R. E. (Eds.), *Advances in Fingerprint Technology*, 2<sup>nd</sup> ed., CRC Press, Boca Raton, 2001, pp. 105-176.
- [49] Daeid, N. N., Carter, S., Laing K., Comparison of Vacuum Metal Deposition and Powder Suspension for Recovery of Fingerprints on Wetted Nonporous Surfaces, *J. Forensic Iden.* **58** (2008) 600-613.
- [50] Daeid, N., N., Carter, C., Laing, K., The Comparison of Three Types of White Powder Suspensions for the Recovery of Fingerprints on Wetted Nonporous Surfaces, *J. Forensic Inden.* **58** (2008) 590-613.
- [51] Kimble, G. W., Powder Suspension Processing, *J. Forensic Iden.* **46** (1996) 273-280.
- [52] Sneddon, N., Black Powder Method to Process Duct Tape, *J. Forensic Iden.* **49** (1999) 347-356.
- [53] Jones, B. J., Reynolds, A. J., Richardson, M., Sears, V. G., Nano-scale Composition of Commercial White Powders for Development of Latent Fingerprints on Adhesives, *Sci. Justice* **50** (2010) 150-155.
- [54] Theys, P., Turgis, Y., Lepareux, A., Chevet, G., Ceccaldi, P. F., New Technique for Bringing out Latent Fingerprints on Paper: Vacuum Metallisation, *Int. Crim. Police Rev.* **217** (1968) 106.

- [55] Jones, N., Stoilovic, M., Lennard, C., Roux, C., Vacuum Metal Deposition: Factors Affecting Normal and Reverse Development of Latent Fingerprints on Polyethylene Substrates, *Forensic Sci. Int.* **115** (2001) 73-88.
- [56] Masters, N., DeHaan, J., Vacuum Metal Deposition (VMD) and Cyanoacrylate Detection of Older Latent Prints, *J. Forensic Iden.* **46** (1996) 32–45.
- [57] Jones, B. J., Downham, R., Sears, V. G., Nanoscale Analysis of the Interaction Between Cyanoacrylate and Vacuum Metal Deposition in the Development of Latent Fingermarks on Low Density Polyethylene, *J. Forensic Sci.* **57** (2012) 196-200.
- [58] Oden, S., von Hofsten, B., Detection of Fingerprints by the Ninhydrin Reaction, *Nature* **173** (1954) 449.
- [59] Almog, J., Fingerprint Development by Ninhydrin and its Analogues, in: Lee, H. C., Gaensslen, R. E. (Eds.), *Advances in Fingerprint Technology*, 2<sup>nd</sup> ed., CRC Press, Boca Raton, 2001, pp. 177-210.
- [60] Paine, M., Bandey, H. L., Bleay, S. M., Wilson, H., The Effect of Relative Humidity on the Effectiveness of the Cyanoacrylate Fuming Process for Fingerprint Development and on the Microstructure of the Developed Marks, *Forensic Sci. Int.* **212** (2011) 130-142.
- [61] Wargacki, S. P., Lewis, L. A., Dadmun, M. D., Understanding the Chemistry of the Development of Latent Fingerprints by Superglue Fuming, *J. Forensic Sci.* **52** (2007) 1057-1062.
- [62] Lewis, L. A., Smithwick, R., Devault, G., Bolinger, B., Lewis, S. A., Processes Involved in the Development of Latent Fingerprints Using the Cyanoacrylate Fuming Method, *J. Forensic Sci.* **46** (2001) 241–246.
- [63] Czekanski, P., Fasola, M., Allison, J., A Mechanistic Model for the Superglue Fuming of Latent Fingerprints, *J. Forensic Sci.* **51** (2006) 1323-1328.
- [64] Almog, J., Azoury, M., Elmaliah, Y., Berenstein, L., Zaban, A., Fingerprints' Third Dimension: The Depth and Shape of Fingerprint Penetration into Paper – Cross Section Examination by Fluorescence Microscopy, *J. Forensic Sci.* **49** (2004) 981-985.
- [65] Zhang, S., Li, L., Kumar, A., *Materials Characterization Techniques*, CRC Press, Boca Raton, 2009.



- [66] SEM and its Applications for Polymer Science, 2011. Accessed at <http://cnx.org/content/m38344/latest/?collection=col10699/latest> on 27/12/11.
- [67] Leng, Y., *Materials Characterization: Introduction to Microscopic and Spectroscopic Methods*, Wiley, New York, 2008.
- [68] Buckingham, J. D., Thermionic Emission Properties of a Lanthanum Hexaboride/Rhenium Cathode, *Brit. J. Appl. Phys.* **16** (1965) 1821-1832.
- [69] Kaufmann, E. N., *Characterization of Materials*, Wiley, New Jersey, 2003.
- [70] Scrivener, K. L., Backscattered Electron Imaging of Cementitious Microstructures: Understanding and Quantification, *Cement Concrete Comp.* **26** (2004) 935-945.
- [71] Dekker, A. J., Secondary Electron Emission, *Solid State Phys.* **6** (1958) 251.
- [72] Bogner, A., Jouneau, P. H., Thollet, G., Basset, D., Gauthier, C., A History of Scanning Electron Microscopy Developments: Towards “wet-STEM” Imaging, *Micron* **58** (2007) 390-401.
- [73] Energy-Dispersive X-ray Microanalysis, Noran Instruments, 1999. Accessed at <http://cime.epfl.ch/webdav/site/cime2/shared/Files/Teaching/EDX/Introduction%20to%20EDS.pdf> on 06/12/11.
- [74] Au, C., Jackson-Smith, H., Quinones, I., Jones, B. J., Daniel, B., Wet Powder Suspensions as an Additional Technique for the Enhancement of Bloodied Marks. *Forensic Sci. Int.* **204** (2011) 13-18.
- [75] Choi, M. J., McBean, K. E., Ng, P. H., McDonagh, A. M., Maynard, P. J., Lennard, C., Roux, C., An Evaluation of Nanostructured Zinc Oxide as a Fluorescent Powder for Fingerprint Detection, *J. Mater. Sci.* **43** (2008) 732-737.
- [76] Ma, R., Bullock, E., Maynard, P., Reedy, B., Shimmon, R., Lennard, C., Roux, C., McDonagh, A., Fingerprint Detection on Non-porous and Semi-Porous Surfaces Using NaYF<sub>4</sub>:Er,Yb Up-converter Particles, *Forensic Sci. Int.* **207** (2011) 145-149.
- [77] Williams, P., Secondary Ion Mass Spectrometry, *Am. Rev. Mater. Sci.* **15** (1985) 517-548.
- [78] Benninghoven, A., Analysis of Sub-Monolayers on Silver by Secondary Ion Emission, *Physica Status Solidi* **34** (1969) 169-171.
- [79] Hermann, A. M., Clode, P.L., Fletcher, I. R., Nunan, N., Stockdale, E. A., O'Donnell, A. G., Murphy, D. V., A Novel Method for the Study of the

- Biophysical Interface in Soils Using Nano-scale Secondary Ion Mass Spectrometry, *Rapid Commun. Mass Sp.* **21** (2007) 29-34.
- [80] Kovac, J., Surface Characterization of Polymers by XPS and SIMS Techniques, *Mater. Tehnol.* **45** (2011) 191-197.
- [81] Grehl, T., *Improvement in TOF-SIMS Instrumentation for Analytical Application and Fundamental Research*, PhD Thesis, University of Münster, 2003.
- [82] Sodhi, R. N. S., Time-of-flight Secondary Ion Mass Spectrometry (ToF-SIMS): Versatility in Chemical and Imaging Surface Analysis, *Analyst* **129** (2004) 483-487.
- [83] Bailey, M. J., Jones, B. N., Hinder, S., Watts, J., Bleay, S., Webb, R. P., Depth Profiling of Fingerprint and Ink Signals by SIMS and MeV SIMS, *Nucl. Instrum. Meth. B* **268** (2010) 1929-1932.
- [84] Szyrkowska, M. I., Czerski, K., Rogowski, J., Paryjczak, T., Parczewski, A., Detection of Exogenous Contaminants of Fingerprints Using ToF-SIMS, *Surf. Interface Anal.* **42** (2010) 393-397.
- [85] Hinder, S. J., Watts, F. F., SIMS Fingerprint Analysis on Organic Substrates, *Surf. Interface Anal.* **42** (2010) 826-829.
- [86] *FT-IR vs. Dispersive Infrared*, Thermo Nicolet Publication No. TN-00128 12/02, 2002.
- [87] *FT-IR Spectroscopy: Attenuated Total Reflectance (ATR)*, Perkin Elmer Publication No. 007024B\_01, 2005.
- [88] Bhargava, R., Perlman, R. S., Fernandez, D. C., Levin, I. W., Bartick, E. G., Non-invasive Detection of Superimposed Latent Fingerprints and Inter-ridge Trace Evidence by Infrared Spectroscopic Imaging, *Anal. Bioanal. Chem.* **394** (2009) 2069-2075.
- [89] Crane, N. J., Bartick, E. G., Perlman, R. S., Huffman, S., Infrared Spectroscopic Imaging for Noninvasive Detection of Latent Fingerprints, *J. Forensic Sci.* **52** (2007) 48-53.
- [90] Tahtouh, M., Kalman, J. R., Roux, C., Lennard, C., Reedy, B. J., The Detection and Enhancement of Latent Fingermarks Using Infrared Chemical Imaging, *J. Forensic Sci.* **50** (2005) 1-9.

- [91] Ricci, C., Kazarian, S. G., Collection and Detection of Latent Fingermarks Contaminated with Cosmetics on Nonporous and Porous Surfaces, *Surf. Interface Anal.* **42** (2009) 386-392.
- [92] Grant, A., Wilkinson, T. J., Holman, D. R., Martin, M. C., Identification of Recently Handled Materials by Analysis of Latent Human Fingerprints Using Infrared Spectromicroscopy, *Appl. Spectrosc.* **59** (2005) 1182-1187.
- [93] Antoine, K. M., Mortazavi, S., Miller, A. D., Miller, L. M., Chemical Differences are Observed in Children's Versus Adults' Latent Fingerprints as a Function of Time, *J. Forensic Sci.* **55** (2010) 513-518.
- [94] Williams, D. K., Schwartz, R. L., Bartick, E. G., Analysis of Latent Fingerprint Deposit by Infrared Microspectroscopy, *Appl. Spectrosc.* **58** (2004) 313-316.
- [95] Williams, D. K., Brown, C. J., Bruker, J., Characterization of Children's Latent Fingerprint Residues by Infrared Microspectroscopy: Forensic Implications, *Forensic Sci. Int.* **206** (2011) 161-165.
- [96] Binnig, G., Quate, C. F., Gerber, Ch., Atomic Force Microscope, *Phys. Rev. Lett.* **56** (1986) 930-933.
- [97] Blanchard, C. R., Atomic Force Microscope, *The Chemical Educator* **1** (1996) 1-8.
- [98] *A Practical Guide to Scanning Probe Microscopy*, Veeco Publication No. 08/05, 2005.
- [99] Eaton, P., West, P., *Atomic Force Microscopy*, Oxford University Press, New York, 2010.
- [100] Wilson, R. A., Bullen, H. A., Basic Theory – Atomic Force Microscopy, 2006. Accessed at [http://asdlib.org/onlineArticles/ecourseware/Bullen/SPMModule\\_BasicTheoryAFM.pdf](http://asdlib.org/onlineArticles/ecourseware/Bullen/SPMModule_BasicTheoryAFM.pdf) on 18/01/11.
- [101] Melitz, W., Shen, J., Kummel, A. C., Lee, S., Kelvin Probe Force Microscopy and its Application, *Surf. Sci. Rep.* **66** (2011) 1-27.
- [102] Skerry, F. M., Kjoller, K., Thornton, J. T., Tench, R. J., Cook, D., *Electric Force Microscopy, Surface Potential Imaging, and Surface Electric Modification with the Atomic Force Microscope (AFM)*, Veeco Publication No. AN27, 2004.
- [103] Shier, D., Butler, J., Lewis, R., *Hole's Human Anatomy and Physiology*, McGraw-Hill, New York, 2010.

- [104] Wittke, J. H., Microprobe-SEM, 2008. Accessed at <http://www4.nau.edu/microanalysis/Microprobe-SEM/Signals.html> on 27/12/11.
- [105] Infrared Absorption Spectroscopy, Sheffield Hallam University. Accessed at <http://teaching.shu.ac.uk/hwb/chemistry/tutorials/molspec/irspec3.htm> on 27/12/11.
- [106] FTIR Analysis Service, SEM Lab, 2011. Accessed at <http://www.semlab.com/ftir.html> on 27/12/11.
- [107] Lehenkari, P. P., Charras, G. T., Nesbitt, S. A., Horton, M. A., How the Atomic Force Microscope Scans Surfaces, 2000. Accessed at [http://journals.cambridge.org/fulltext\\_content/ERM/ERM2\\_02/S1462399400001575sup002.htm](http://journals.cambridge.org/fulltext_content/ERM/ERM2_02/S1462399400001575sup002.htm) on 27/12/11.
- [108] Williams, G., McMurray, H. N., Latent Fingermark Visualisation using a Scanning Kelvin Probe, *Forensic Sci. Int.* **167** (2007) 102-109.
- [109] Watson, P., Prance, R. J., Beardsmore-Rust, S. T., Prance, H., Imaging Electrostatic Fingerprints with Implications for a Forensic Timeline, *Forensic Sci. Int.* **209** (2011) e41-e45.
- [110] Sperling, M. L., *Introduction to Physical Polymer Science*, 4<sup>th</sup> ed., Wiley-Interscience, New Jersey, 2006.
- [111] McLaren, C., Lennard, C., Stoilovic, M., Methylamine Pretreatment of Dry Latent Fingermarks on Polyethylene for Enhanced Detection by Cyanoacrylate Fuming, *J. Forensic Iden.* **60** (2010) 199-222.
- [112] Huntsman Pigments, The Way Forward For Titanium Dioxide. *Plastics, Additives & Compounding* **10** (2008) 36-39.
- [113] Chen, X., Mao, S. S., Titanium Dioxide Nano Materials: Synthesis, Properties, Modifications and Applications, *Chem. Rev.* **107** (2007) 2891-2959.
- [114] DuPont to Increase Titanium Dioxide Production, Reuters, 2011. Accessed at <http://www.reuters.com/article/2011/05/11/dupont-idUKN1123780520110511> on 20/09/11.
- [115] Edge, M., Liauw, C. M., Allen, S. N., Herrero, R., Surface Pinking in Titanium Dioxide/Lead Stabiliser Filled PVC Profiles, *Polym. Degrad. Stabil.* **95** (2010) 2022-2040.

- [116] Jones, B. J., *Interactions Between Latent Fingerprints, Surfaces and Fingerprint Development Techniques*, 36th Fingerprint Society Annual Conference, 2011.
- [117] Pearson, B. N. J., Contact Mechanics for Randomly Rough Surfaces, *Surf. Sci. Rep.* **61** (2006) 201-227.
- [118] Skoog, D. A., Leary, J. J., *Principles of Instrument Analysis*, Saunders College Publishing, Philadelphia, 1992.
- [119] Conley, R. T., *Infrared Spectroscopy*, Allyn and Bacon, Boston, 1972.
- [120] Wade, L. G., *Organic Chemistry*, Prentice-Hall, New Jersey, 1995.